AD-A141 535 DEVELOPMENT AND COMPARISON OF ESTIMATION ALGORITHMS FOR AIRBORNE MISSILES(U) MISSISSIPPI STATE UNIV MISSISSIPPI STATE DEPT OF AEROPHYSICS A... K R HALL FEB 83 1/2

UNCLASSIFIED AFATL-TR-83-14 F08635-82-K-0107 F/G 12/1 NL

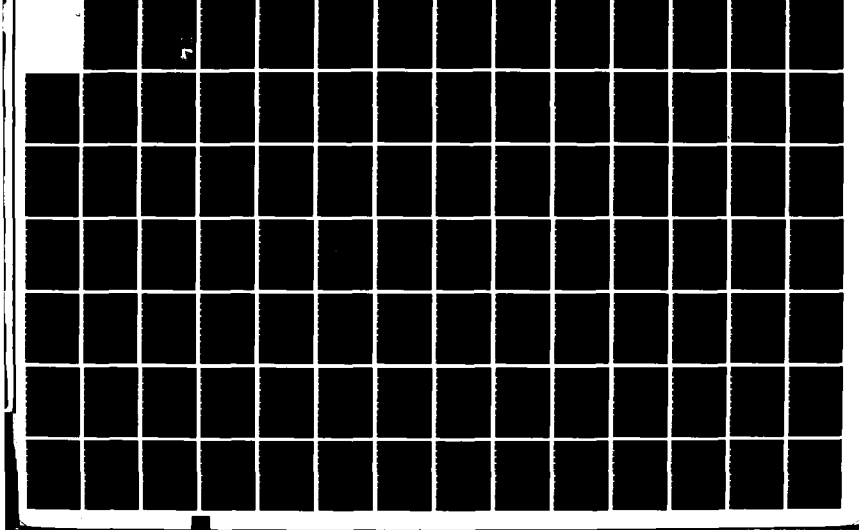

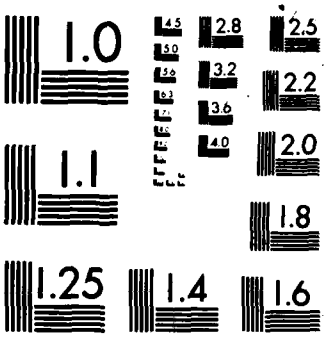

(2)

AD-A141 535

AFATL-TR-83-14

Development and Comparison of Estimation Algorithms for Airborne Missiles

K R Hall

DEPARTMENT OF AEROSPACE ENGINEERING
MISSISSIPPI STATE UNIVERSITY
MISSISSIPPI STATE, MISSISSIPPI 39762

FEBRUARY 1983

FINAL REPORT FOR PERIOD DECEMBER 1981 - DECEMBER 1982

Approved for public release; distribution unlimited

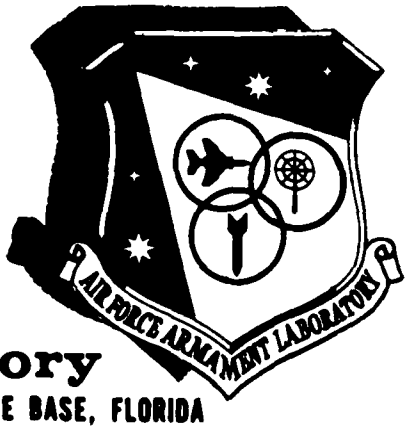

Air Force Armament Laboratory
AIR FORCE SYSTEMS COMMAND★UNITED STATES AIR FORCE★EGLIN AIR FORCE BASE, FLORIDA

NOTICE

Please do not request copies of this report from the Air Force Armament Laboratory. Additional copies may be purchased from:

National Technical Information Service
5285 Port Royal Road
Springfield, Virginia 22161

Federal Government agencies and their contractors registered with Defense Technical Information Center should direct requests for copies of this report to:

Defense Technical Information Center
Cameron Station
Alexandria, Virginia 22314

UNCLASSIFIED

SECURITY CLASSIFICATION OF THIS PAGE (When Data Entered)

REPORT DOCUMENTATION PAGE		READ INSTRUCTIONS BEFORE COMPLETING FORM
1. REPORT NUMBER AFATL-TR-83-14	2. GOVT ACCESSION NO. AD A141 535	3. RECIPIENT'S CATALOG NUMBER
4. TITLE (and Subtitle) DEVELOPMENT AND COMPARISON OF ESTIMATION ALGORITHMS FOR AIRBORNE MISSILES		5. TYPE OF REPORT & PERIOD COVERED Final Report: December 1981-December 1982 6. PERFORMING ORG. REPORT NUMBER
7. AUTHOR(s) K. R. Hall		8. CONTRACT OR GRANT NUMBER(s) F08635-82-K-0107
9. PERFORMING ORGANIZATION NAME AND ADDRESS Department of Aerospace Engineering Mississippi State University Mississippi State, Mississippi 39762		10. PROGRAM ELEMENT, PROJECT, TASK AREA & WORK UNIT NUMBERS PE: 61102F JON: 2304-E1-34
11. CONTROLLING OFFICE NAME AND ADDRESS Air Force Armament Laboratory (DLMA) Armament Division Eglin Air Force Base, Florida 32542		12. REPORT DATE February 1983 13. NUMBER OF PAGES 125
14. MONITORING AGENCY NAME & ADDRESS(if different from Controlling Office)		15. SECURITY CLASS. (of this report) UNCLASSIFIED 15a. DECLASSIFICATION/DOWNGRADING SCHEDULE

16. DISTRIBUTION STATEMENT (of this Report)

Approved for Public Release; Distribution Unlimited

17. DISTRIBUTION STATEMENT (of the abstract entered in Block 20, if different from Report)

18. SUPPLEMENTARY NOTES

Availability of this report is specified on verso of front cover.

19. KEY WORDS (Continue on reverse side if necessary and identify by block number)

Airborne Missile Guidance, Linear Quadratic Gaussian Control Extended Kalman Filter, Advanced Estimation Techniques

20. ABSTRACT (Continue on reverse side if necessary and identify by block number)

Basic development of the estimation, guidance, and control algorithms for guidance of an airborne missile during air-to-air combat engagements are examined. The extended Kalman filter is improved through the use of sample measurement statistics, through time-weighting the measurements, and through iterating within the Kalman filter. Numerical results are presented for comparing the performance of different filters.

DD FORM 1 JAN 73 1473 EDITION OF 1 NOV 65 IS OBSOLETE
S/N 0102-LF-014-6601

UNCLASSIFIED

SECURITY CLASSIFICATION OF THIS PAGE (When Data Entered)

PREFACE

This report was prepared by the Department of Aerospace Engineering, Mississippi State University, Mississippi State, Mississippi 39762 under Contract F08635-82-K-0107 with the Air Force Armament Laboratory, Aramament Division, Eglin Air Force Base, Florida 32542. Mr. Norman O. Speakman (DLMA) monitored the program for the Armament Laboratory. This work was accomplished during the period from December 1981 to December 1982.

The Public Affairs Office has reviewed this report, and it is releasable to the National Technical Information Service, (NTIS), where it will be available to the general public, including foreign nationals.

This technical report has been reviewed and is approved for publication.

FOR THE COMMANDER

Hugh T. Bainter

HUGH T. BAINTER, Colonel, USAF
Chief, Guided Weapons Division

Accession For	
NTIS GRA&I	☑
DTIC TAB	☐
Unannounced	☐
Justification	
By	
Distribution/	
Availability Codes	
Dist	Avail and/or Special
A-1	

(The reverse of this page is blank.)

TABLE OF CONTENTS

LIST OF FIGURES

LIST OF FIGURES (CONTINUED)

LIST OF FIGURES (CONTINUED)

LIST OF SYMBOLS

Symbol	Definition
A	..state coefficient matrix
$\underline{A}$	..acceleration vector
A1,A2,A3	..state coefficient matrix for each axis
AZ	..azimuth angle
B	..control coefficient matrix
B1,B2,B3	..control coefficient matrix for each axis
CM	..estimated measurement error covariance
CS	..sample estimated measurement error covariance
DT	..constant sampling interval
em	..sample estimated measurement error mean
EL	..elevation angle
F	..state transition matrix
G	..control transition matrix
GN	..gain coefficient
H	..Hamiltonian
J	..performance index
$\underline{J}$	..jerk vector
J1,J2,J3	..performance index for each axis
KG	..Kalman gain matrix
MB	..estimated measurement
MBe	..estimated measurement error
MT	..actual measurement
P	..costate vector
PB	..propagated state estimate error covariance
PF	..costate vector value at TF
PH	..updated state estimate covariance
P1,P2,P3	..costate vector components along x axis
q	..state propagation process error
Q	..process error covariance matrix

LIST OF SYMBOLS (CONTINUED)

Symbol	Definition
r	..measurement noise
R	..measurement noise covariance matrix
$\underline{R}$	..position vector
S	..state weighting matrix
T	..current time
TF	..final time
TTG	..time to go (TF-T)
U1,U2,U3	..control vector components
$\underline{V}$	..velocity vector
W	..control weighting matrix
XB	..propagated state estimate
XBe	..propagated state estimate error
XF	..state variable value at TF
XH	..updated state estimate
XHe	..updated state estimate error
XI,YI,ZI	..inertial position vector components
XT	..true state value
X1,X2,X3	..state vector components along x-axis
Y	..unforced state propagation response
Y1,Y2,Y3	..state vector components along y-axis
Z	..forced state propagation response
Z1,Z2,Z3	..state vector components along z-axis
	SUBSCRIPTS
M	..missile inertial quantity
R	..target quantity relative to missile
T	..target inertial quantity
	MISCELLANEOUS
XX'	..transpose of the matrix XX
XX^{-1}	..inverse of the square matrix XX
E{ XX }	..expected value of the quantity XX

SECTION I

INTRODUCTION

The guidance systems for modern airborne missiles are increasing in complexity with the introduction of onboard computational power in the form of minicomputers and microcomputers. The traditional form of guidance systems for airborne missiles employs some form of proportional navigation (pro-nav), a guidance scheme developed in the 1950's for use with analog equipment. Modern technology with microminiaturization of digital components allows a redefinition of the guidance schemes to utilize the computational power of current state-of-the-art equipment. Adaptive control systems with variable gains and onboard processing capabilities provide the potential for increased performance and versatility for these weapons. The price paid for the increase in potential is the development and application of modern optimal control and estimation techniques to the missile guidance problem.

The sensor complement employed in air-to-air missiles is usually composed of rate gyros and accelerometers for determining information about the states of the missile and a seeker for determining information about the target. The seeker may be classified as passive if it provides measurements of line-of-sight data only, and active or semi-active if it provides measurements of line-of-sight data and range data. Range data and line-of-sight data may be obtained from onboard radar while line-of-sight data only may be obtained from an infrared sensor. Many short range air-to-air missiles employ passive seekers and that is the type of seeker to be employed for this study.

The missile model to be employed in this study is that of a generic short-range bank-to-turn (BTT) missile. This

type of missile employs short aerodynamic surfaces (wings) which can be used to generate large aerodynamic forces in the pitch plane of the missile. For steering, the missile rolls to orient the pitch plane in the direction of the desired control force and uses the lift force as the control force. This type of steering differentiates the bank-to-turn missile from the skid-to-turn (STT) missile which does not employ wings to produce the turning maneuver. The skid-to-turn missile does not need to orient any plane during the turning maneuver, but it also cannot generate the turning maneuver forces comparable to the bank-to-turn missile.

Proportional navigation control laws are developed around passive seekers where the objective is to null the rotational rate of the line-of-sight vector from the missile to the target. For non-maneuvering targets, this will lead to an optimal interception. For maneuvering targets, pro-nav control laws are quickly seen to be suboptimal. The use of modern optimal control theory is ideally suited to this problem. In the majority of cases, the development of the control law follows the form of the linear quadratic optimal control problem in which the control is assumed to be composed of a linear combination of the states and the optimal control is chosen to minimize a quadratic function known as the performance index. The assumption that all of the states are measured and available is not true in general and a computational technique must be developed to obtain the desired state information from the available measurements.

An estimation algorithm is employed to convert the available measurement information into the desired state information. For problems governed by linear state differential equations with linear relationships between state and measurement variables, the optimal estimator is

the Kalman filter algorithm. For problems with non-linear state differential equations, or with non-linear state-measurement relationships, or both the extended Kalman filter is the most widely used estimation algorithm. While these are powerful estimation algorithms and do perform well in the presence of noise and uncertainty, most people use the "cookbook approach" of applying the algorithms without understanding the theory or even the results.

The Kalman filter employs a model of the state propagation process to determine estimated state values at a point in time. With these estimated state values, an estimate of the measurements can be made and compared to the true measurements made at that time. The discrepancy between the estimated measurements and the actual measurements may then be used to update the state estimates to a more correct value.

One of the problems with the application of the Kalman filter algorithm is that the characteristics of the error associated with the process of propagating the state estimate (process error) and the error associated with the taking of the measurements (measurement error) must be specified for use by the algorithm. The specification of these characteristics for a certain problem configuration is known as "tuning" of the filter and may lead to degraded performance of the filter under another problem configuration. A method of alleviating this tuning difficulty is to allow the filter to be self-tuning. This process is known as adaptive filtering and will be the subject of the adaptive filtering section of this report.

In summary, the application of modern optimal control techniques and the attendant estimation techniques to the guidance of an airborne missile pursuing a maneuvering target provides an excellent means of demonstrating the

application of modern guidance schemes. In addition, the problem provides an opportunity for a comparison of modern guidance schemes to traditional guidance schemes and, most of all, an excellent problem for development and testing of new guidance and estimation techniques. The current study places perspective upon the techniques employed in modern missiles while providing means of increasing the accuracy and performance of the missile guidance systems.

It should be emphasized that the guidance and control algorithms of this study along with the attendant estimation algorithms are being designed with the idea of microcomputer or minicomputer implementation onboard the missile. For this reason, algorithms of the recursive form are emphasized rather than algorithms which require large memory storage areas or extended computational time per iteration. Computational efficiency and minimal storage requirements are desirable characteristics of the optimal guidance scheme which is to be physically realizable onboard the missile.

SECTION II

PROBLEM DESCRIPTION

This section of the report provides a physical description of the problem to be studied and defines the coordinate systems which will be used in the problem description. Conventional right-handed coordinate systems are employed for the problem description.

1. Coordinate Systems

At the instant the airborne missile is launched from its carrier aircraft, an inertial coordinate system is established with its origin at the center of mass of the missile, with x-axis and y-axis in the horizontal plane and z-axis vertical. The positive x-axis is in the original direction of travel for the missile, the z-axis is positive downward, and the y-axis completes the right-handed system. This is the base coordinate system for all conversions.

As the missile moves away from the point of launch, a set of missile body axes moves with the missile. This set of axes has an origin always at the center of mass of the missile, the x-axis is the missile longitudinal axis with the positive direction forward, the y-axis is in the plane of the missile wings with the positive direction out the right wing, and the z-axis completes the right-handed system. The missile body axes coincide with the inertial axes at the instant of launch, but then the body axes translate and rotate with the missile whereas the inertial axes remain fixed. The missile position and orientation are described in terms of the relationship between the inertial axes and the missile body axes.

In a manner similar to the missile body axes, a set of

target body axes is established with origin at the center of mass of the target, the x-axis is the longitudinal axis of the target with the positive direction forward, the y-axis is in the plane of the wings with the positive direction out the right wing of the target, and the z-axis completes the right-handed system. The target body axes directions rarely coincide with the missile inertial axes directions established at the instant of launch. The target orientation is therefore described in terms of the relationship between the inertial axes and the target body axes.

Figure 1 provides pictorial representation of the above information for a number of air-to-air engagements.

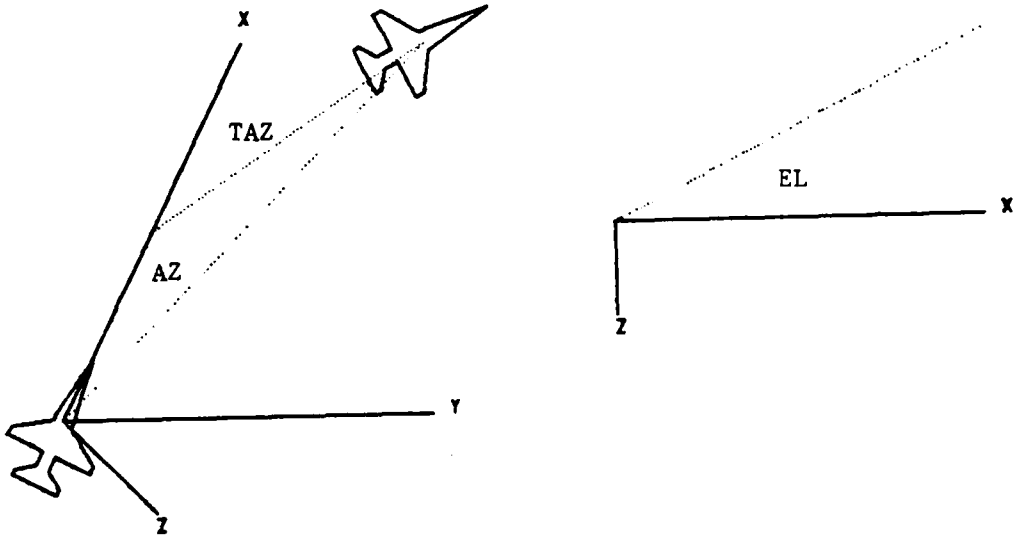

Figure 1. Engagement Geometry Definitions

2. Missile Model

The missile model used in the simulation represents a generic bank-to-turn missile. This is a highly maneuverable, short range, air-to-air missile which employs short aerodynamic surfaces (wings) to produce large aerodynamic forces in a plane perpendicular to the wings to effect a turn. This means that a turning maneuver by the missile requires banking the missile to orient the plane of the aerodynamic force and then generating the aerodynamic force to cause the turn. This leads to the common designator of bank-to-turn for this category of missiles. This type of missile is capable of generating large turning accelerations for maneuvers (in excess of 100 Gs at moderate angles of attack), and care must be exercised or the structural limits of the missile will be exceeded. In this phase of the study, an autopilot furnished by the USAF Armament Laboratory, Eglin AFB, Florida, was used to transform the commands from the guidance system to the appropriate bank-to-turn maneuver for the missile. The missile is launched from the carrier aircraft and guidance commands are ignored for the first half-second to allow the missile to clear the carrier aircraft. Guidance commands are then obeyed as dictated by the guidance system. The fuel on board the missile lasts for approximately two and one-half seconds.

Following the thrusting phase, the missile follows a ballistic trajectory utilizing the bank-to-turn capability to attain the target. Sensors on board the missile consist of rate gyros and accelerometers to detect the linear and angular accelerations of the missile, but these sensors provide noisy information.

Additionally, the missile has a sensing system for detecting the target. A passive sensor system consisting of

an infrared seeker is used to provide angular position data for the target relative to the missile. Angular rate data was not used for this study. This passive seeker does not provide information directly usable by the guidance system, so an estimation process must be employed to extract the desired information. An active seeker (one which provides range data in addition to angular data) would make the estimation process much more accurate, but the study was restricted to use of the passive seeker, as the use of the active seeker was prohibitive in both weight and cost.

3. Target Model

The target used in this report is a "smart" target which employs an evasive maneuver in an attempt to escape the incoming airborne missile. The target maintains a constant speed and heading until the missile is within 6000 feet. At this time, the target begins a 9-G acceleration maneuver in a direction dictated by the engagement geometry. This maneuver is continued until the missile is within 1000 feet. At this time, the target executes a "last chance" maneuver consisting of a 9-G acceleration vertically downward. This evasive maneuver has been tested by research at Eglin AFB and determined to be the type of maneuver which exercises the estimation and guidance algorithms in the maximum for the engagements studied.

Target aerodynamics are not modeled in this study as that would restrict the validity of the study to the type of target used in the model. Instead, the target is modeled as a rigid body whose original orientation is specified by the target body axes orientation. The target velocity vector is along the target body x-axis, and the evasive maneuver acceleration is along the target body z-axis. Due to the short time periods involved in these air-to-air combat

engagements, the target thrust acceleration may be ignored, and the evasive acceleration is obtained from aerodynamic forces acting upon the target. The 9-G evasive acceleration was chosen as a typical structural limit and may be changed in the simulation if so desired.

SECTION III

MATHEMATICAL DEVELOPMENT

This section of the report describes the development of the differential equations of motion utilized in the problem development. In addition, the equations relating the measured quantities obtained from the sensors to the quantities needed by the guidance system are provided.

1. State Equation

The state vector differential equation of motion for an airborne missile pursuing an airborne target can be expressed in a number of different ways. One possible means of expression is in terms of the target inertial state vector consisting of target position, velocity, and acceleration quantities, and the missile inertial state vector consisting of missile position, velocity, and acceleration quantities. This provides a total of 18 quantities to be determined. Choosing the missile acceleration vector as the control to be specified reduces the number to 15 quantities to be determined. The guidance system requires full knowledge of the state vectors, so the estimation process would have to furnish 15 quantities from its input sensor information (2 angular measurements). In order to reduce the dimensionality of the estimation process, note that the missile guidance system is trying to reduce the distance between the target and the missile to a minimum. This does not require the inertial position of the missile and the target, but the relative position of the target to the missile. Also, the inertial velocity of the target and missile are not required, but the velocity of the target relative to the missile is required. Lastly, the

inertial acceleration of the target and the missile could be replaced by the relative acceleration of the target to the missile. This last replacement is not needed as the inertial acceleration of the missile is the control quantity which will be specified to produce the state quantities. Replacing the target inertial acceleration with the target relative acceleration does not reduce the dimensionality of the problem. Use of the relative position and velocity of the target and the inertial acceleration of the target provides a problem state vector with nine quantities to be determined along with three control quantities (the missile inertial acceleration) to be specified.

All vectors in the following developments are expressed in terms of components along the inertial axes which were established at the instant of missile launch. Let $\underline{R}$ denote position vector, $\underline{V}$ denote velocity vector, $\underline{A}$ denote acceleration vector, and $\underline{J}$ denote the jerk vector (time derivative of acceleration vector). Let subscript "T" denote target inertial quantities, subscript "M" denote missile inertial quantities, and subscript "R" denote target quantities relative to the missile. Once these symbols have been defined, the following equations governing the problem state variables may be written.

$$\dot{\underline{R}}_R = \underline{V}_T - \underline{V}_M = \underline{V}_R$$

$$\dot{\underline{V}}_R = \underline{A}_T - \underline{A}_M$$

$$\dot{\underline{A}}_T = \underline{J}_T$$

In order to continue with the mathematical description of the problem, the time derivative of the target inertial acceleration must be examined. If a non-zero value is used for this term, then these equations would imply

foreknowledge of the target's actions, whereas these actions could be totally random and not describable by differential equations at all. However, an assumption can be made concerning the time correlation of the target acceleration (a random variable). The success of this practice for this particular problem did not warrant using an assumed correlation function for target acceleration with the attendant complexity. Therefore, the time derivative of the target acceleration should be set equal to zero. This action does not preclude target acceleration but assumes that the target acceleration is constant. If the target acceleration is indeed changing, then it becomes the task of the estimation process to adapt to the new acceleration as rapidly as possible.

Again, using the inertial axes established at the instant of missile launch, define the inertial components of the nine-element state vector for the problem in the following manner.

X1 = target position relative to missile along x-axis
X2 = target velocity relative to missile along x-axis
X3 = target inertial acceleration along x-axis
Y1 = target position relative to missile along y-axis
Y2 = target velocity relative to missile along y-axis
Y3 = target inertial acceleration along y-axis
Z1 = target position relative to missile along z-axis
Z2 = target velocity relative to missile along z-axis
Z3 = target inertial acceleration along z-axis

In a similar way, define the three-element control vector for this problem in the following manner.

U1 = missile inertial acceleration along x-axis
U2 = missile inertial acceleration along y-axis
U3 = missile inertial acceleration along z-axis

With the state vector elements and the control vector elements defined, the nine scalar differential equations of motion for this problem may be written in the following manner.

$$\dot{X}1 = X2$$
$$\dot{X}2 = X3 - U1$$
$$\dot{X}3 = 0$$
$$\dot{Y}1 = Y2$$
$$\dot{Y}2 = Y3 - U2$$
$$\dot{Y}3 = 0$$
$$\dot{Z}1 = Z2$$
$$\dot{Z}2 = Z3 - U3$$
$$\dot{Z}3 = 0$$

The state variable differential equations of motion may now be written in the standard linear equation format as follows.

$$\dot{X} = A\,X + B\,U$$

Where:

$$X' = [\,X1, X2, X3, Y1, Y2, Y3, Z1, Z2, Z3\,]$$

$$U' = [\,U1, U2, U3\,]$$

$$A = \begin{bmatrix} 0 & 1 & 0 & 0 & 0 & 0 & 0 & 0 & 0 \\ 0 & 0 & 1 & 0 & 0 & 0 & 0 & 0 & 0 \\ 0 & 0 & 0 & 0 & 0 & 0 & 0 & 0 & 0 \\ 0 & 0 & 0 & 0 & 1 & 0 & 0 & 0 & 0 \\ 0 & 0 & 0 & 0 & 0 & 1 & 0 & 0 & 0 \\ 0 & 0 & 0 & 0 & 0 & 0 & 0 & 0 & 0 \\ 0 & 0 & 0 & 0 & 0 & 0 & 0 & 1 & 0 \\ 0 & 0 & 0 & 0 & 0 & 0 & 0 & 0 & 1 \\ 0 & 0 & 0 & 0 & 0 & 0 & 0 & 0 & 0 \end{bmatrix} \quad : \quad B = \begin{bmatrix} 0 & 0 & 0 \\ -1 & 0 & 0 \\ 0 & 0 & 0 \\ 0 & 0 & 0 \\ 0 & -1 & 0 \\ 0 & 0 & 0 \\ 0 & 0 & 0 \\ 0 & 0 & -1 \\ 0 & 0 & 0 \end{bmatrix}$$

Note the natural division of the full nine-state differential equation into three independent three-state differential equations.

$$\dot{X} = A1\ X + B1\ U1$$

$$\dot{Y} = A2\ Y + B2\ U2$$

$$\dot{Z} = A3\ Z + B3\ U3$$

Where:

$$X' = [\ X1, X2, X3\ ]$$

$$Y' = [\ Y1, Y2, Y3\ ]$$

$$Z' = [\ Z1, Z2, Z3\ ]$$

$$A1 = A2 = A3 = \begin{bmatrix} 0 & 1 & 0 \\ 0 & 0 & 1 \\ 0 & 0 & 0 \end{bmatrix}$$

$$B1 = B2 = B3 = \begin{bmatrix} 0 \\ -1 \\ 0 \end{bmatrix}$$

The state variable differential equations are now in the standard form of linear differential equations with constant coefficients whether the standard form refers to the full nine-state system or to one of the three independent three-state systems. The state differential equation is a linear, non-homogenous, vector differential equation with constant coefficients and standard solution techniques involving the state transition matrix may be applied. Refer to Appendix A for a review of this solution technique.

2. Measurement Equations

The measurements by which the missile control system relates to the real world consist of two angular measurements made by the passive seeker on board the missile. From the discussion on the coordinate systems used

in this problem, remember that an inertial coordinate system is established at the instant of launch. If the seeker is an inertial platform initialized at launch with measurements made in the inertial axes, then the angles are exactly the ones needed for this development. If the seeker is a "strapdown seeker" where the measurements are made in body axes, then a transformation to the inertial axes is necessary. The following development assumes that the angular measurements are made in the inertial axes.

The angular measurements are made by an infrared "heat seeker" on board the missile which provides the angles defining the line-of-sight (LOS) direction from the missile to the target. This direction is specified by two angles--the azimuth angle which is measured in the horizontal plane, and the elevation angle which is measured in the vertical plane. Figure 1 provides a pictorial definition of these two angles. The relationship between the state variables (relative position, relative velocity, and target inertial acceleration) and the angular measurements (inertial azimuth angle and inertial elevation angle) are given by the following equations.

$$\text{Tan}(AZ) = YI / XI$$

$$\text{Tan}(EL) = - ZI / (XI^2 + YI^2)^{.5}$$

Where:

AZ is the current LOS inertial azimuth angle

EL is the current LOS inertial elevation angle

XI is the relative position along the inertial x-axis

YI is the relative position along the inertial y-axis

ZI is the relative position along the inertial z-axis

3. Problem Definition Angles

In addition to the measurement angles which are used

in the estimation algorithm to establish the relationship between the estimated states and the actual states, there exists a set of angles which are used to identify the particular problem geometry. These angles are the angle in the horizontal plane defining the original direction of the line-of-sight from the carrier aircraft to the target aircraft (the off-boresight angle), and the angle in the horizontal plane defining the original direction of travel for the target aircraft (the target aspect angle). As the problem is extended to different altitudes for the initial positions of the carrier aircraft and the target aircraft, two more angles will become necessary. For the co-altitude engagement, the off-boresight angle and the target aspect angle are sufficient to specify the engagement.

These angles are shown on Figure 1 where:

TAZ is the original target velocity direction

TOB is the original line-of-sight direction

SECTION IV

ESTIMATION ERROR ANALYSIS

The Kalman filter is an optimal estimation process for a totally linear system, but the extended Kalman filter and its derivatives are suboptimal when applied to nonlinear systems. If the propagation equation for the state estimate is known exactly , then the initial uncertainty indicated by the initial value of the state estimation error covariance matrix will soon decay to a small or zero value. If the state propagation equation is not known exactly, then the value of the state process noise covariance matrix will determine if the state estimation error covariance will decrease or increase as the state is propagated forward in time.

The common tendency on all of the estimation algorithms tested was for an initial increase in the state estimation error covariance during the period that the target was furtherest from the missile, followed by a rapid convergence toward zero as the missile nears the target and the measurement changes become large in comparison to the initial measurement changes.

This section of the report will discuss the four types of estimation algorithms which were tested and the five types of air-to-air combat engagements which were studied to analyze the performance of the filters. Results will be produced which will show the time histories of the position error, the velocity error, and the acceleration error for each engagement and for each filter.

Table 1 identifies the individual filters by number and Table 2 identifies the engagements by number.

TABLE 1. FILTER IDENTIFICATION NUMBERS

FILTER NUMBER	FILTER NAME
1	EXTENDED KALMAN FILTER
2	ADAPTIVE KALMAN FILTER
3	ADAPTIVE TIME WEIGHTED KALMAN FILTER
4	ITERATIVE KALMAN FILTER (3 ITERATIONS)

TABLE 2. ENGAGEMENT IDENTIFICATION NUMBERS

ENGAGEMENT (num)	RANGE (ft)	ASPECT (deg)	OFF-BORESIGHT (deg)
1	13000	90	0
2	8000	0	0
3	11000	90	40
4	3000	135	0
5	3500	135	40

1. Filter Comparisons

This section of the report will present a comparison of the four filters for each engagement. The initial engagement geometry is depicted by the first figure of each group, followed by the time histories of the position estimation error, the velocity estimation error, and the acceleration estimation error. In each case, the error is calculated by subtracting the true value of the quantity (taken from the simulation) from the estimated value of the quantity. Note that the position refers to the position of the target relative to the missile, the velocity refers to the velocity of the target relative to the missile, and the acceleration refers to the absolute acceleration of the

target. A final comparison of the filter performance in tabular form will complete the analysis.

a. Engagement 1

The initial problem geometry for engagement 1 is presented in Figure 2. The carrier aircraft is flying northward at a speed of Mach = 0.9 at an altitude of 10,000 feet when the missile is launched. The target aircraft is located directly ahead of the carrier aircraft at the same altitude and a range of 13,000 feet at launch, but is traveling eastward at a speed of Mach = 0.9.

The estimation algorithm is initialized with the correct state values as these are available from the carrier aircraft. As we note on Figure 3, the position error is very small for filter 1 until the missile thrust is cut off at approximately 2.5 seconds. After this time, there is a moderate buildup of position estimation error until the target aircraft begins an escape maneuver at approximately 3.5 seconds. The position estimation error rapidly increases due to the inability of the regular extended Kalman filter to track rapidly changing parameters. As the position estimation error progresses to a peak value, the missile is drawing nearer to the target, so the measurements are becoming more usable in the estimator. This is reflected by a decrease in the estimation error between 5 and 6 seconds. Just after 6 seconds, the target aircraft begins its final maneuver as reflected by a rise in the position estimation error. The missile is within 1000 feet of the target at this time, so the aircraft maneuver is very influential upon the estimation algorithm through large changes in the measurements. The estimation algorithm reacts to this good data by rapidly converging toward the true position with the estimated position. The final miss

distance is 5.23 feet even though the estimated miss is much greater than this. A characteristic of all of these maneuvers is that the estimation algorithm will produce an acceptable miss distance as long as it overestimates the time-to-go.

From Figure 3, the velocity estimation error closely follows the characteristics of the position estimation error until the last second of the trajectory. During the last second, the model must make some drastic changes in order to accommodate the measurements it is receiving. The way that the position error is decreased is by a large change in the model velocity. This leads to an increase in the velocity estimate error which can be appreciable near the end of the trajectory.

From Figure 4, the acceleration estimation error follows the velocity estimation error characteristics as it should since the position, velocity, and acceleration are related through the model.

Figure 5 presents the position estimation error for filter 2, an adaptive extended Kalman filter which uses 20 measurements to produce the sample measurement noise characteristics. One important item to note is that the scale of the position estimation error plot is different for this filter from that of filter 1. Due to the smaller sample, the local noise characteristics are used instead of the global noise characteristics. This allows filter 2 to adjust more rapidly to changing conditions than could filter 1. This fact is apparent in the narrow shape of the position estimate error plot indicating rapid adjustment and in the lowered peak error. In a similar fashion, the velocity estimate error plot and the acceleration estimate error plot filter 2 have reduced values from those of filter 1. The final miss distance filter 2 is 4.47 feet, not a drastic improvement, but the performance (as measured by

miss distance) of filter 1 was pretty good. If the filter performance all along the trajectory is compared, then filter 2 is an obvious improvement over filter 1.

The use of local noise characteristics instead of global characteristics provides an increase in overall filter performance due to the ability of the filter to react rapidly to changing conditions. Filter 3 was created especially to decrease the time required for the filter to adjust to changing conditions. Filter 2 weighted each of the measurements equally in obtaining noise characteristics from the sample. For 20 measurements in the sample window, this means a weight of 19/20 for the previous measurement statistics and a weight of 1/20 for the latest measurement. In an attempt to place more weight on the latest measurement, the weighting was changed to 4/5 for the previous measurement statistics and 1/5 for the current measurement. This represents a fourfold increase in the importance of the latest measurement over that of filter 2.

Figure 7, the position estimate error plot for filter 3, is a very convincing argument for the merit of this idea. Notice once again that the plot scale has changed, and that the plot width (indicating response time) has become very narrow. Peak error on this plot was about one-fourth of the peak error of the corresponding plot for filter 1 and about one-third of the peak error of the corresponding plot for filter 2. Both velocity estimate error and acceleration estimate error filter 3 are smaller than those of filter 1 or 2. This filter does such a good job all along the trajectory that it is no surprise that the final miss distance is only 2.19 feet. Note that if miss distance is the only comparison criterion, then all of the estimation filters provide comparable performance. The use of the error time history allows one to make a more telling comparison. Finally, other weighting was tried, but the

weighting given above provided the best balance of rapid adjustment with small overshoot.

Aesthetically, filter 4, the iterated extended Kalman filter, is very pleasing in that it should yield performance improvement on each iteration. This has not been the case in that the filter diverges for a large number of iterations. This filter is still undergoing evaluation but will be presented here for comparison purposes. The filter performance and final miss distance are comparable to those of the regular extended Kalman filter of filter 1. The smoothing of the peaks and valleys in the error plots points out the potentiality of this technique. More work is being done to improve the performance of the filter, and it is hoped that this filter will compare favorably to filter 3 in the end. Figures 12, 13, and 14 are the error plots for this filter for engagement 1.

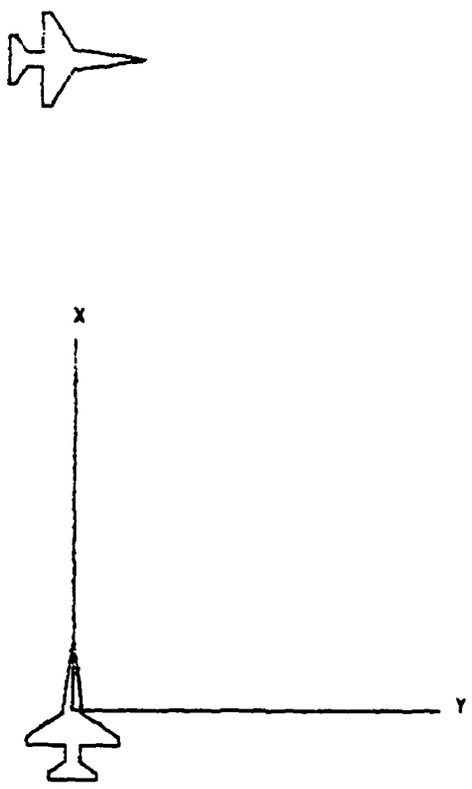

Figure 2. Engagement 1 Geometry

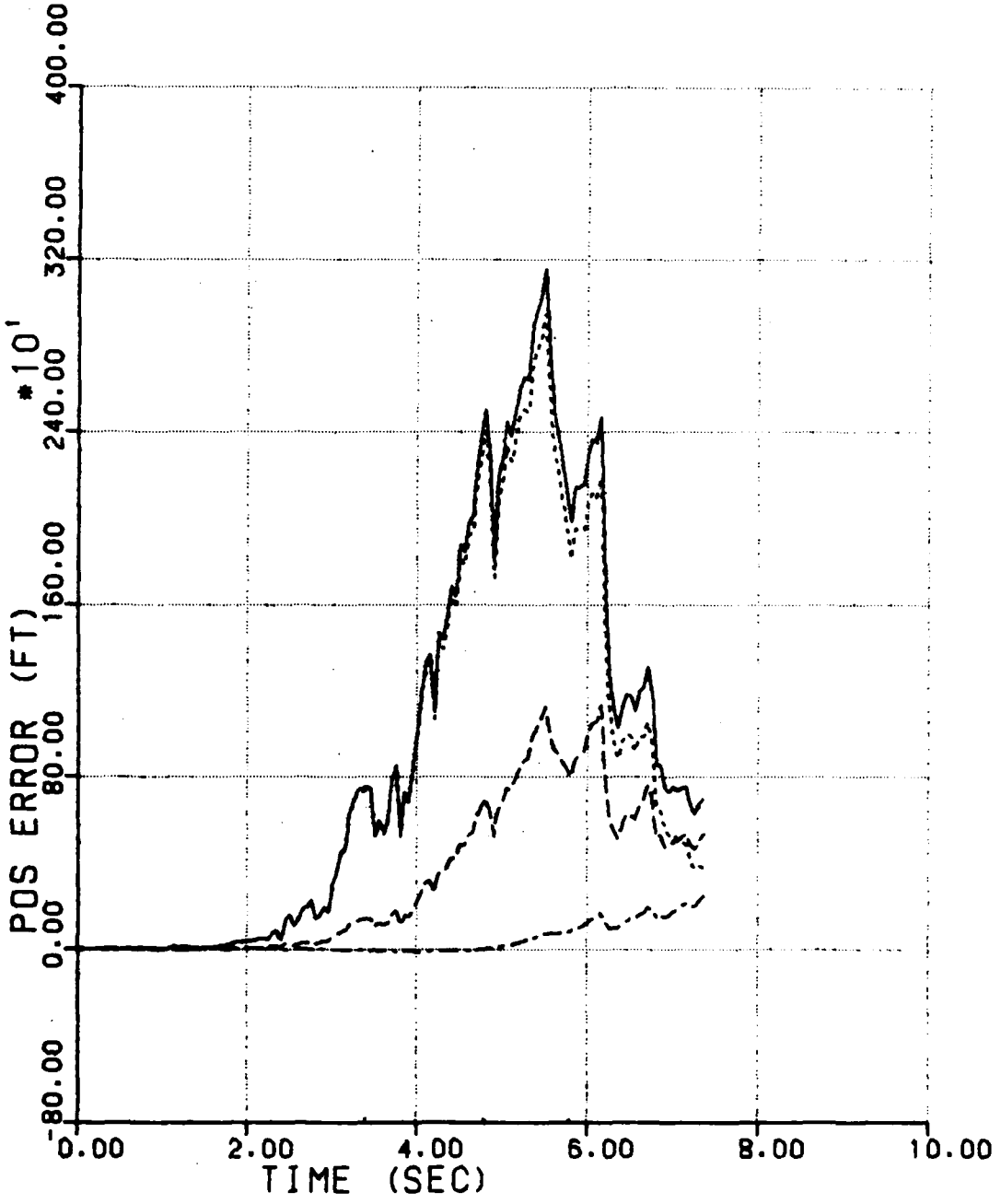

Figure 3. Position Error History for Engagement 1, Filter 1

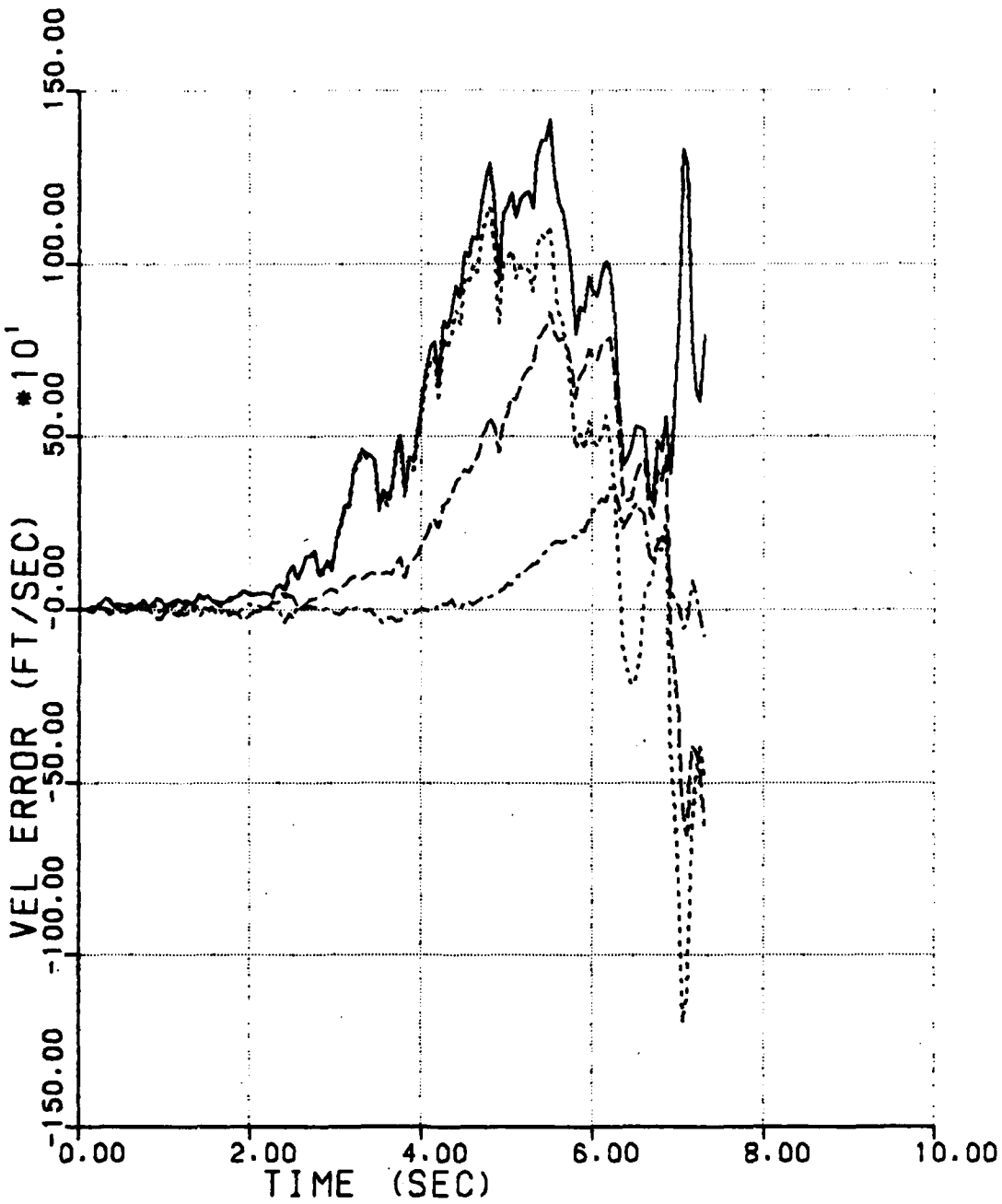

Figure 4. Velocity Error History for Engagement 1, Filter 1

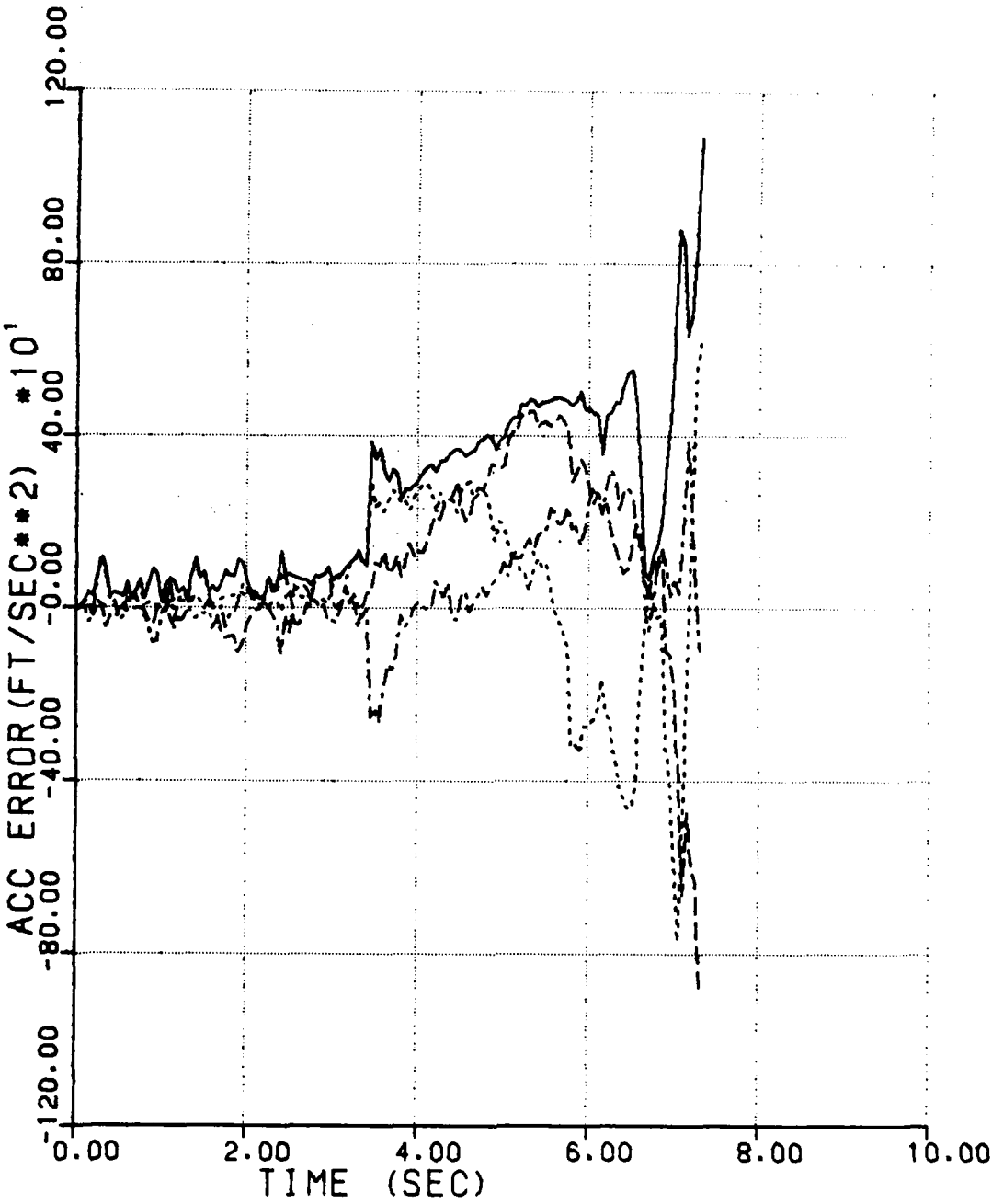

Figure 5. Acceleration Error History for Engagement 1, Filter 1

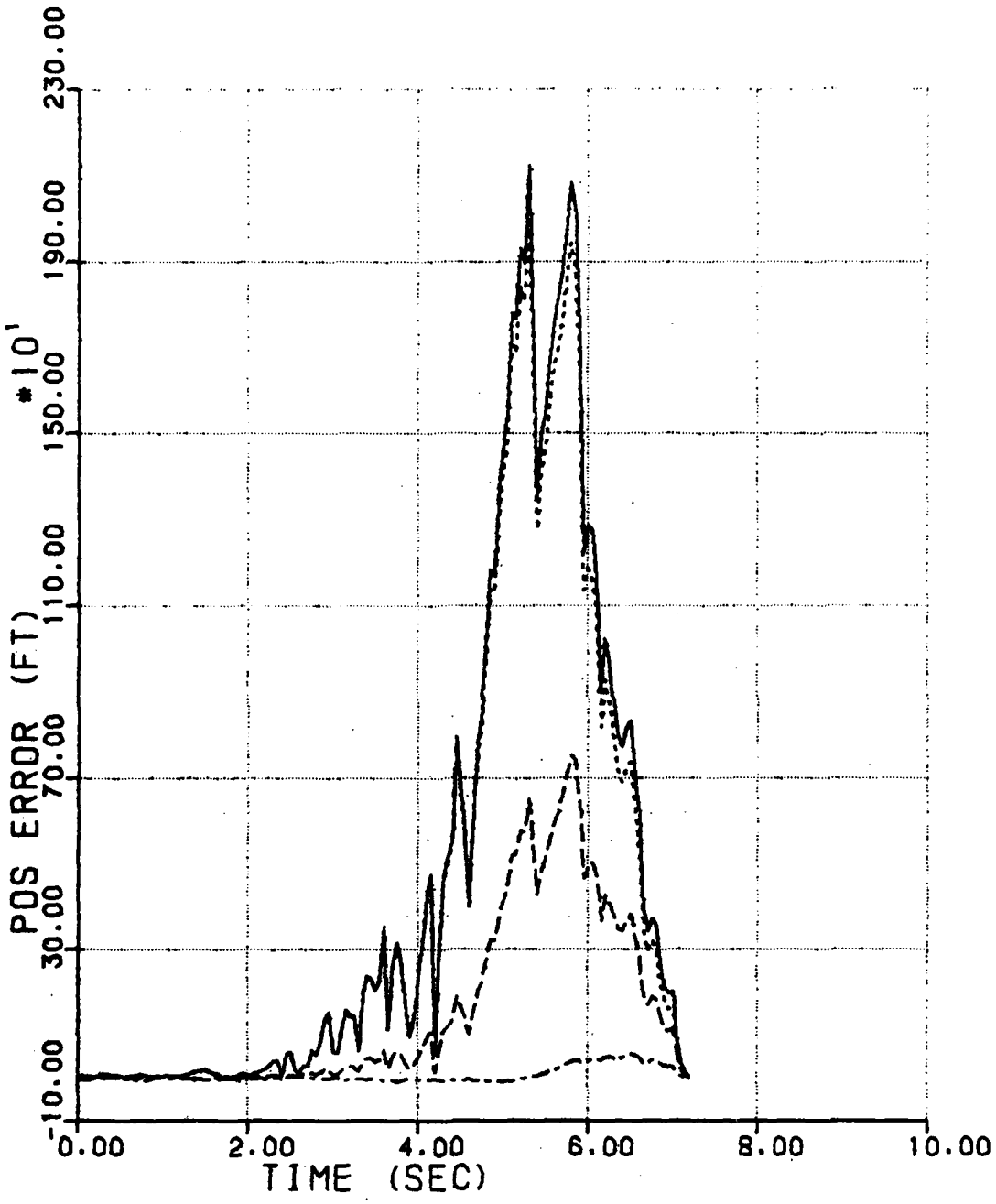

Figure 6. Position Error History for Engagement 1, Filter 2

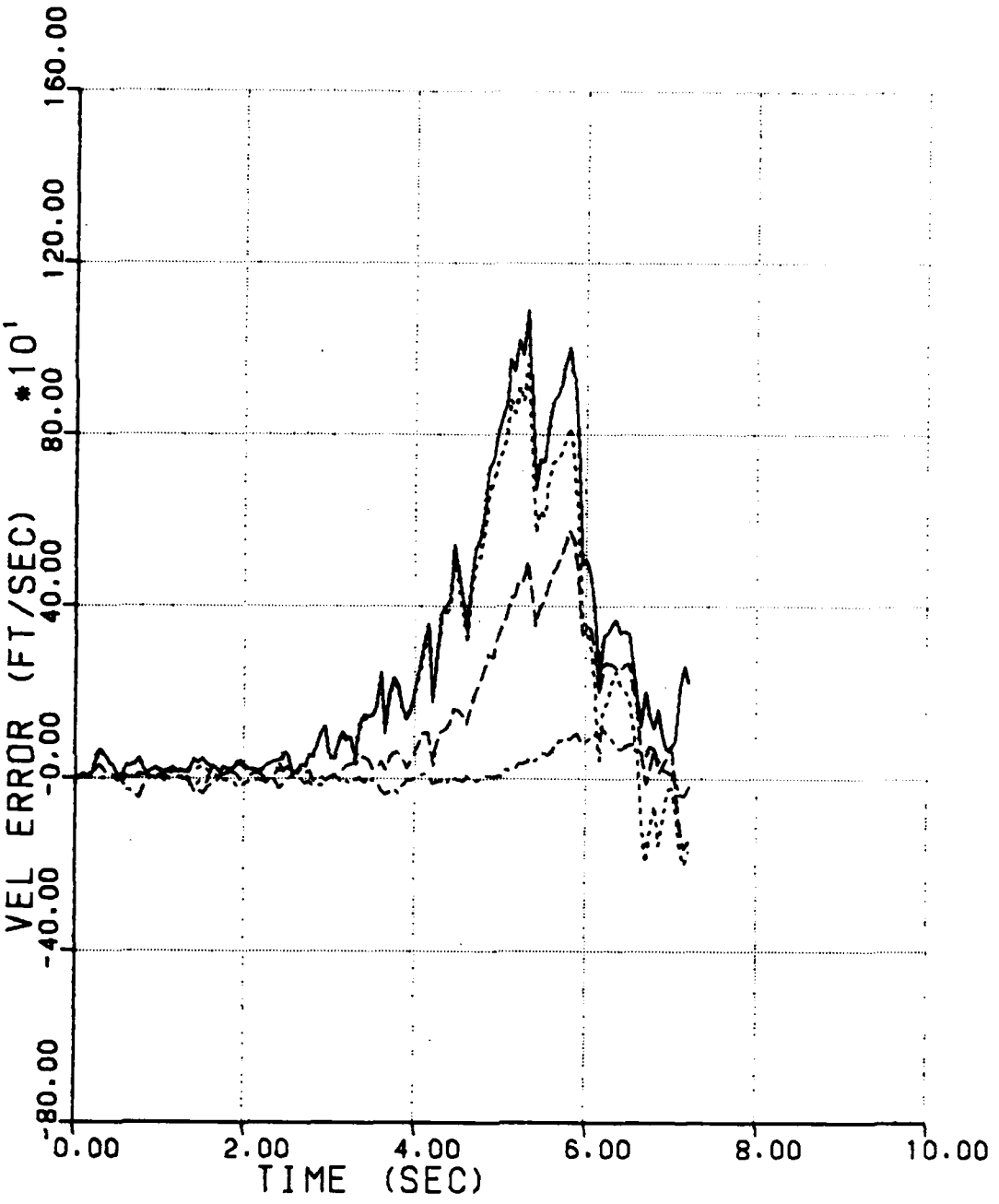

Figure 7. Velocity Error History for Engagement 1, Filter 2

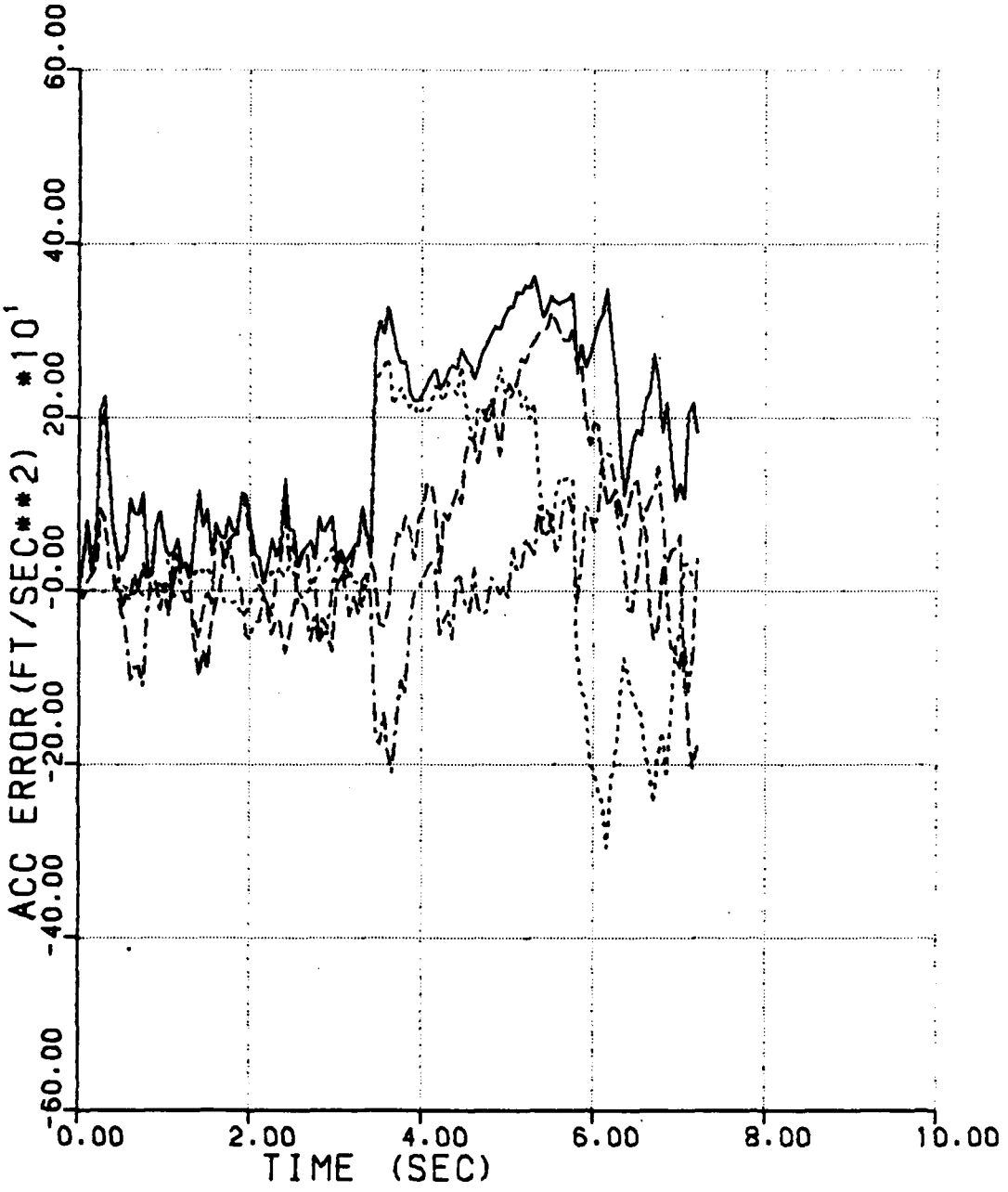

Figure 8. Acceleration Error History for Engagement 1, Filter 2

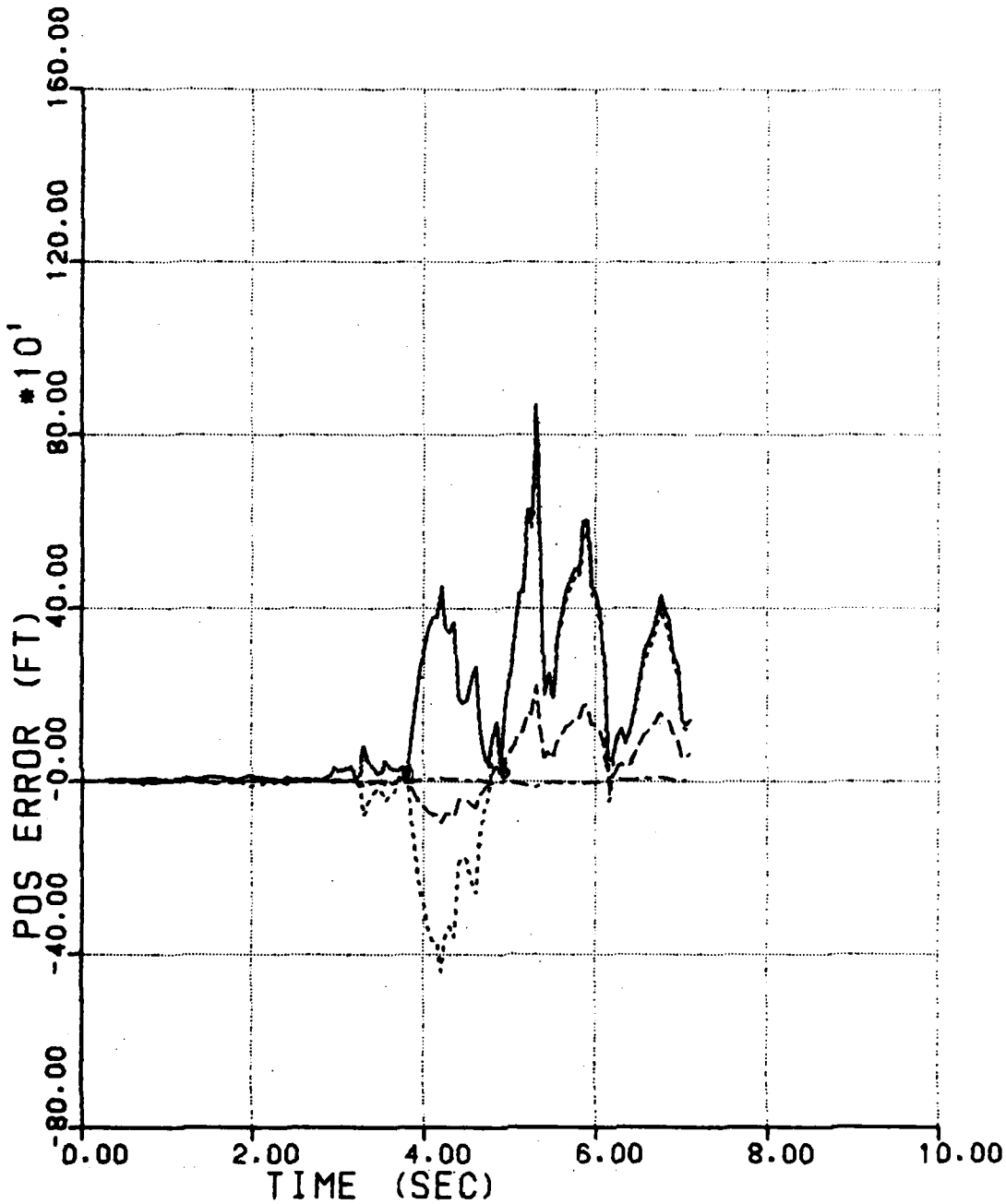

Figure 9. Position Error History for Engagement 1, Filter 3

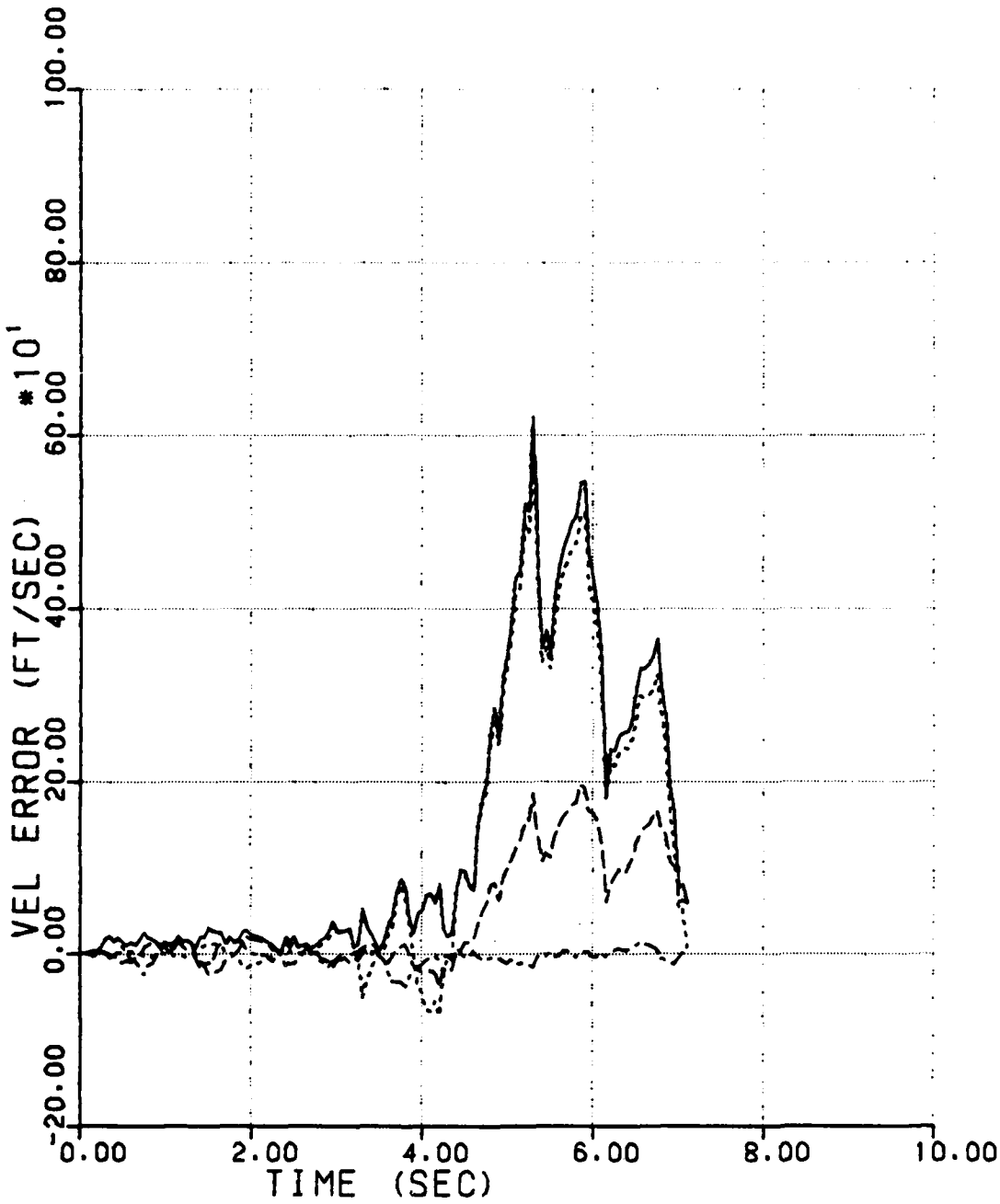

Figure 10. Velocity Error History for Engagement 1, Filter 3

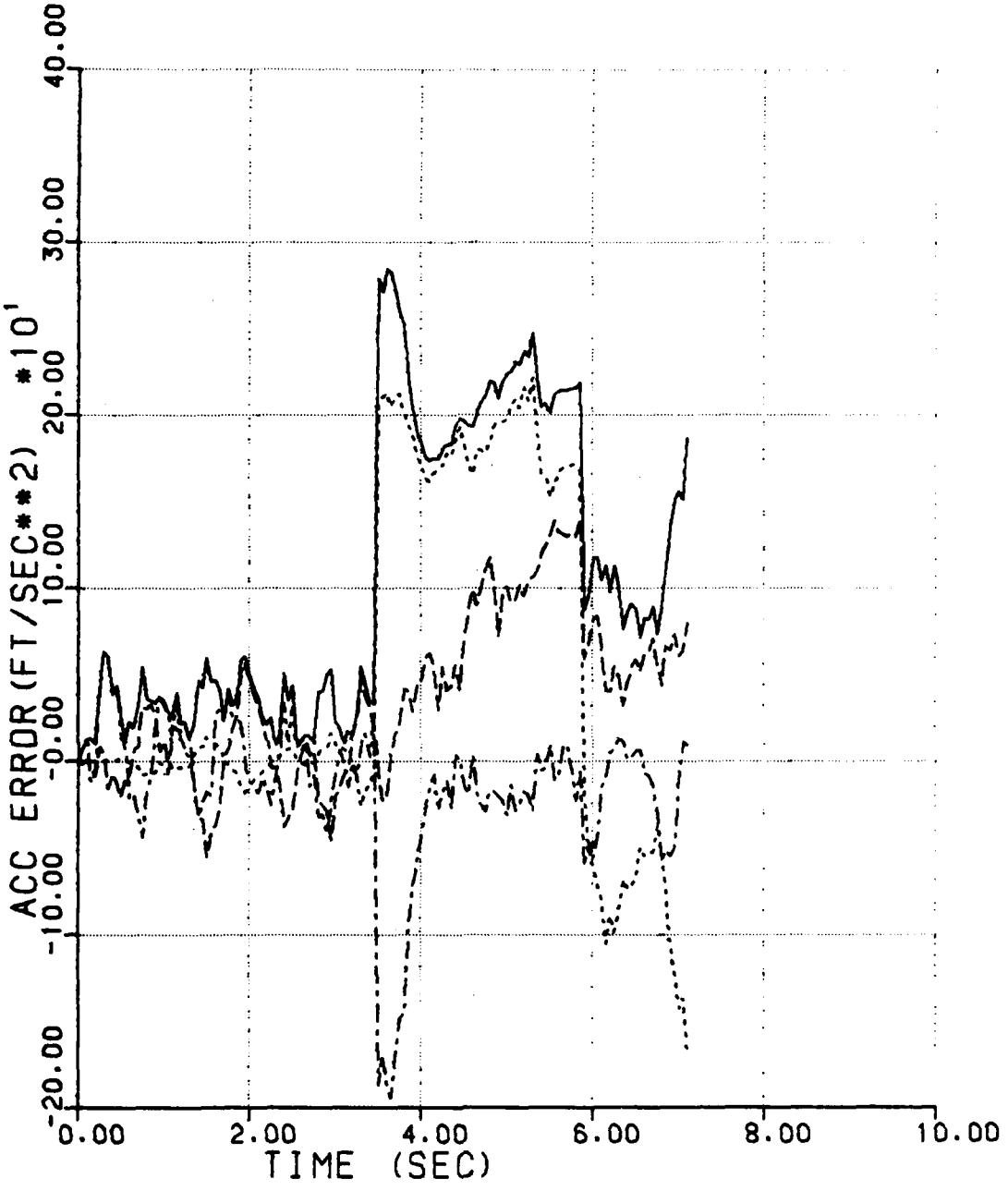

Figure 11. Acceleration Error History for Engagement 1, Filter 3

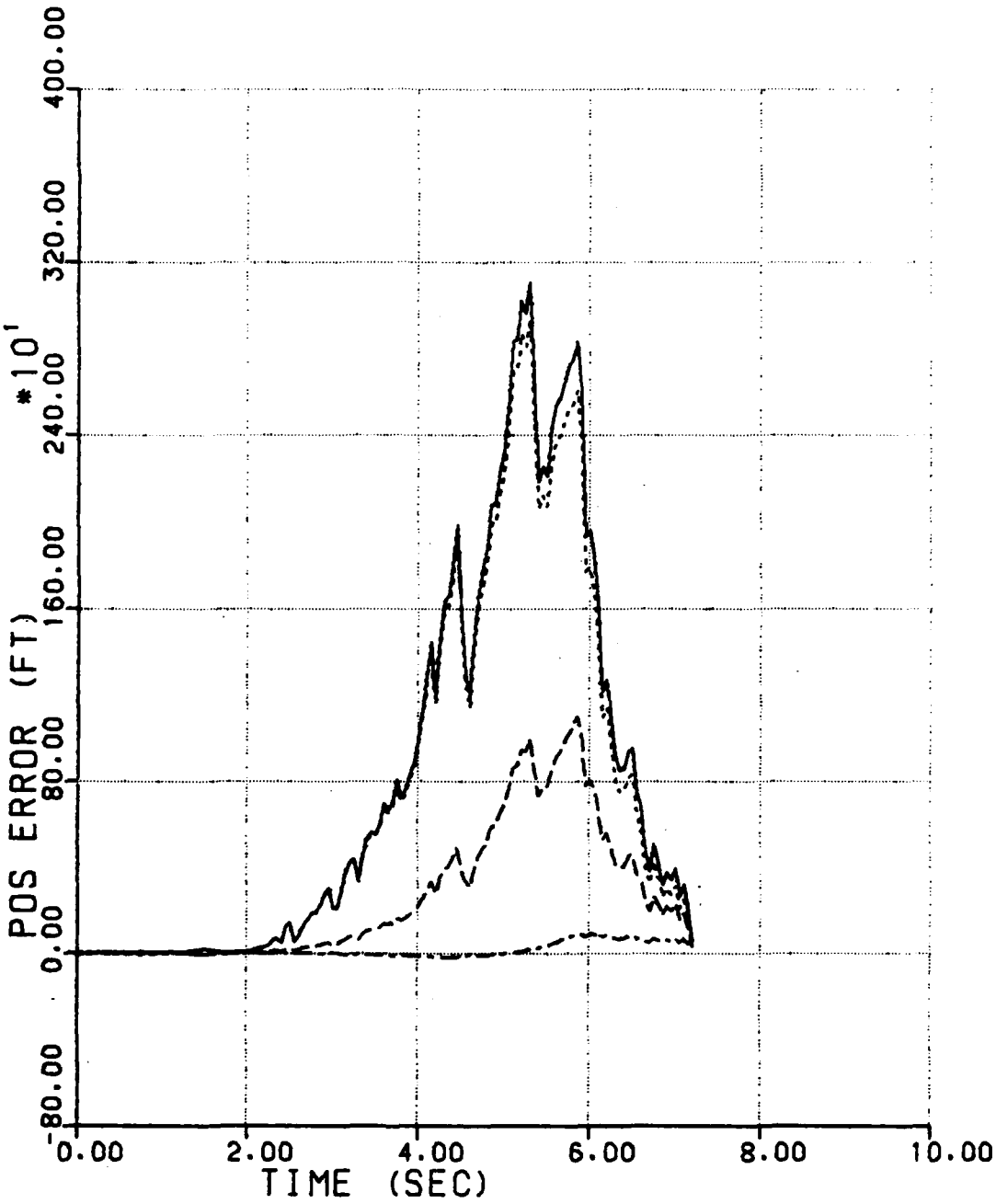

Figure 12. Position Error History for Engagement 1, Filter 4

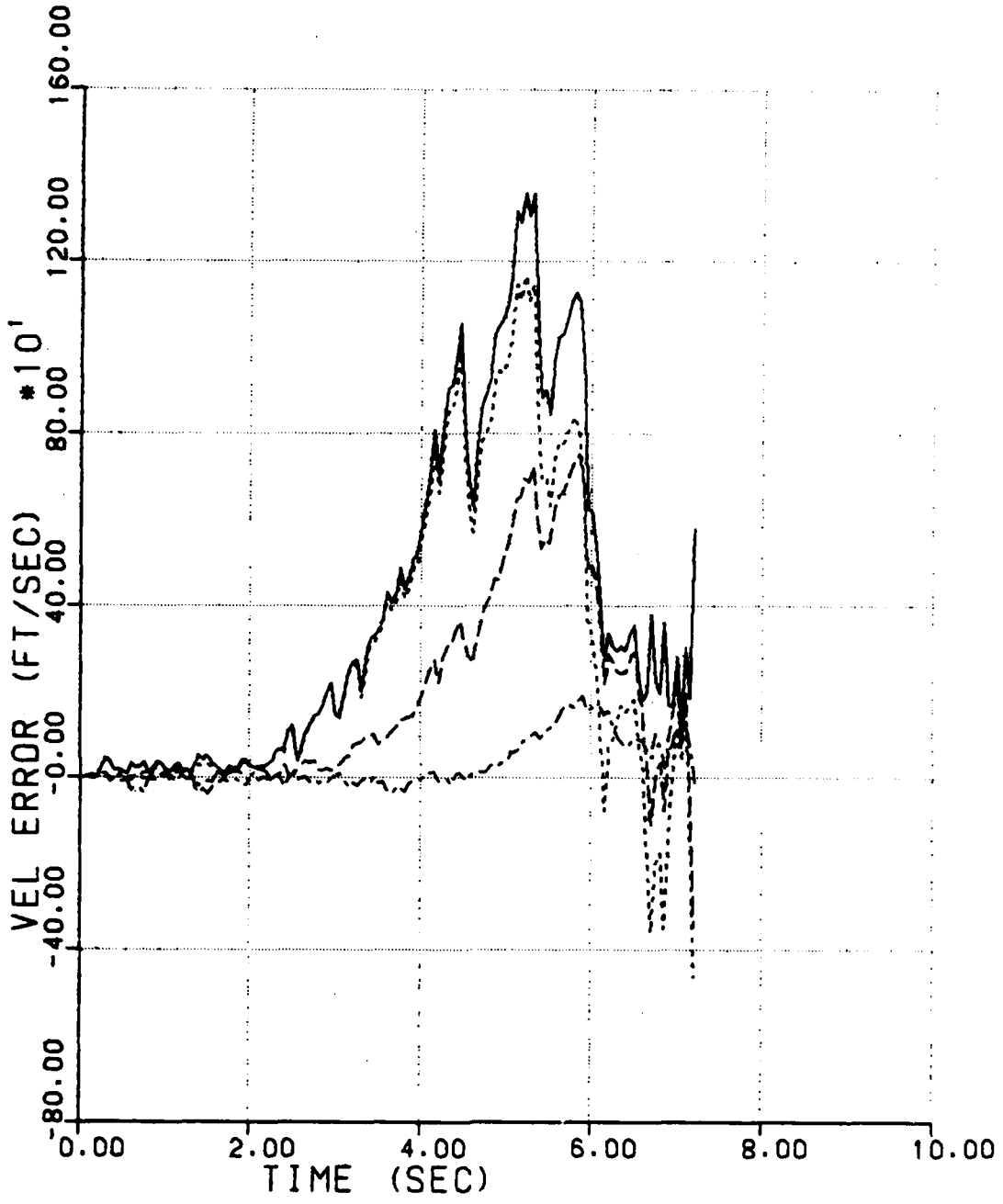

Figure 13. Velocity Error History for Engagement 1, Filter 4

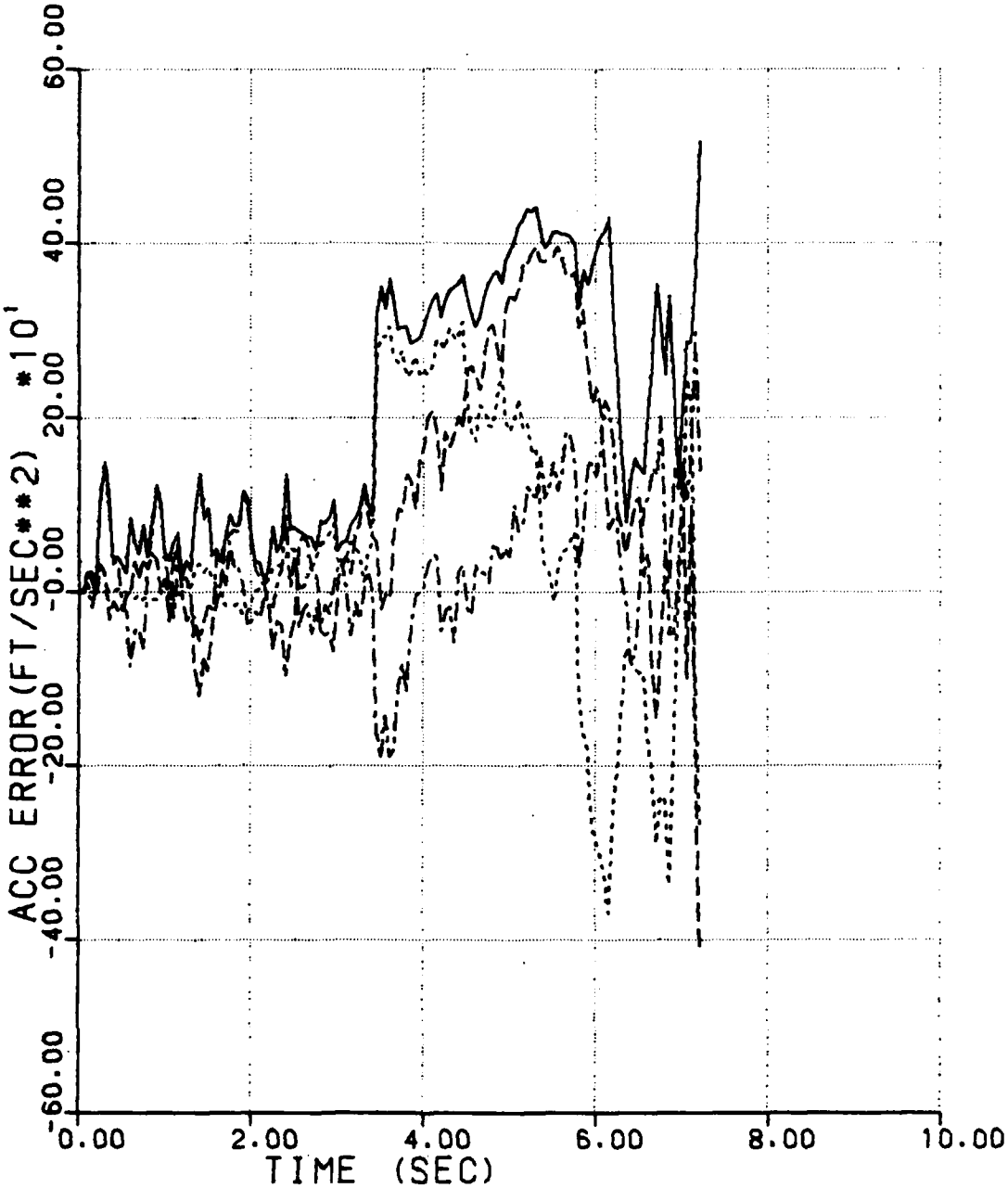

Figure 14. Acceleration Error History for Engagement 1, Filter 4

b. Engagement 2

The initial problem geometry for engagement 2 is given in Figure 15. The carrier aircraft is flying northward at an altitude of 10,000 feet and a speed of Mach = 0.9. The target aircraft is directly ahead of the carrier aircraft at the same altitude and at a range of 8000 feet. The target aircraft is flying northward at a speed of Mach = 0.9.

The performance for each of the filters is similar to that of engagement 1 with the notable exception of filter 3. The use of the time-weighting in combination with the adaptive feature allows this filter to improve its performance such that the maximum position error for engagement 2 is one-half of the maximum position error of engagement 1. This reduction is especially notable when the performance of the other filters is similar for both engagements. Figures 16 through 27 provide the time history error plots for position estimate, velocity estimate, and acceleration estimate for this engagement.

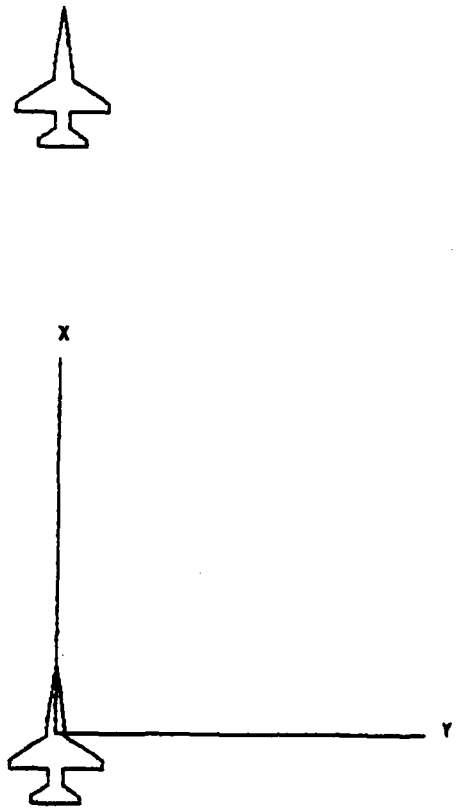

Figure 15. Engagement 2 Geometry

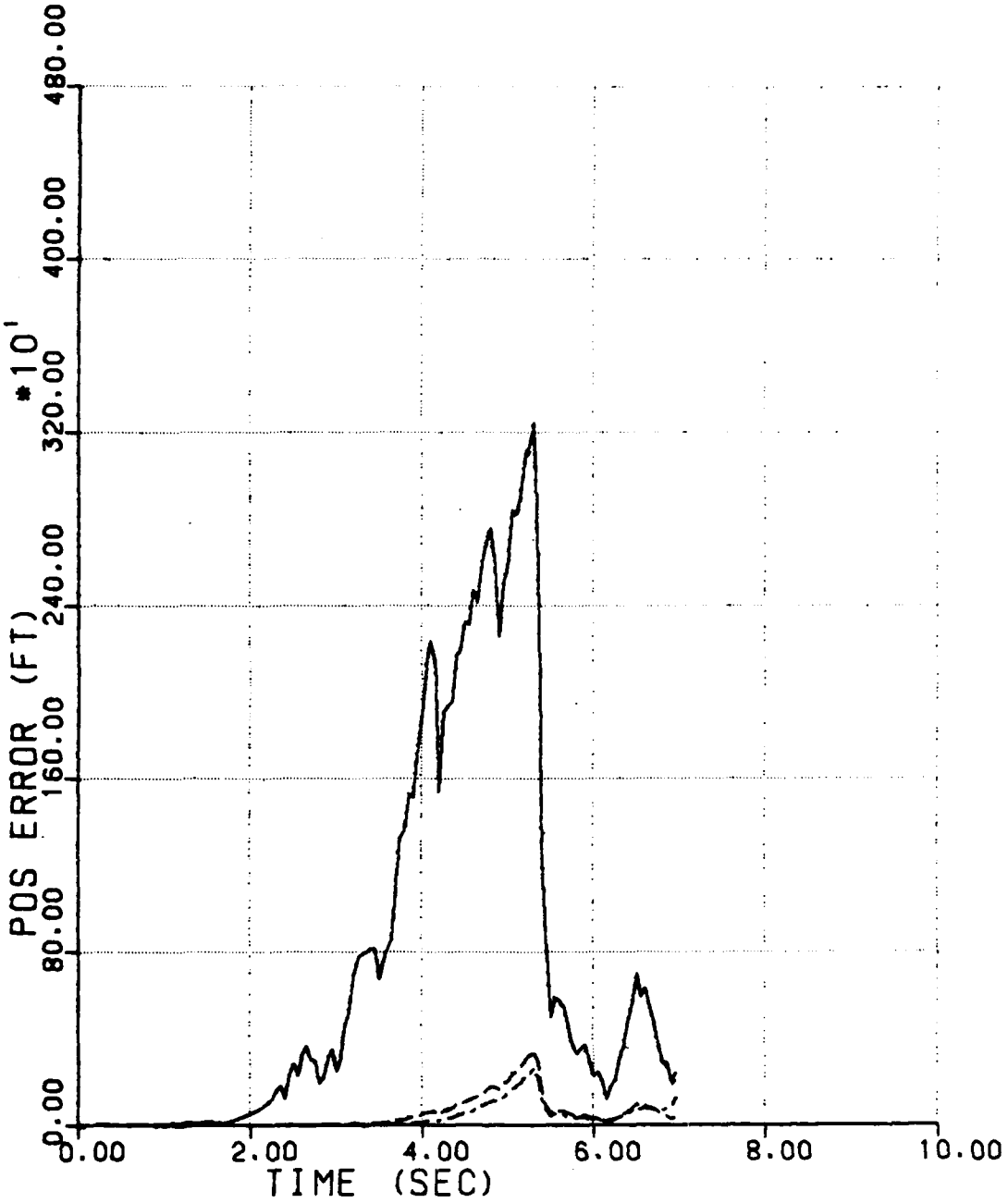

Figure 16. Position Error History for Engagement 2, Filter 1

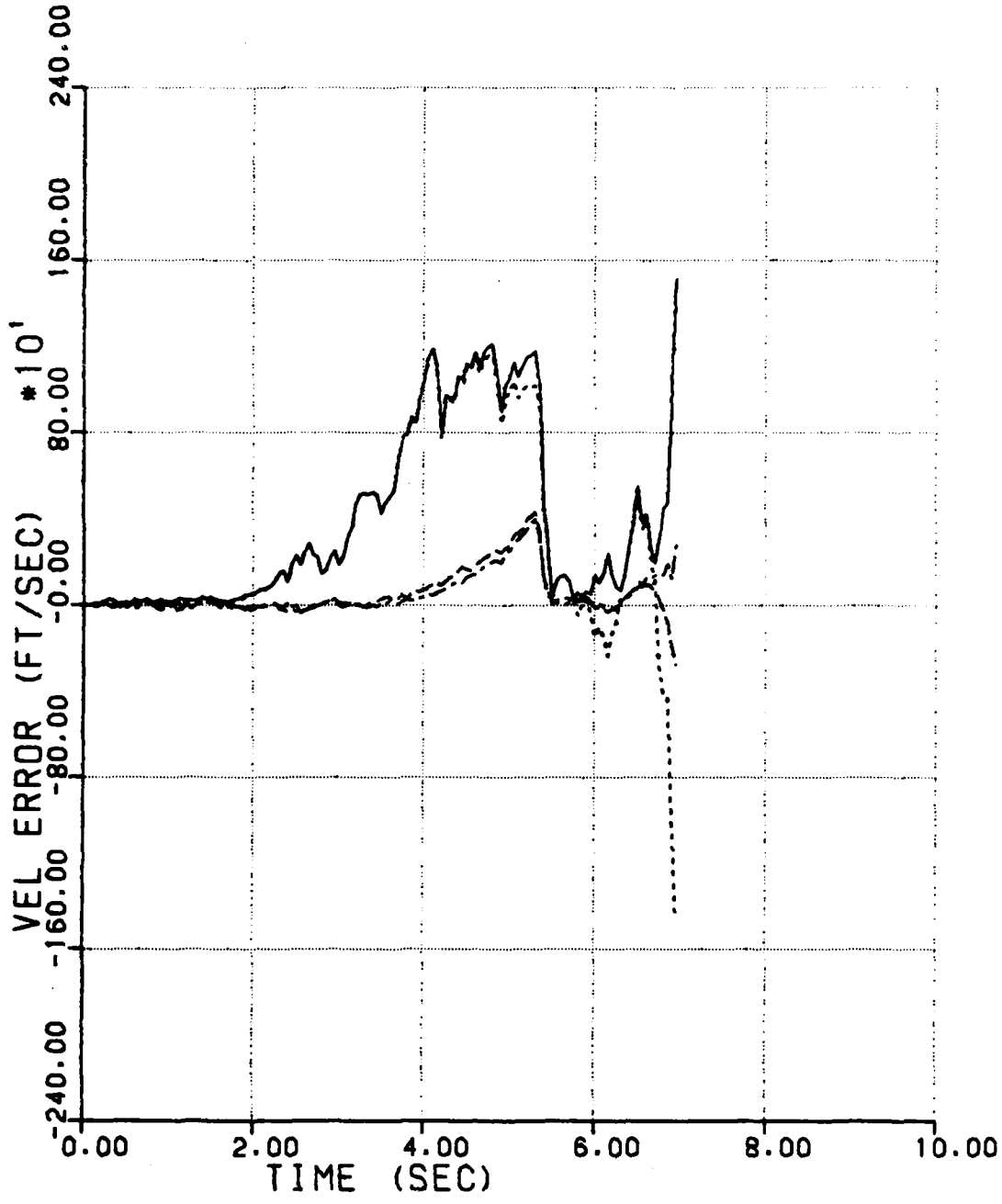

Figure 17. Velocity Error History for Engagement 2, Filter 1

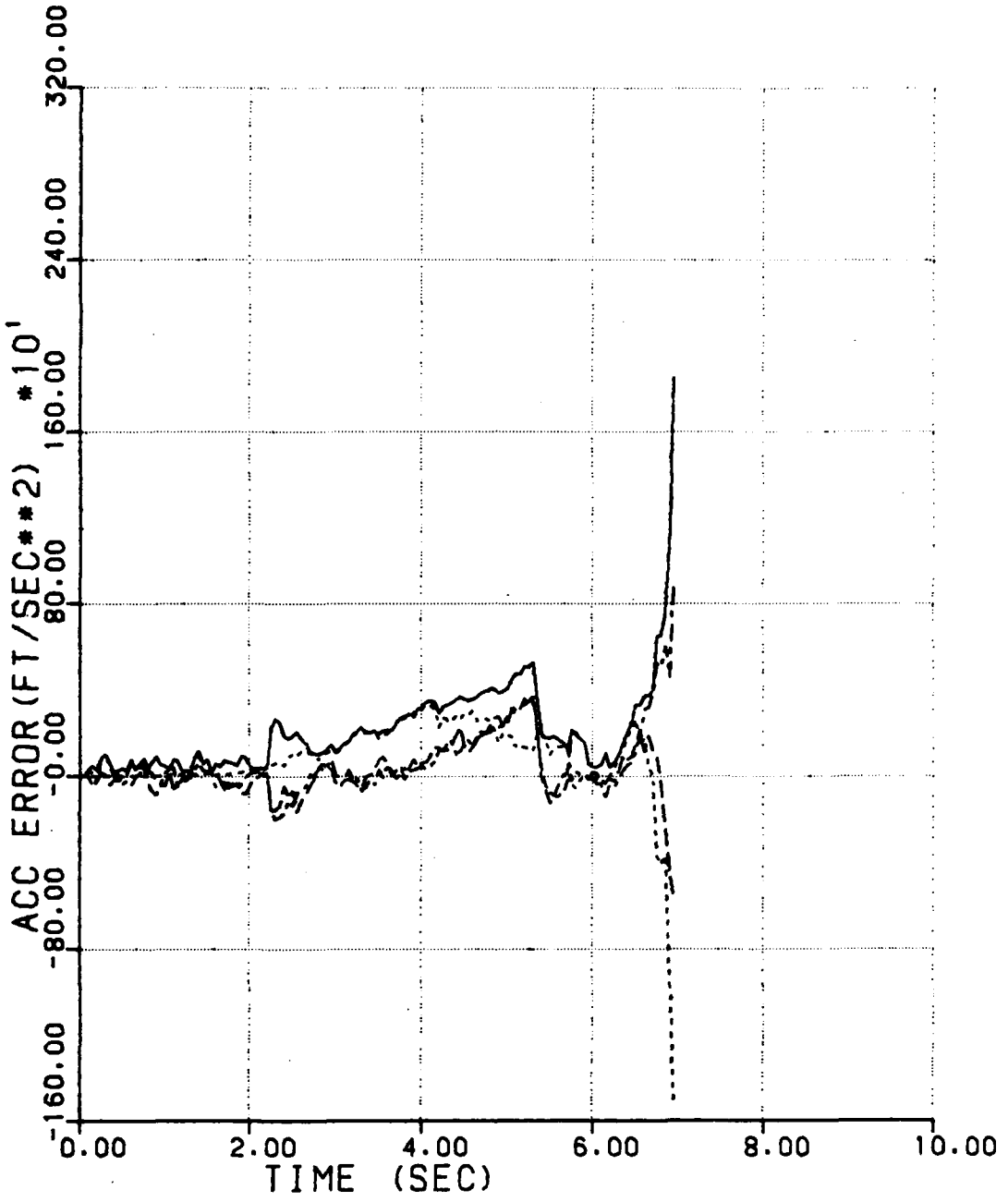

Figure 18. Acceleration Error History for Engagement 2, Filter 1

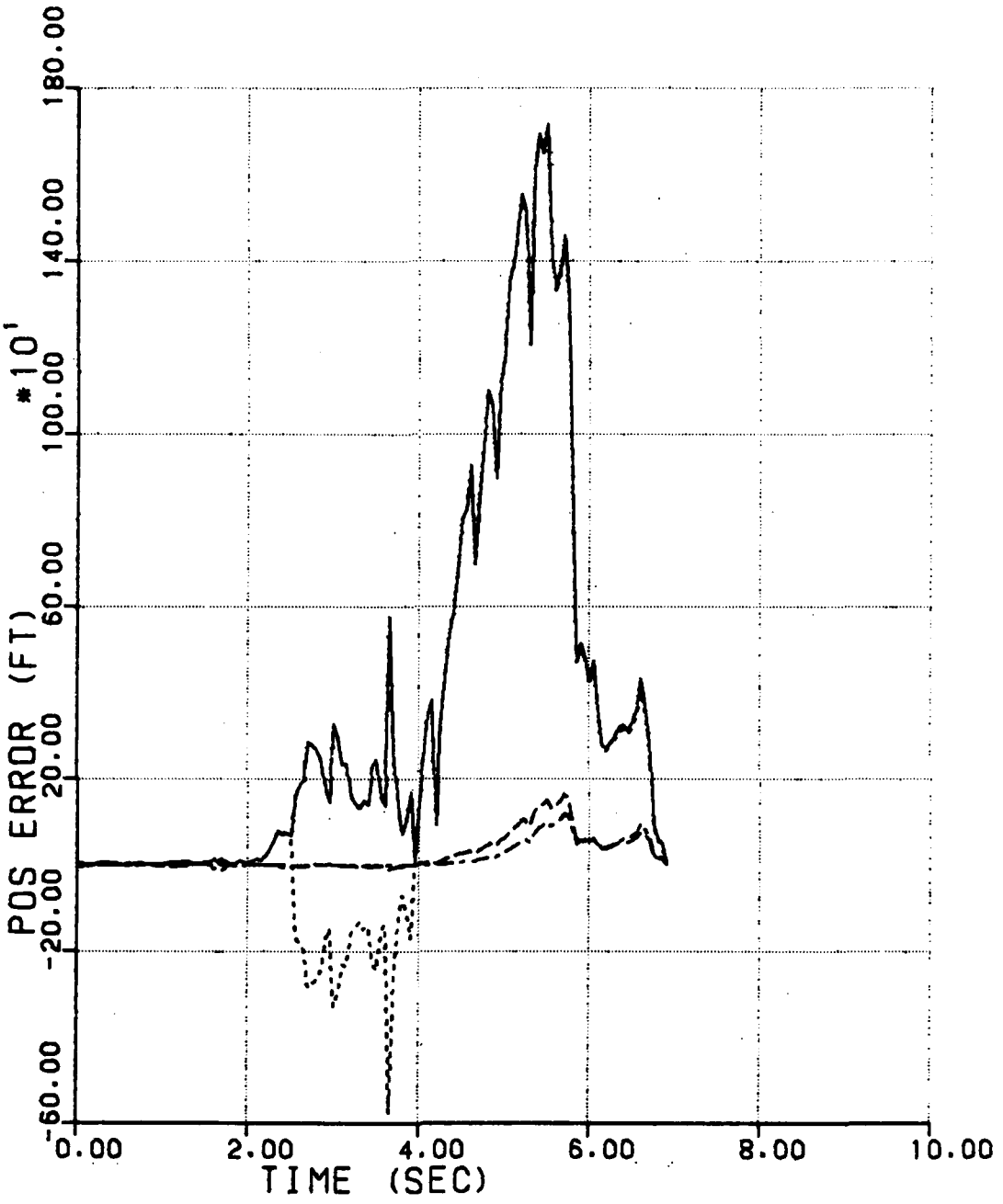

Figure 19. Position Error History for Engagement 2, Filter 2

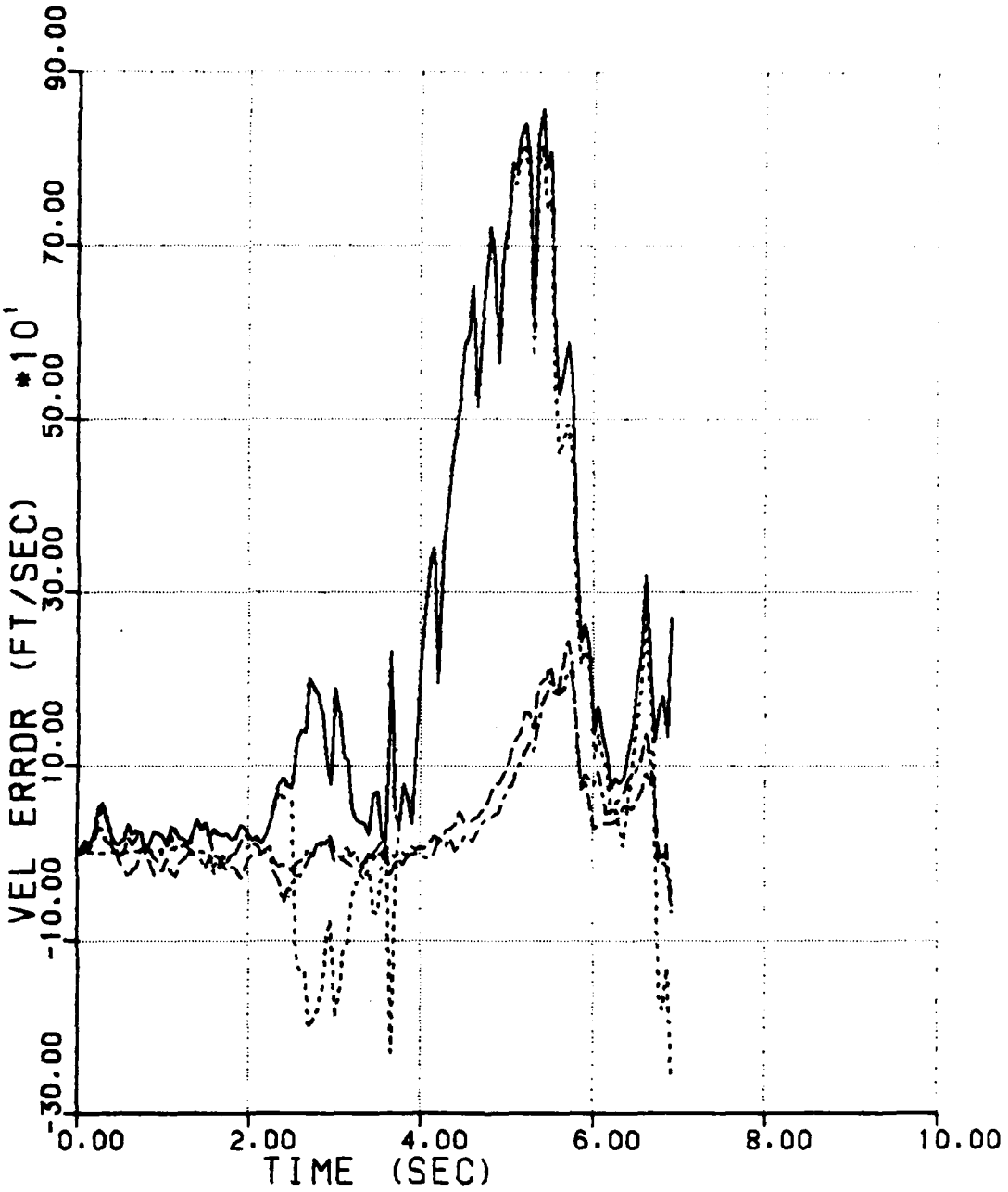

Figure 20. Velocity Error History for Engagement 2, Filter 2

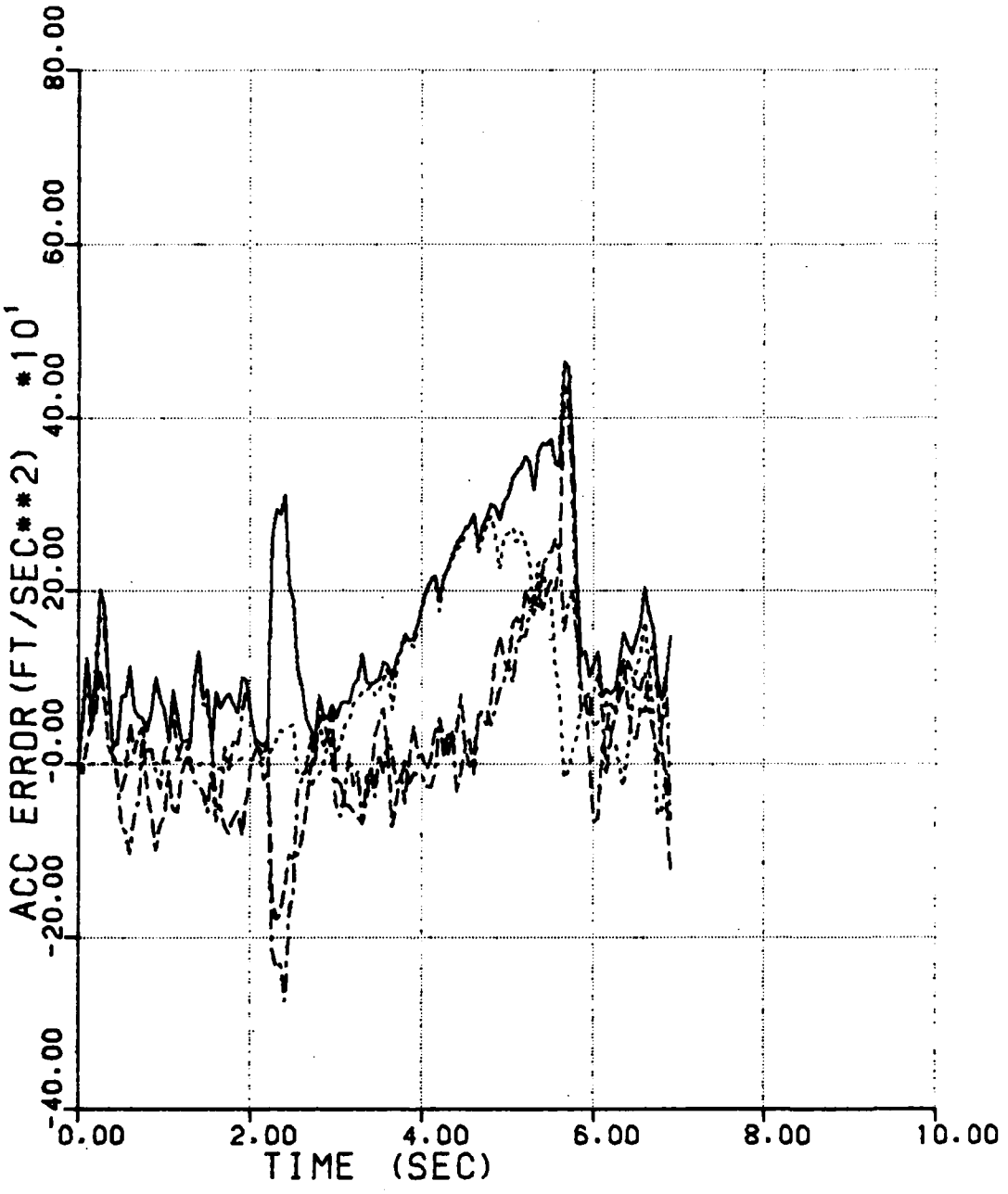

Figure 21. Acceleration Error History for Engagement 2, Filter 2

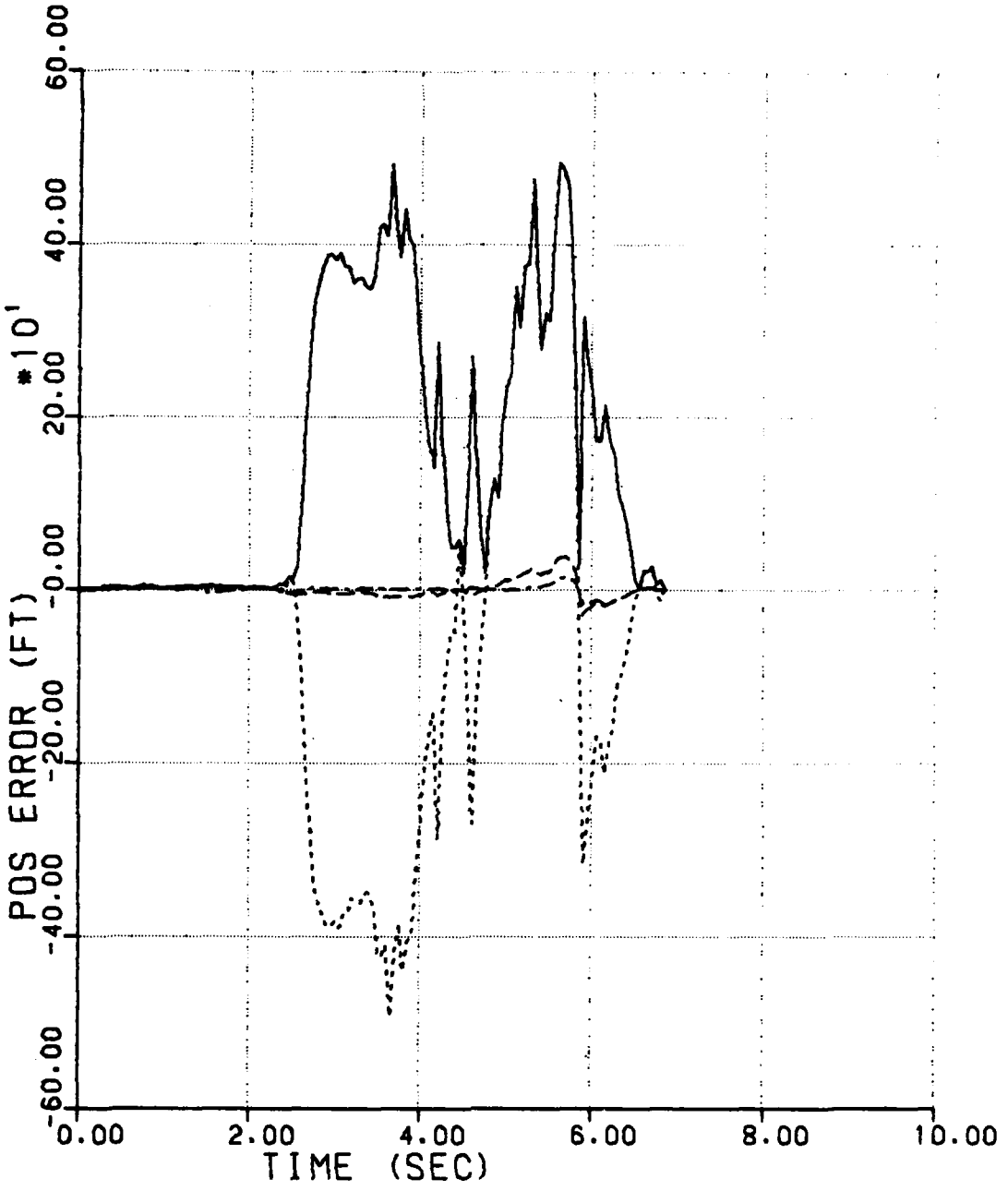

Figure 22. Position Error History for Engagement 2, Filter 3

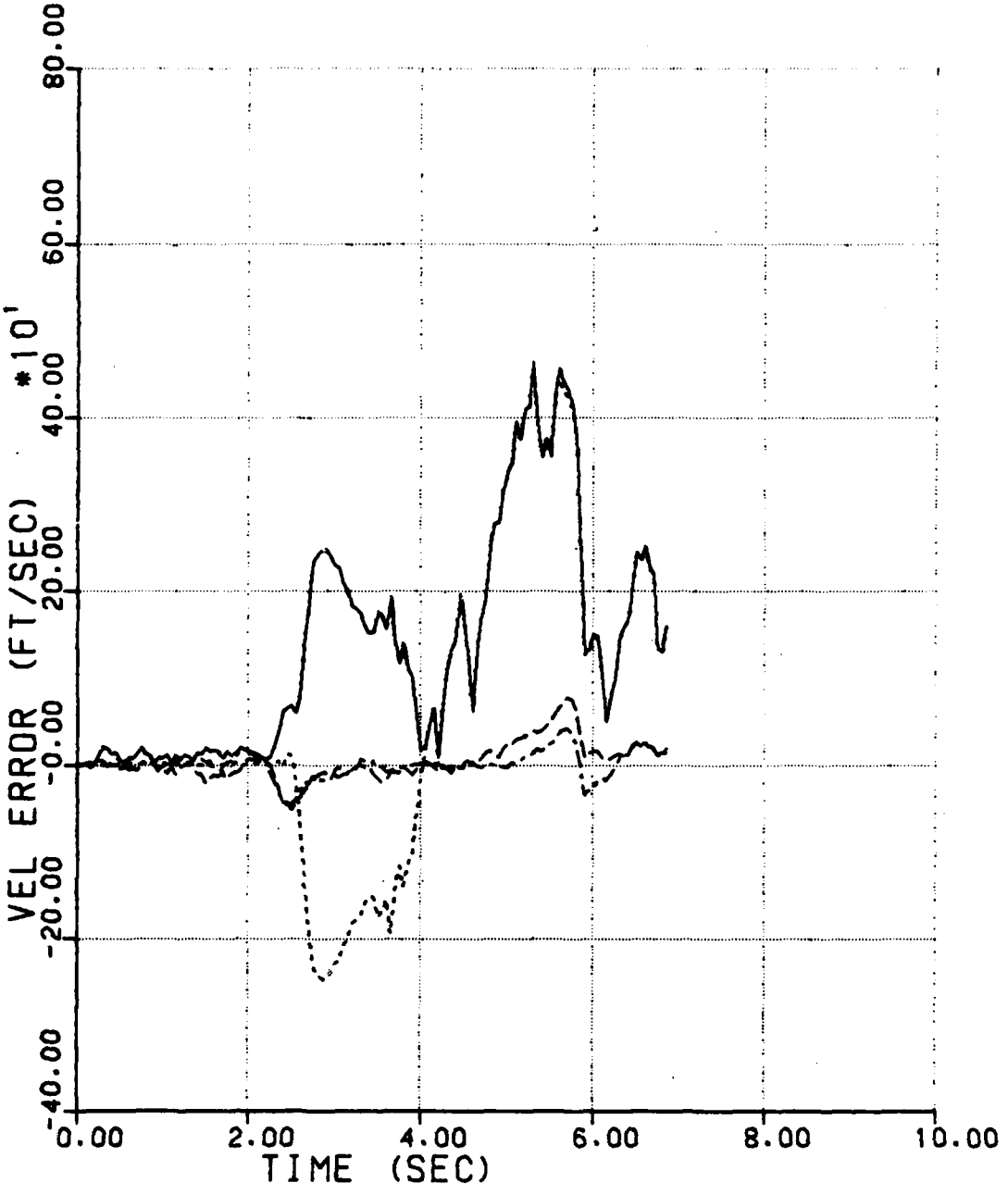

Figure 23. Velocity Error History for Engagement 2, Filter 3

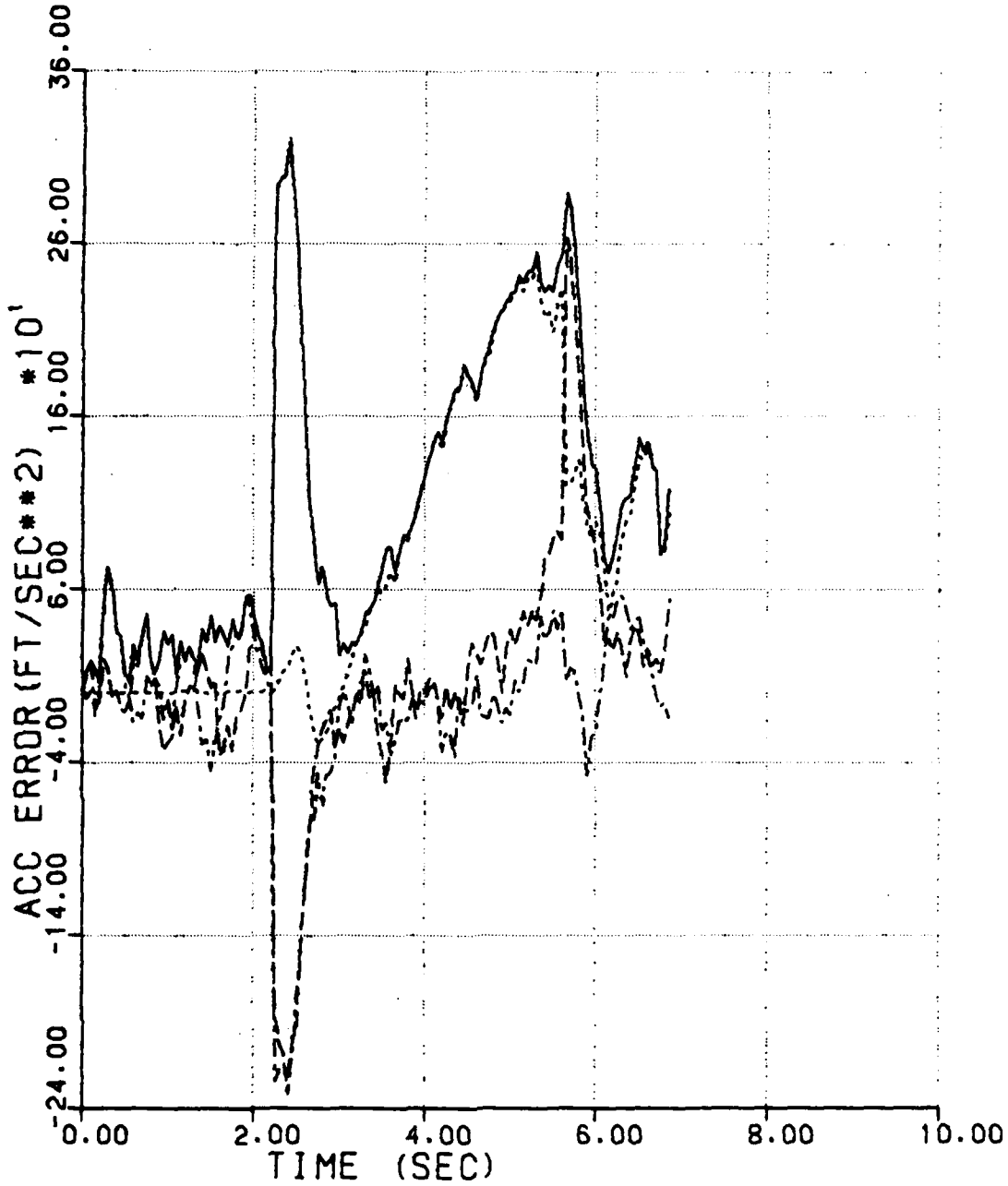

Figure 24. Acceleration Error History for Engagement 2, Filter 3

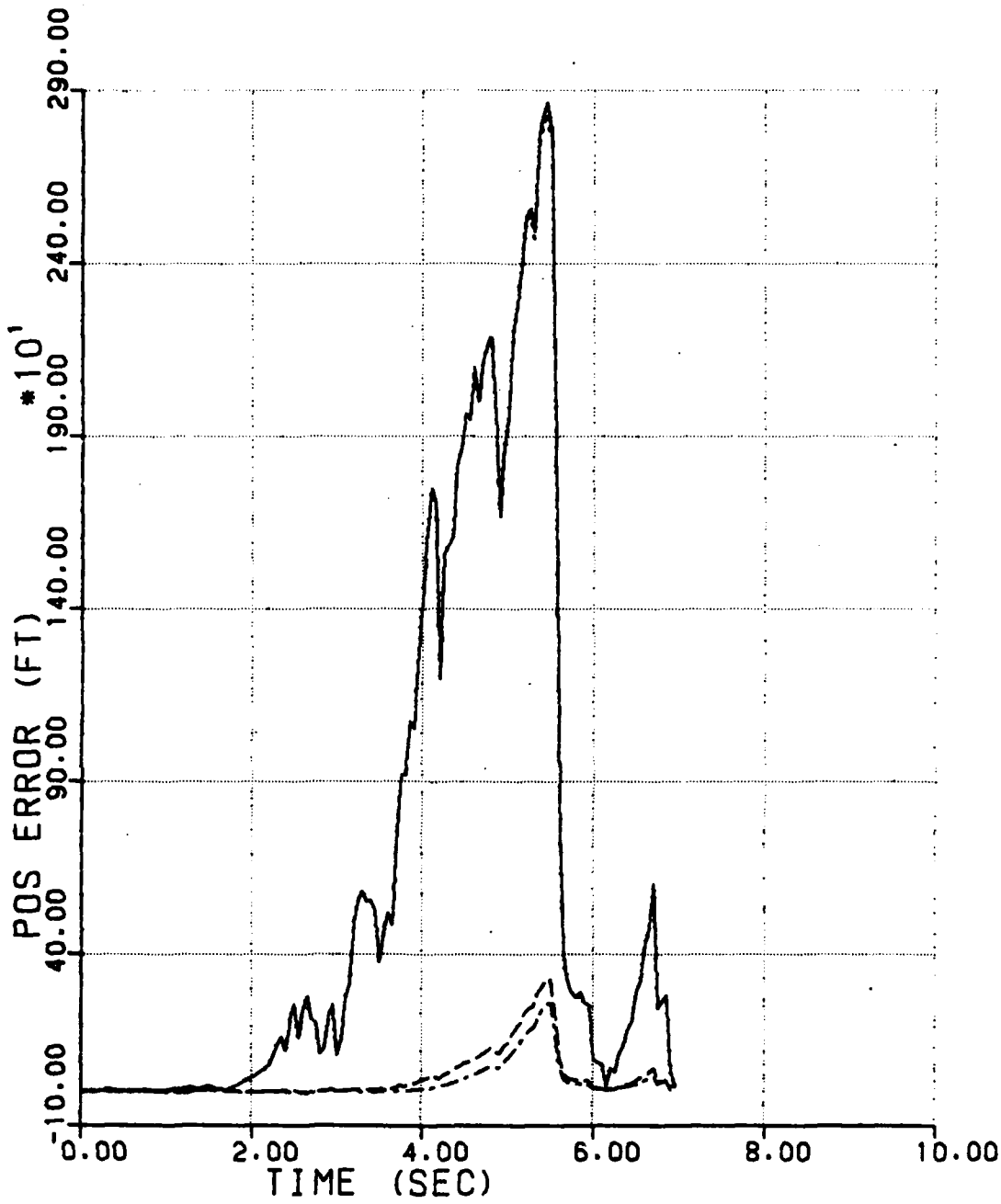

Figure 25. Position Error History for Engagement 2, Filter 4

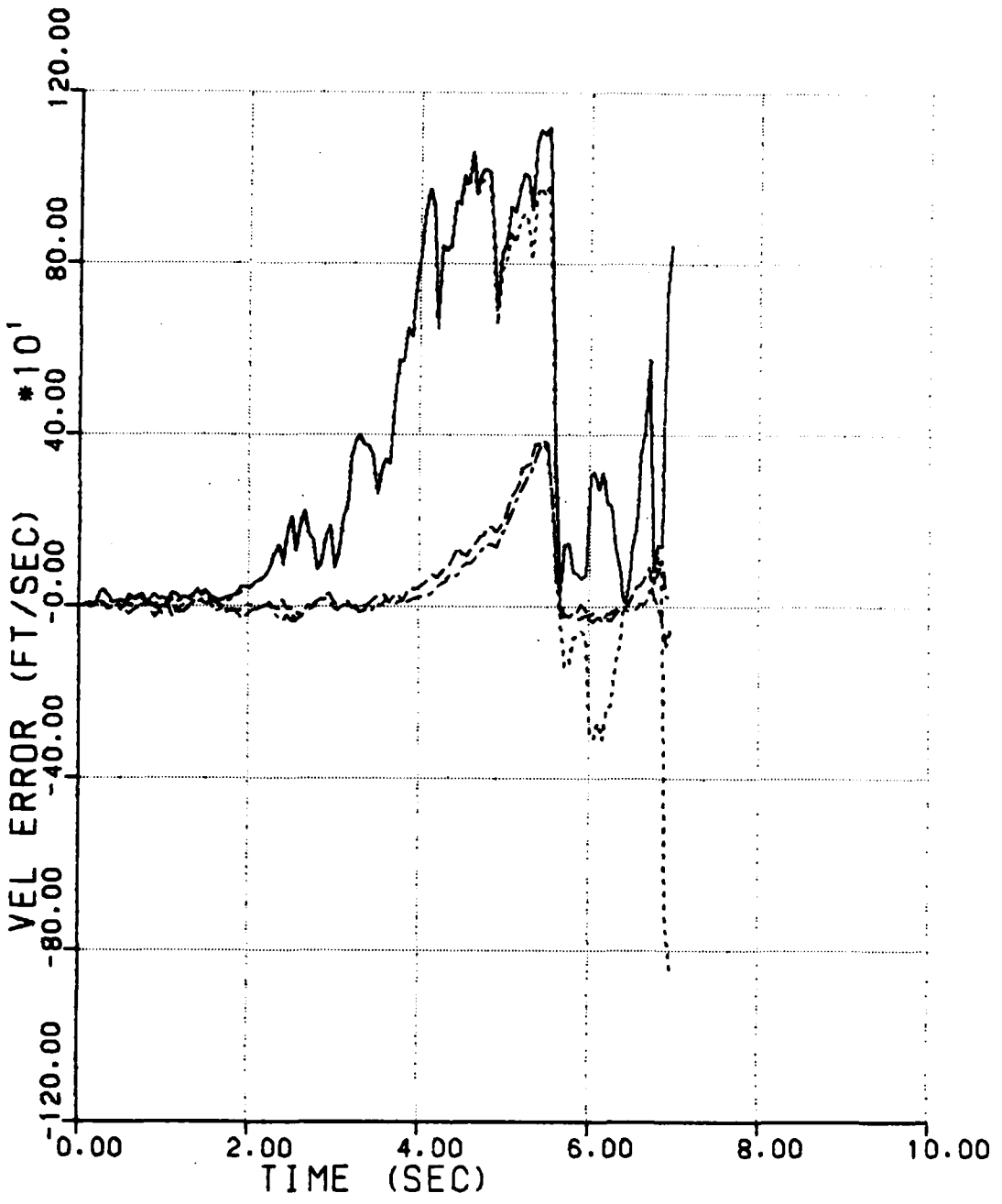

Figure 26. Velocity Error History for Engagement 2, Filter 4

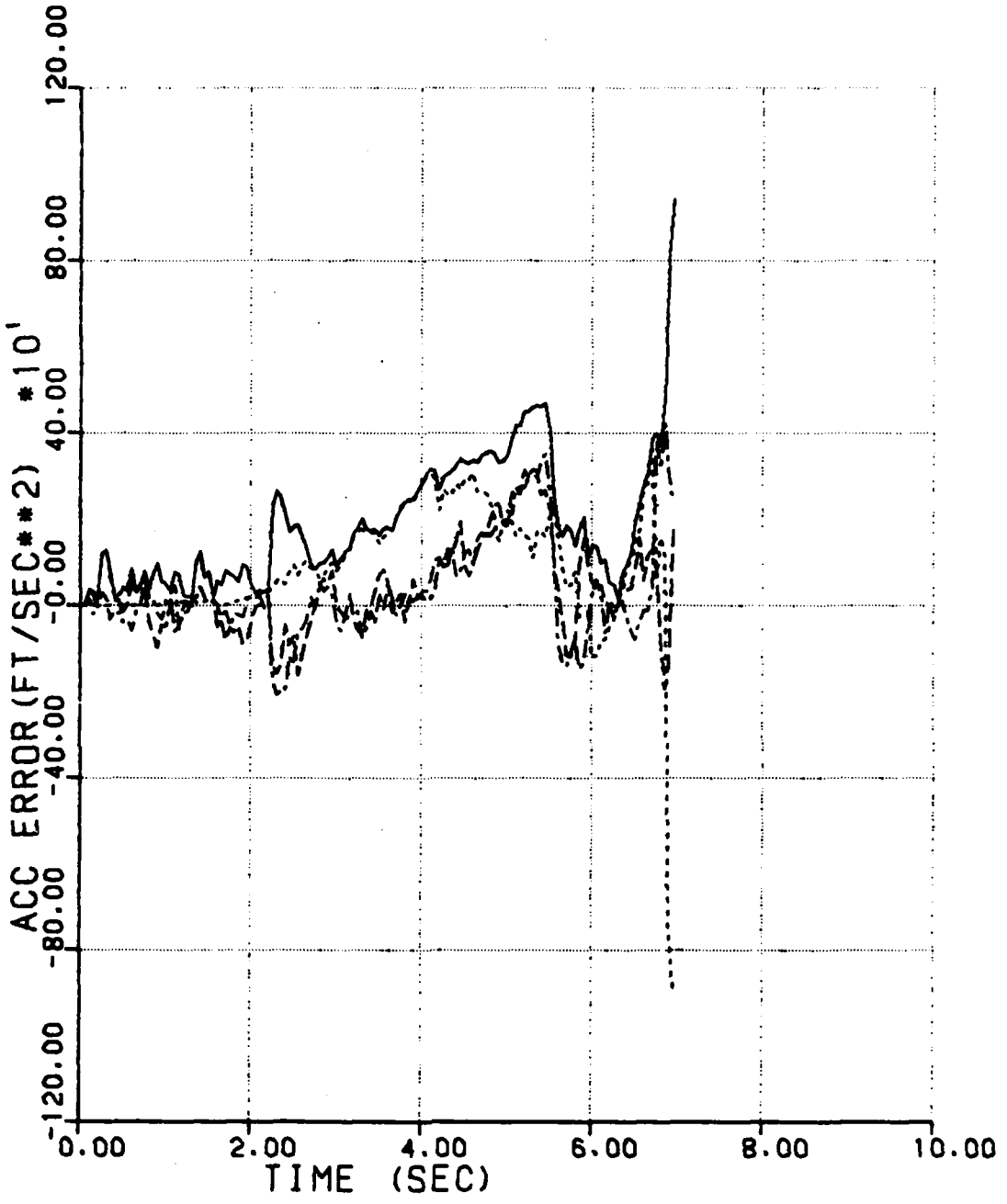

Figure 27. Acceleration Error History for Engagement 2, Filter 4

c. Engagement 3

Figure 28 represents the initial problem geometry for engagement 3. The carrier aircraft is again flying northward at 10,000 feet and Mach = 0.9 at launch. The target aircraft is originally located on a line 40 degrees east of north relative to the carrier aircraft and traveling in an eastward direction at Mach = 0.9. The initial range is 11,000 feet.

Due to the severe starting conditions, the missile guidance system and the estimation algorithm must work very hard to acquire the target. Once again, the results of the filter performance comparisons are similar to those of engagement 1 with the regular extended Kalman filter providing the worst performance followed closely by the iterated extended Kalman filter. Next comes the adaptive extended Kalman filter with approximately half the peak error of the other two, and finally, the time weighted adaptive extended Kalman filter with a peak error of less than one-sixth the peak error of the regular extended Kalman filter. Figures 29 through 40 present the filter error comparisons for engagement 3.

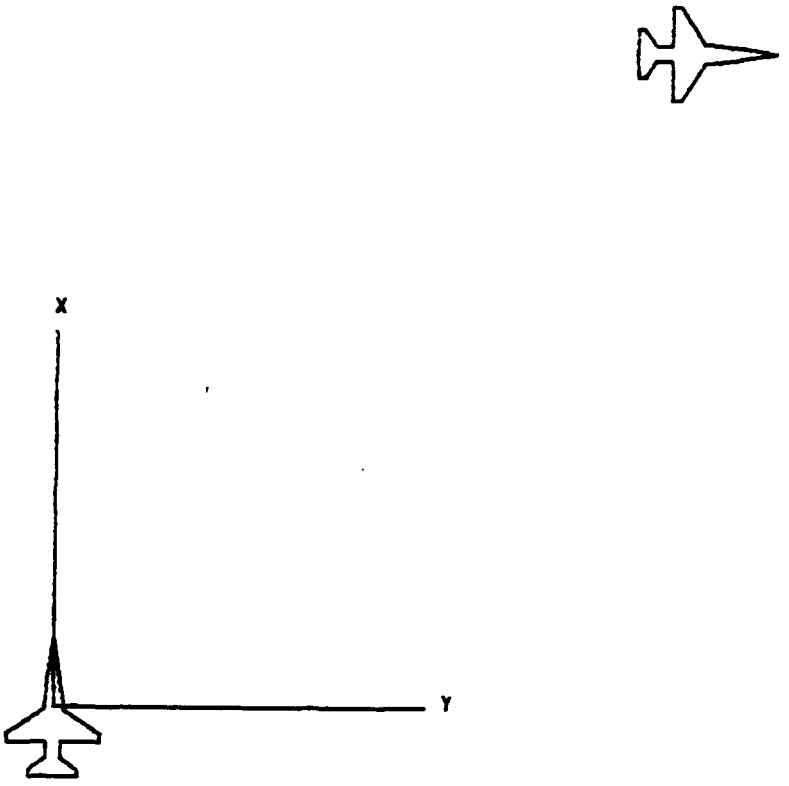

Figure 28. Engagement 3 Geometry

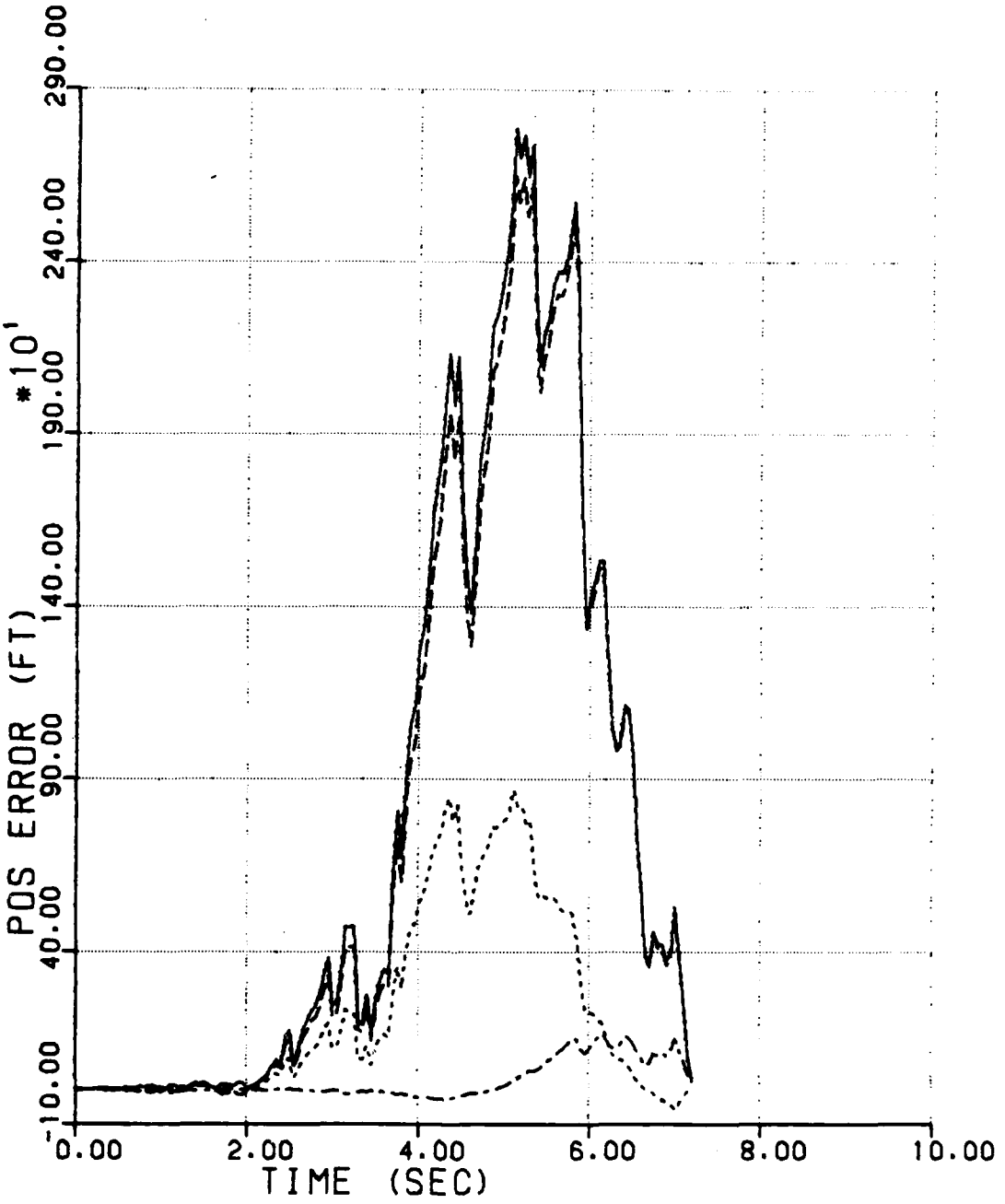

Figure 29. Position Error History for Engagement 3, Filter 1

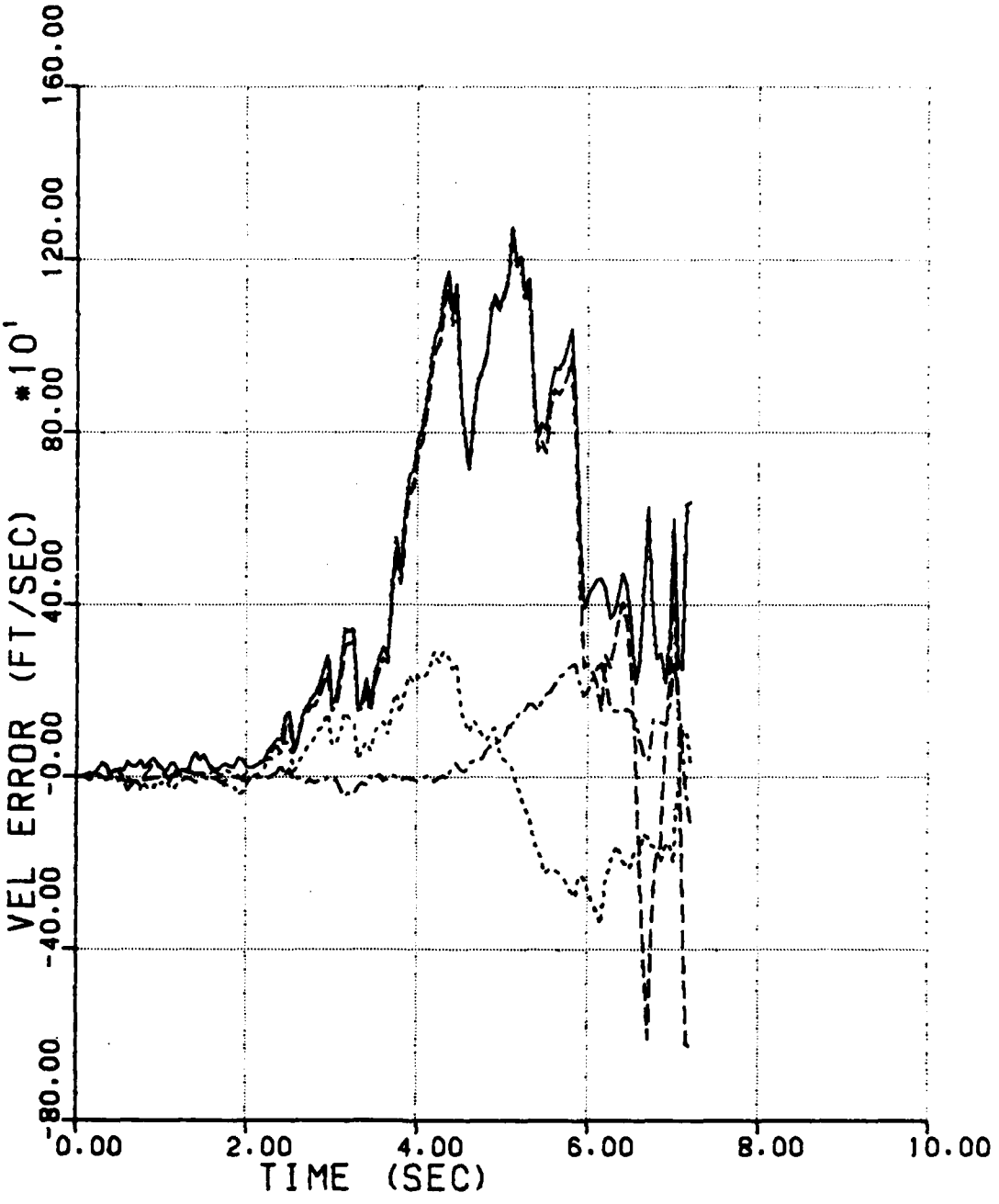

Figure 30. Velocity Error History for Engagement 3, Filter 1

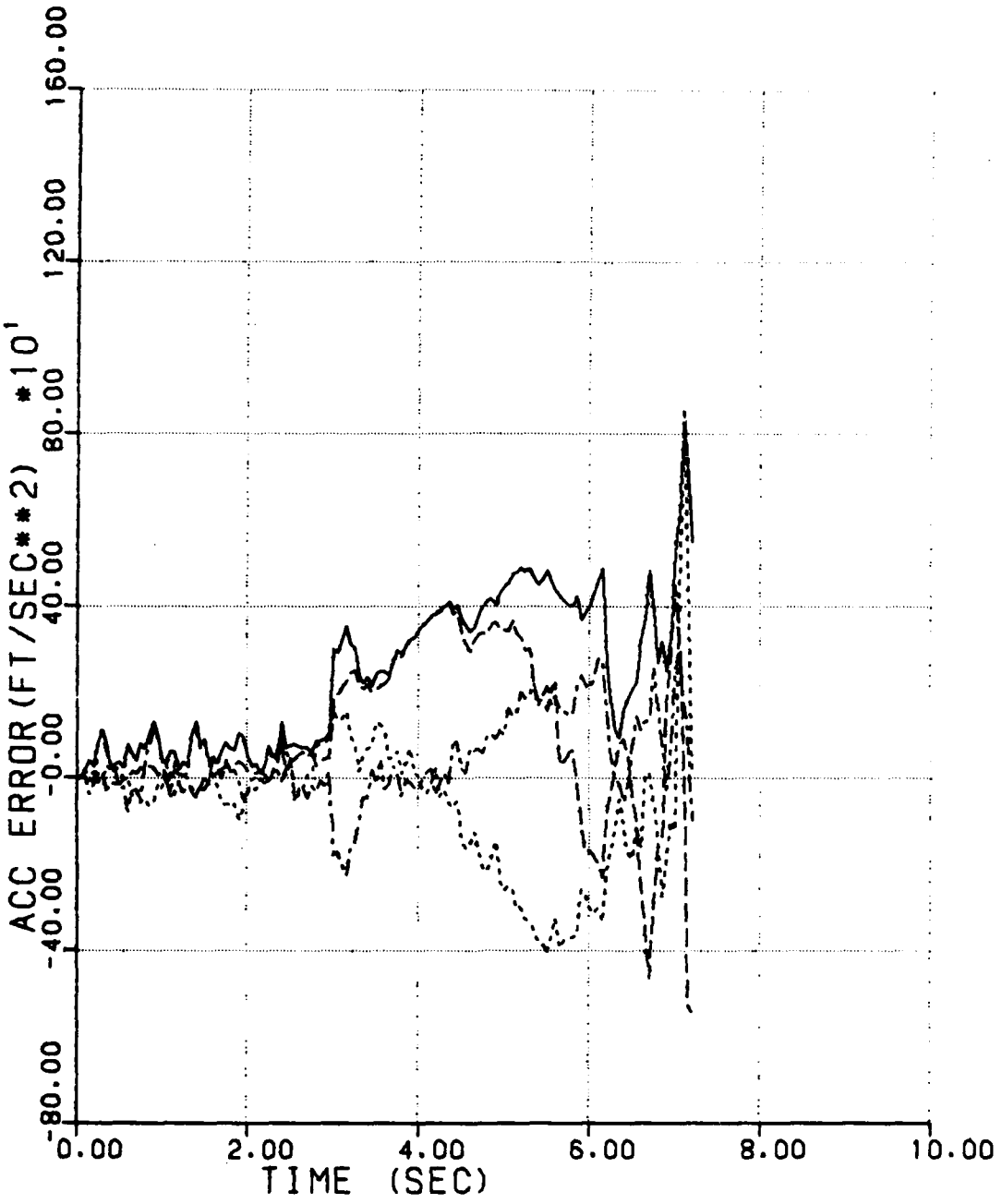

Figure 31. Acceleration Error History for Engagement 3, Filter 1

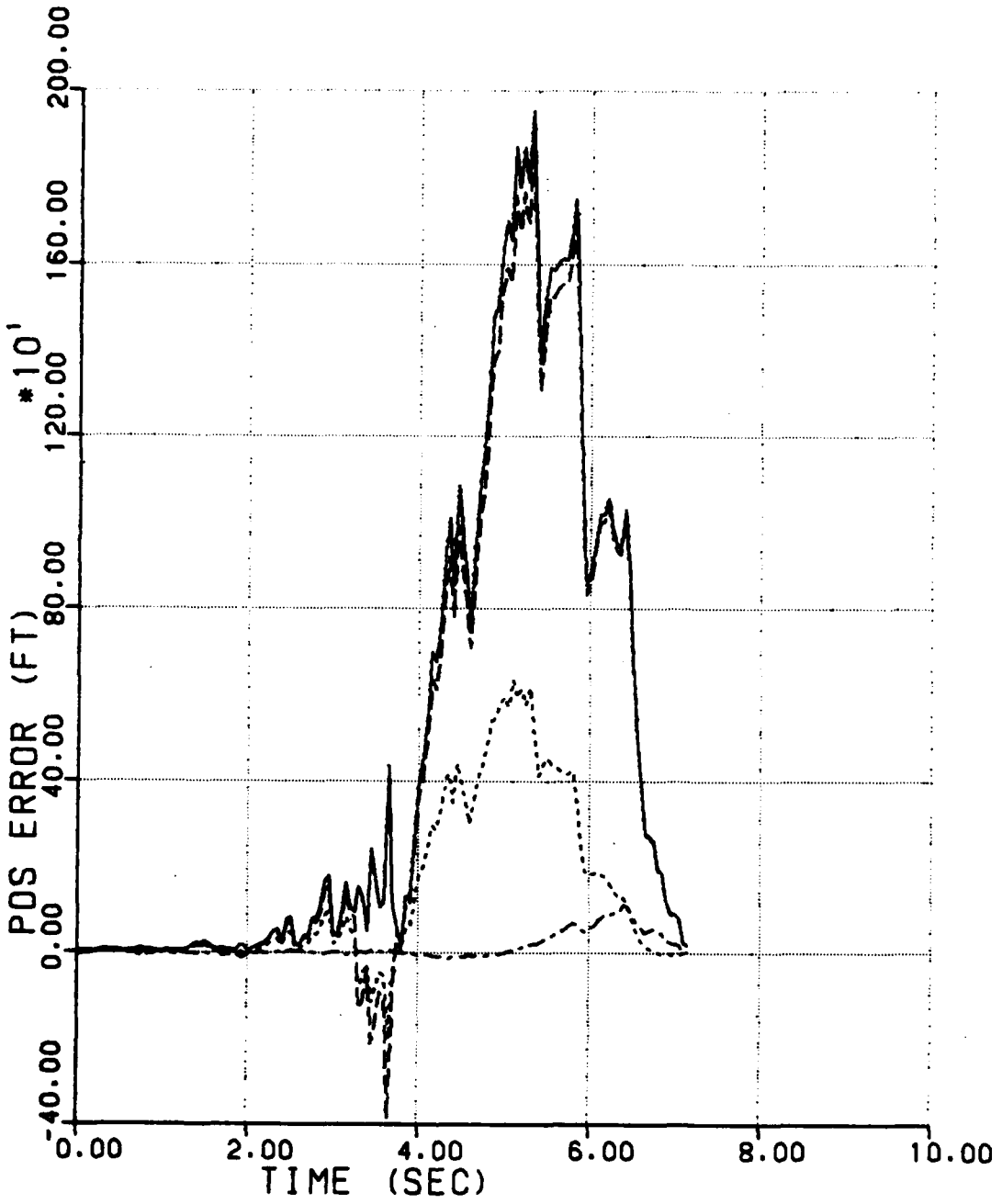

Figure 32. Position Error History for Engagement 3, Filter 2

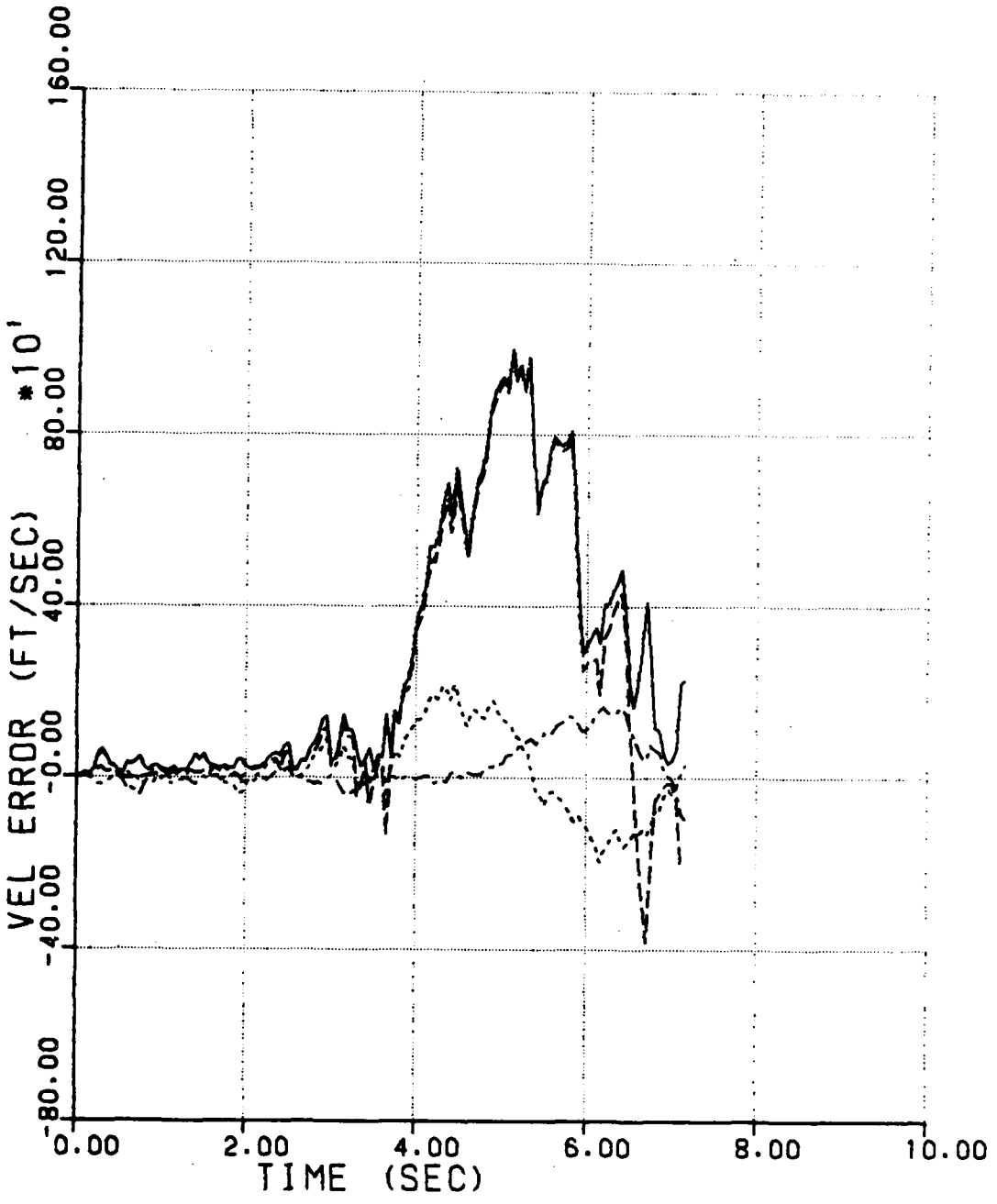

Figure 33. Velocity Error History for Engagement 3, Filter 2

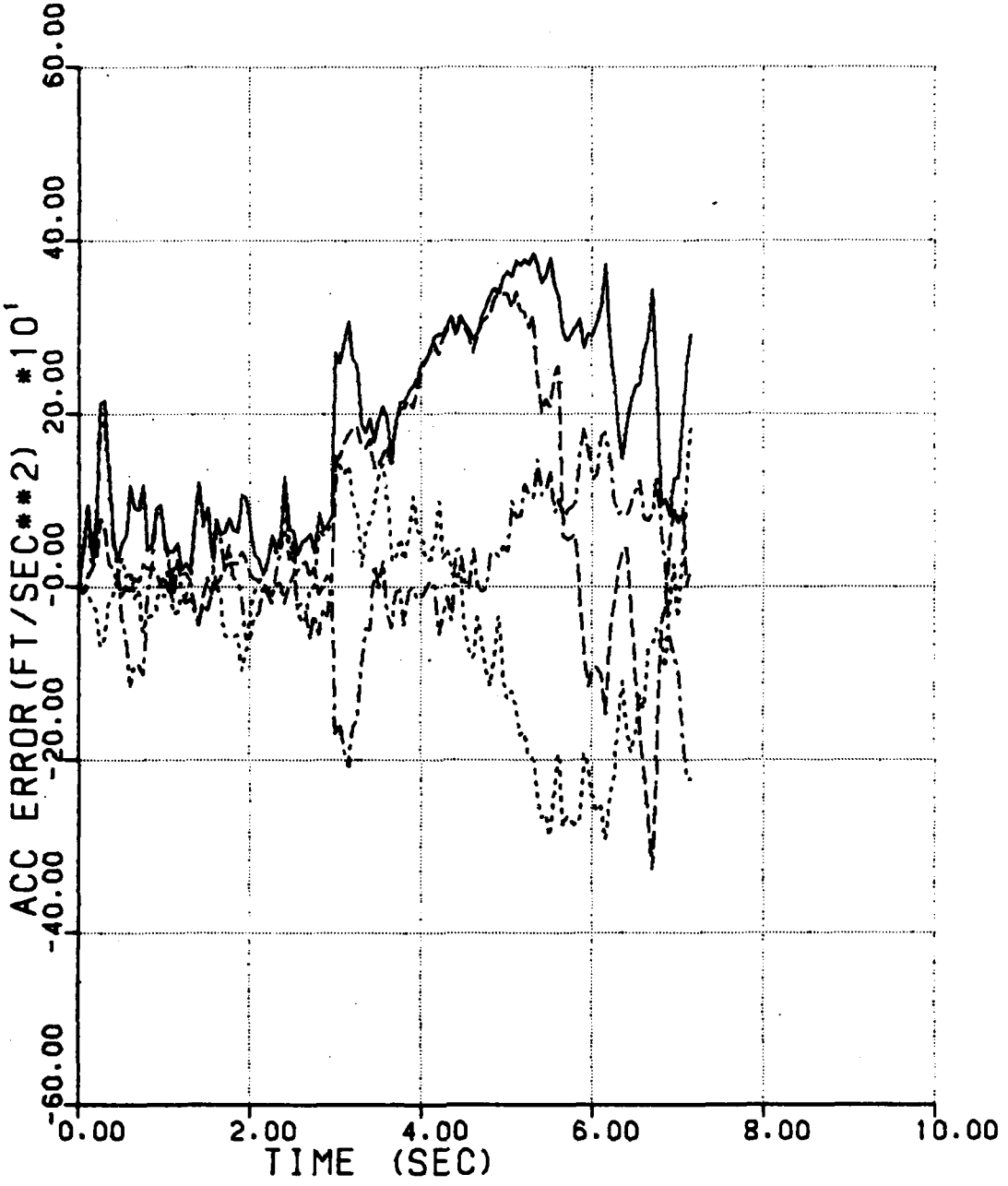

Figure 34. Acceleration Error History for Engagement 3, Filter 2

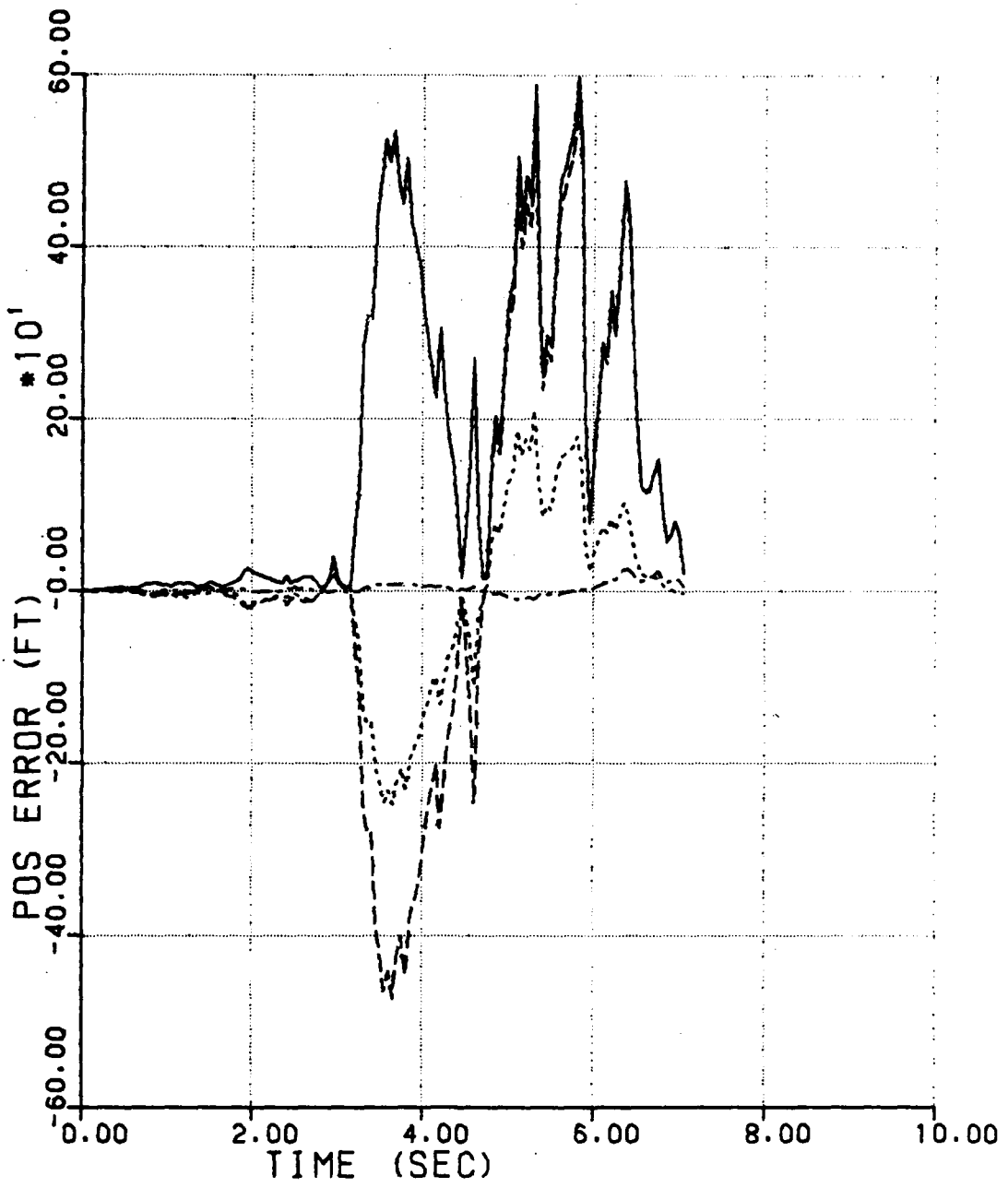

Figure 35. Position Error History for Engagement 3, Filter 3

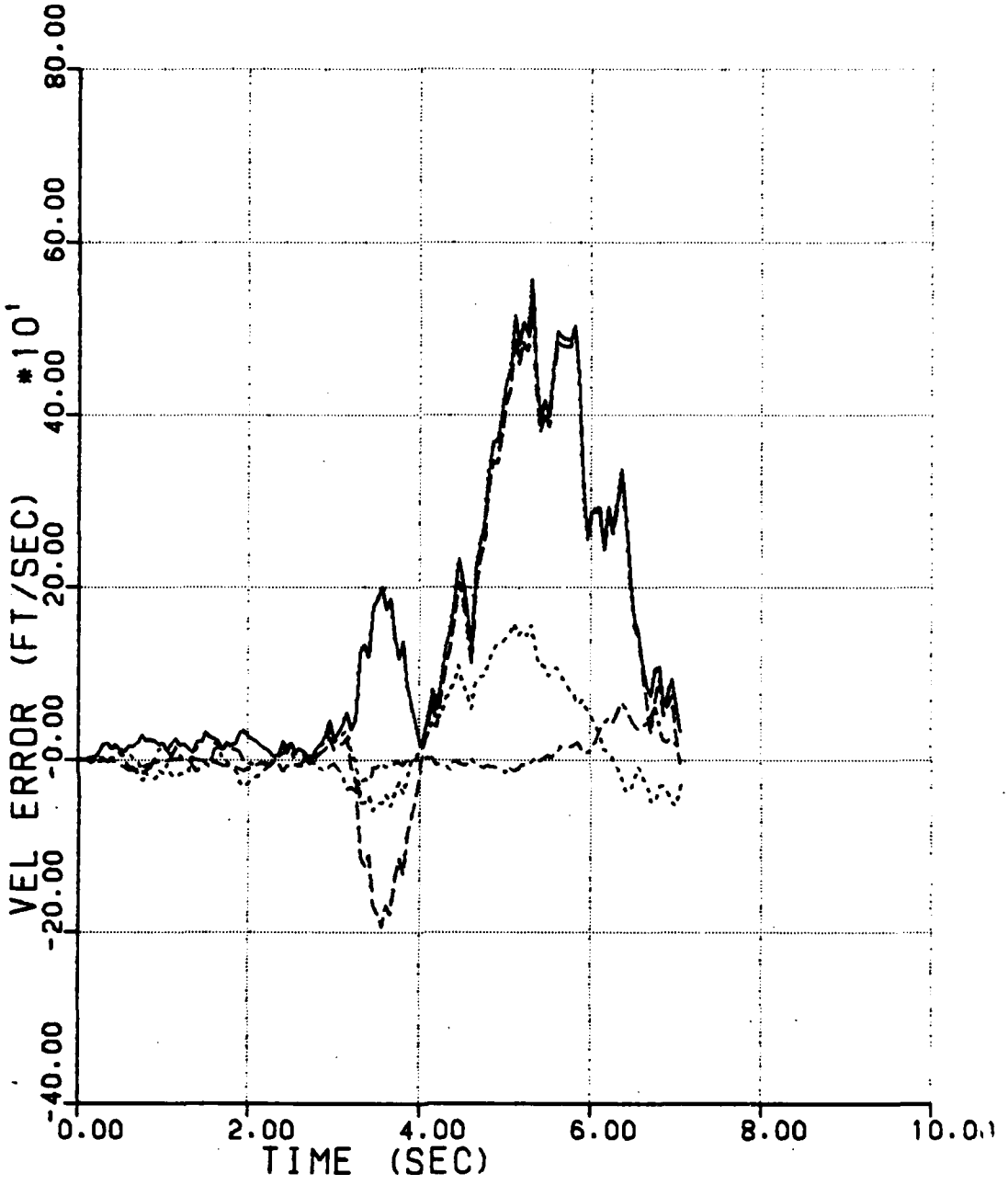

Figure 36. Velocity Error History for Engagement 3, Filter 3

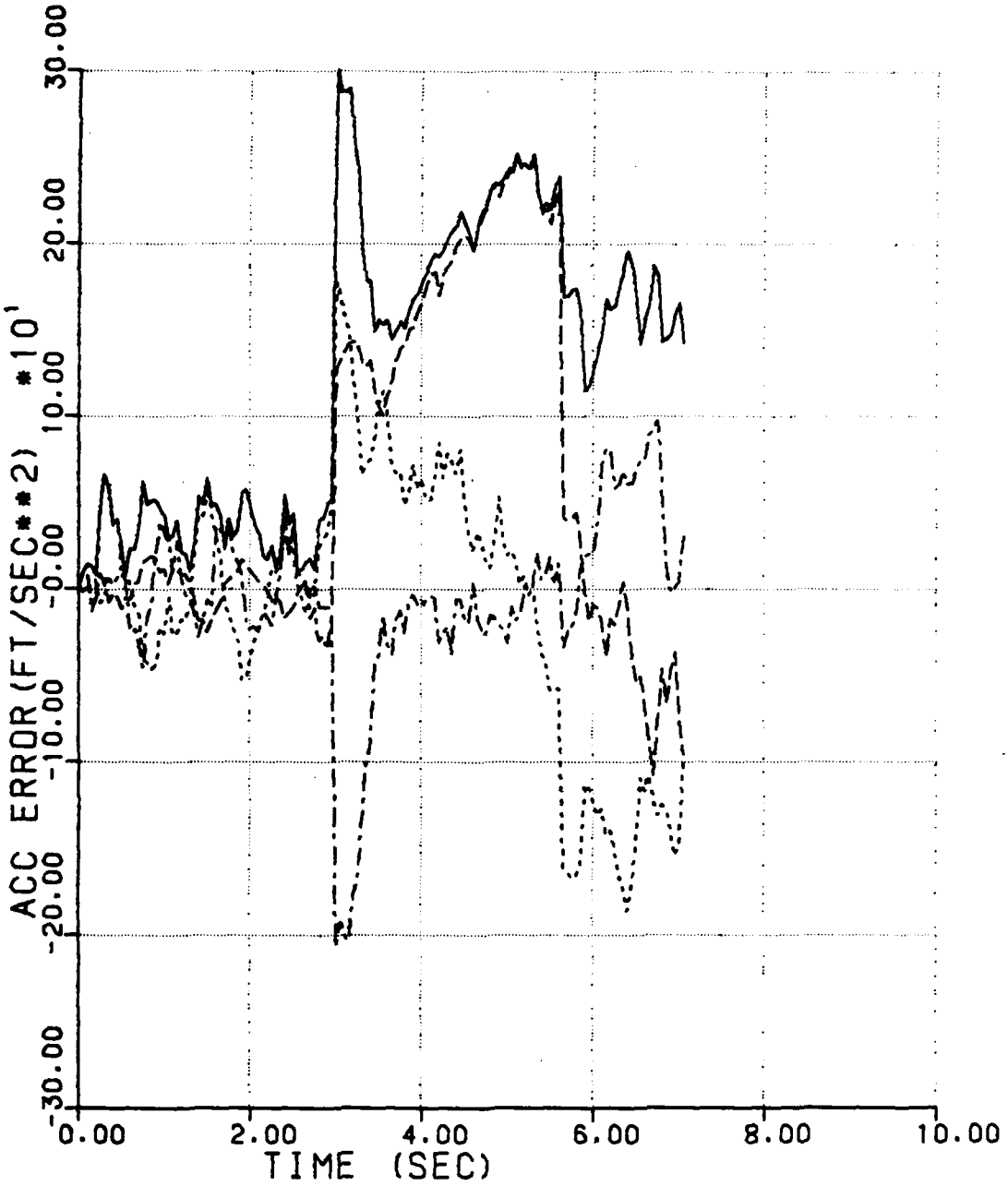

Figure 37. Acceleration Error History for Engagement 3, Filter 3

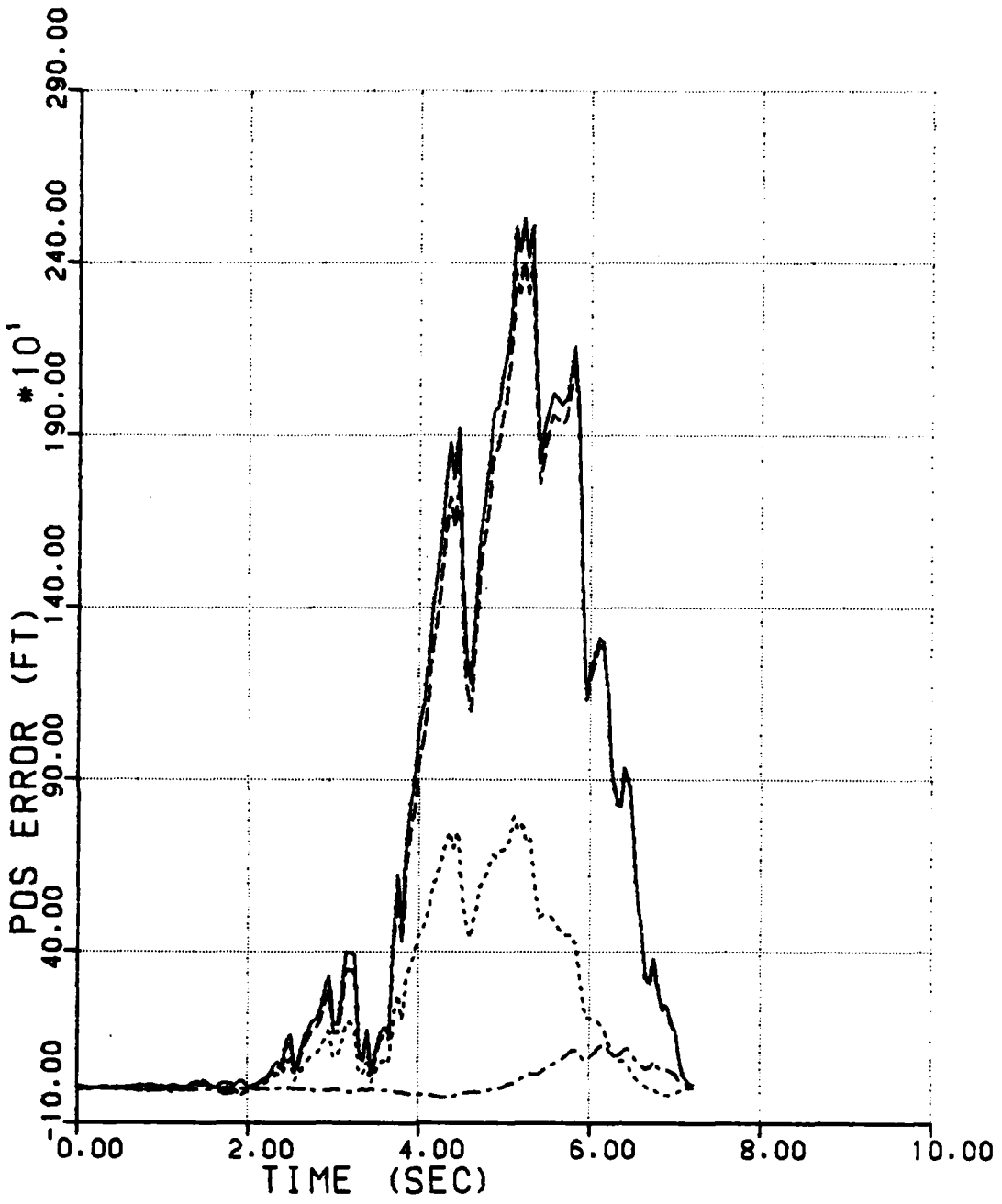

Figure 38. Position Error History for Engagement 3, Filter 4

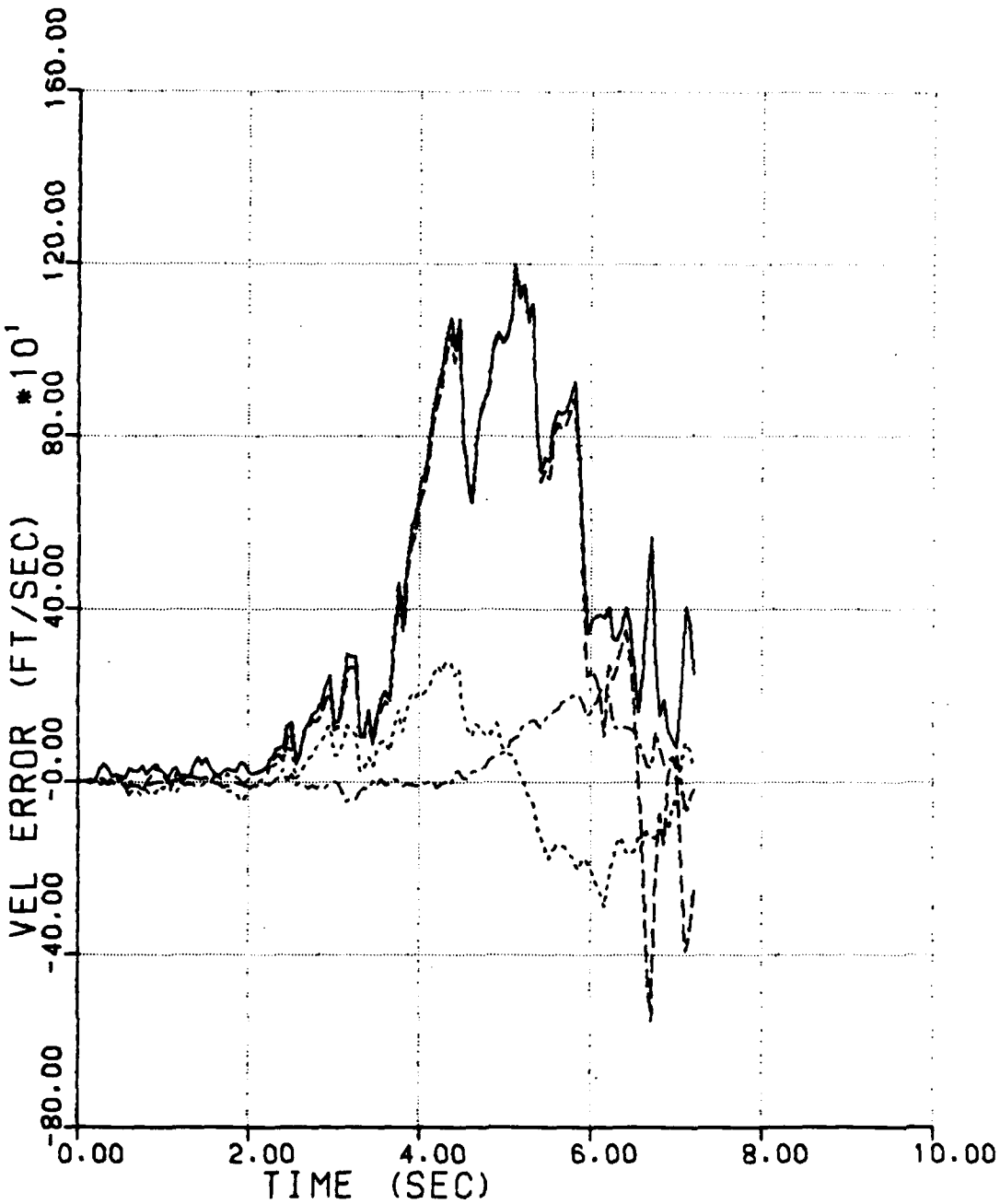

Figure 39. Velocity Error History for Engagement 3, Filter 4

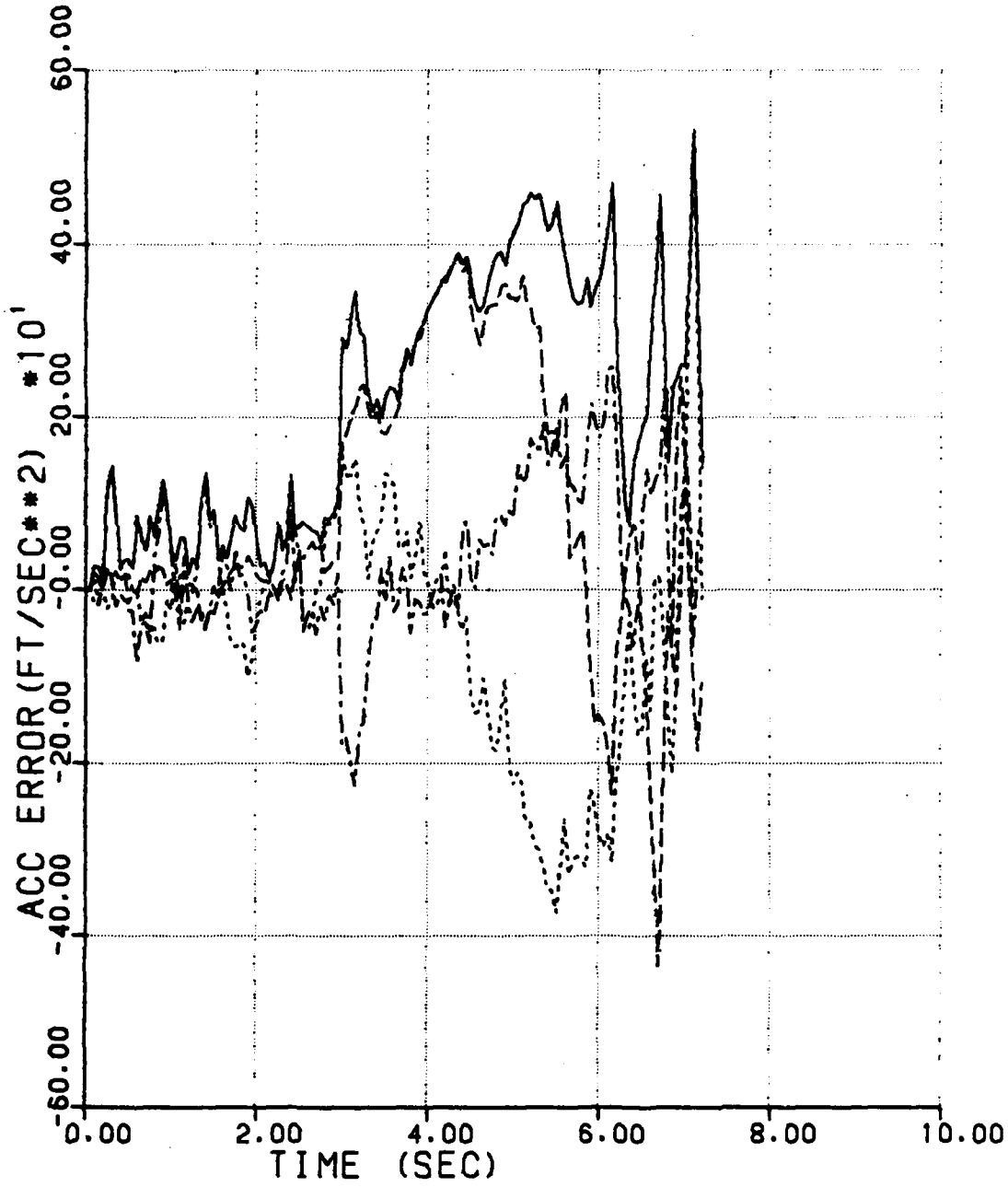

Figure 40. Acceleration Error History for Engagement 3, Filter 4

d. Engagement 4

Figure 41 represents the initial problem geometry for engagement 4. The carrier aircraft is again traveling north at 10,000 feet and a speed of Mach = 0.9 at launch. The target aircraft is directly ahead of the carrier at the same altitude and a range of 3,000 feet, but is traveling in a southeastward direction at a speed of Mach = 0.9. This is a short duration missile flight due to the initial range. This also means that the measurement differences are large enough to cause good estimation of the states. All of the filters performed well with the notable fact that the maximum position estimate error of the four filters was experienced by filter 3. This maximum error was less than 80 feet, however, and filter 3 still managed to attain the smallest miss distance in the end.

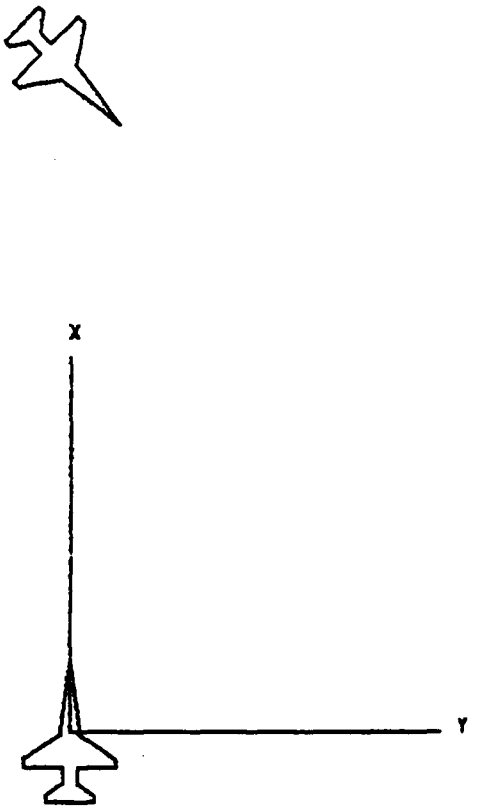

Figure 41. Engagement 4 Geometry

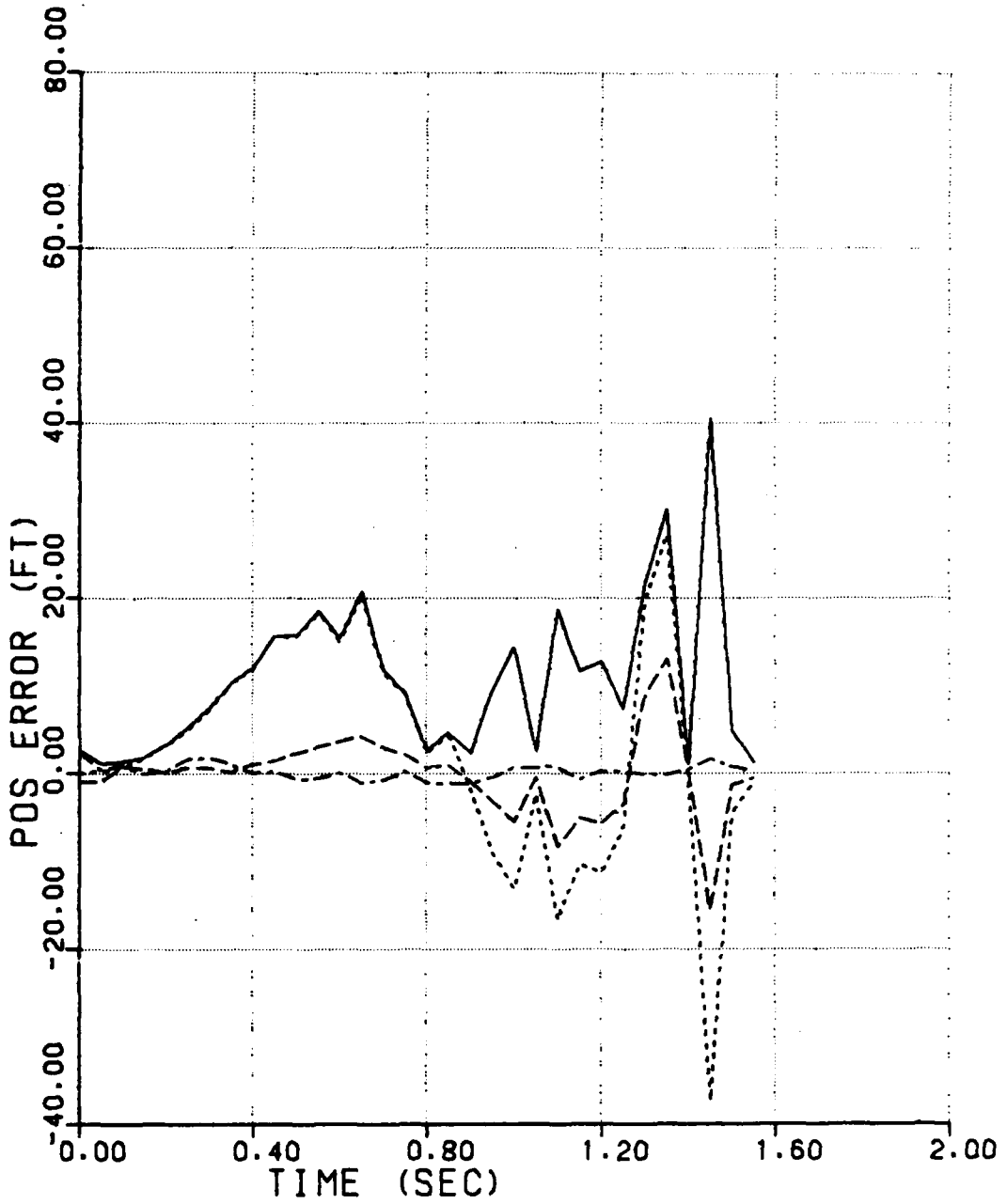

Figure 42. Position Error History for Engagement 4, Filter 1

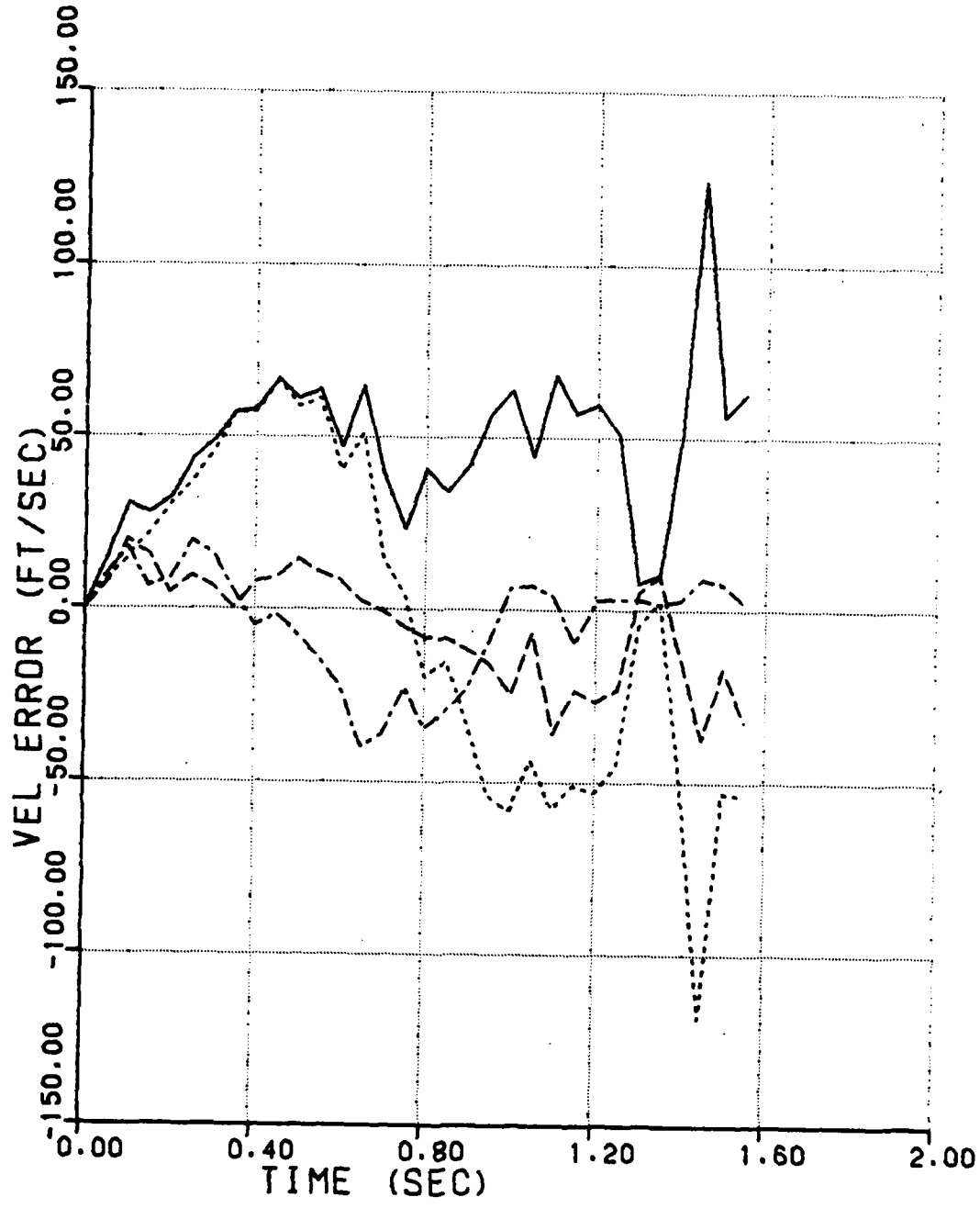

Figure 43. Velocity Error History for Engagement 4, Filter 1

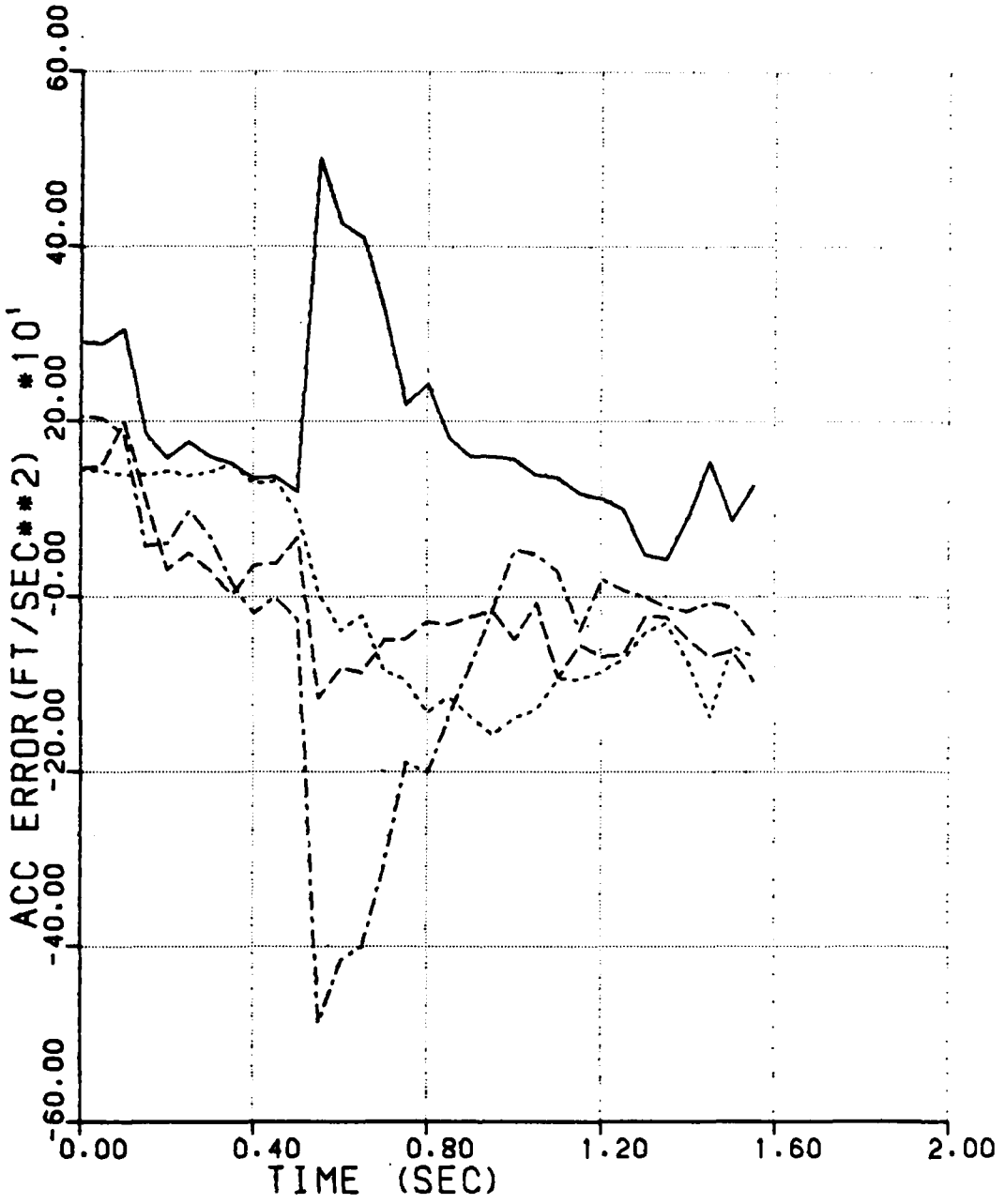

Figure 44. Acceleration Error History for Engagement 4, Filter 1

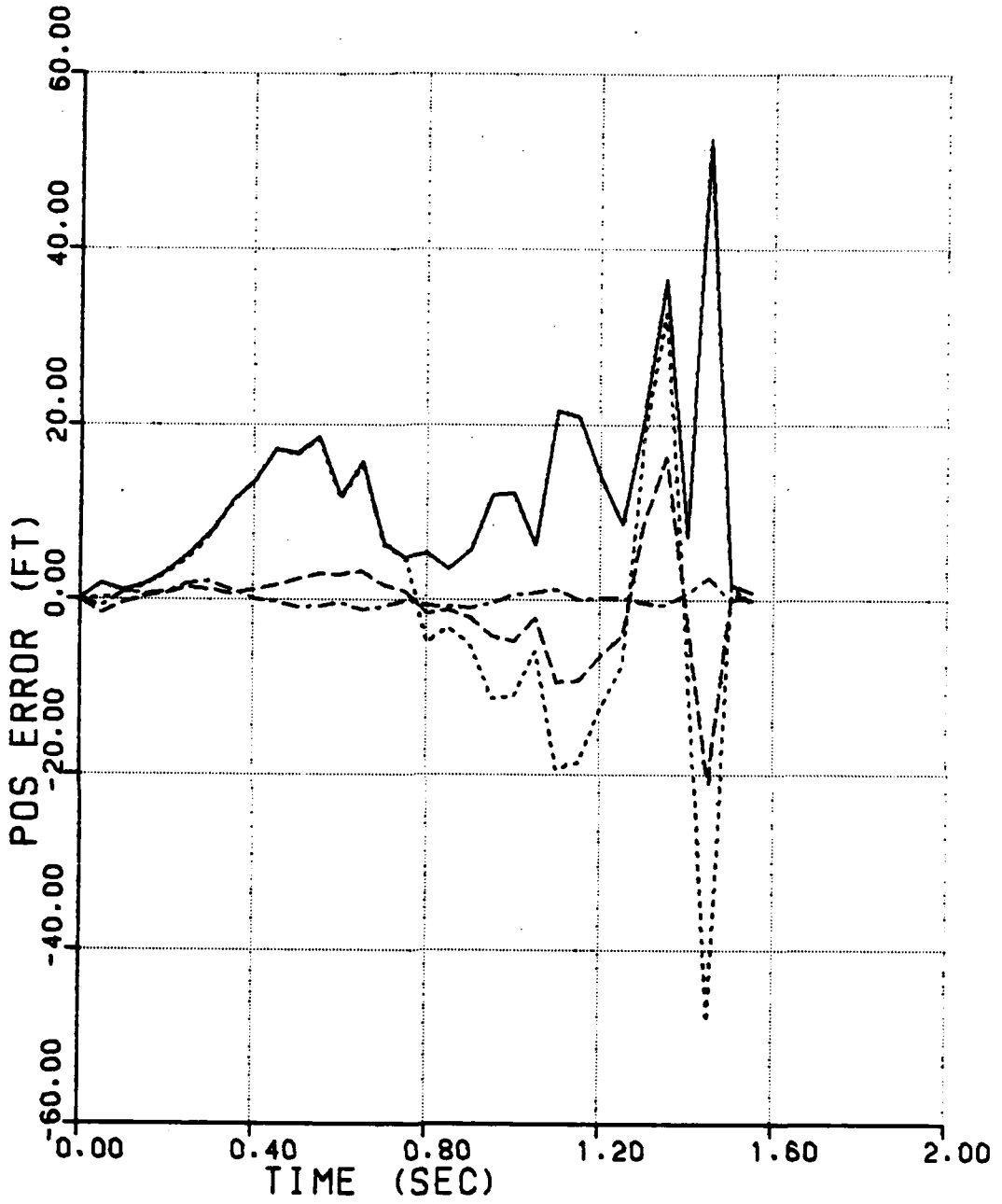

Figure 45. Position Error History for Engagement 4, Filter 2

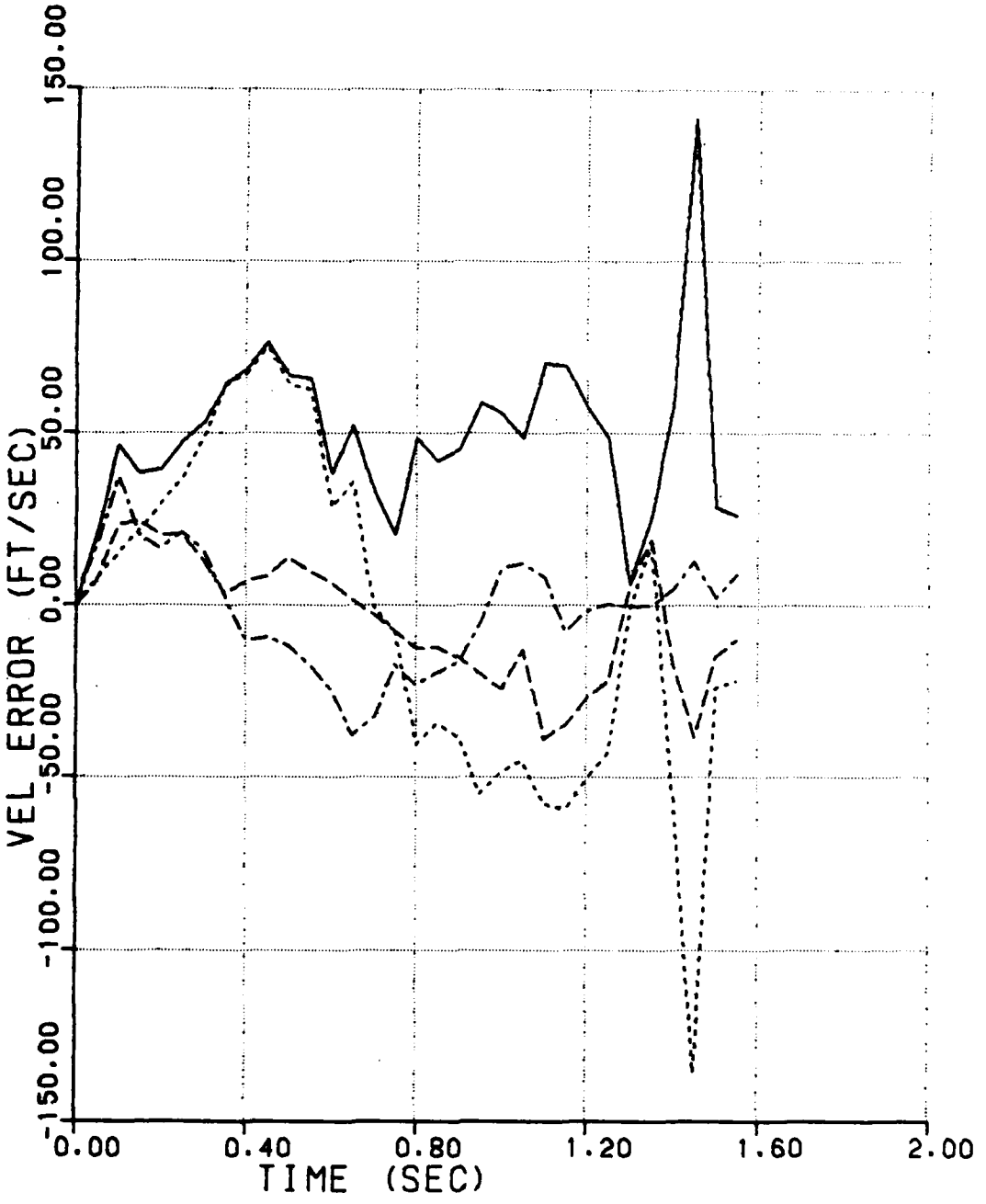

Figure 46. Velocity Error History for Engagement 4, Filter 2

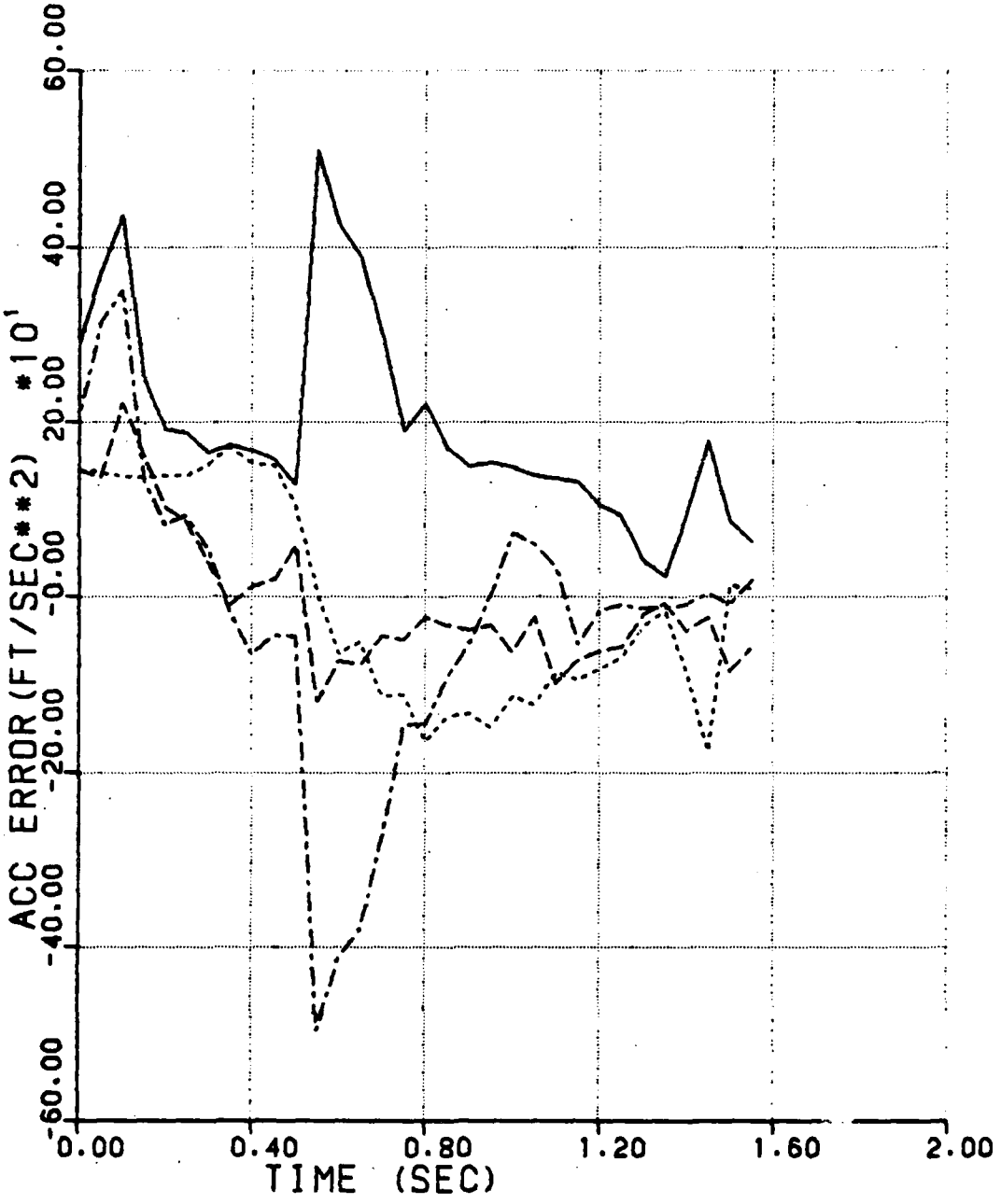

Figure 47. Acceleration Error History for Engagement 4, Filter 2

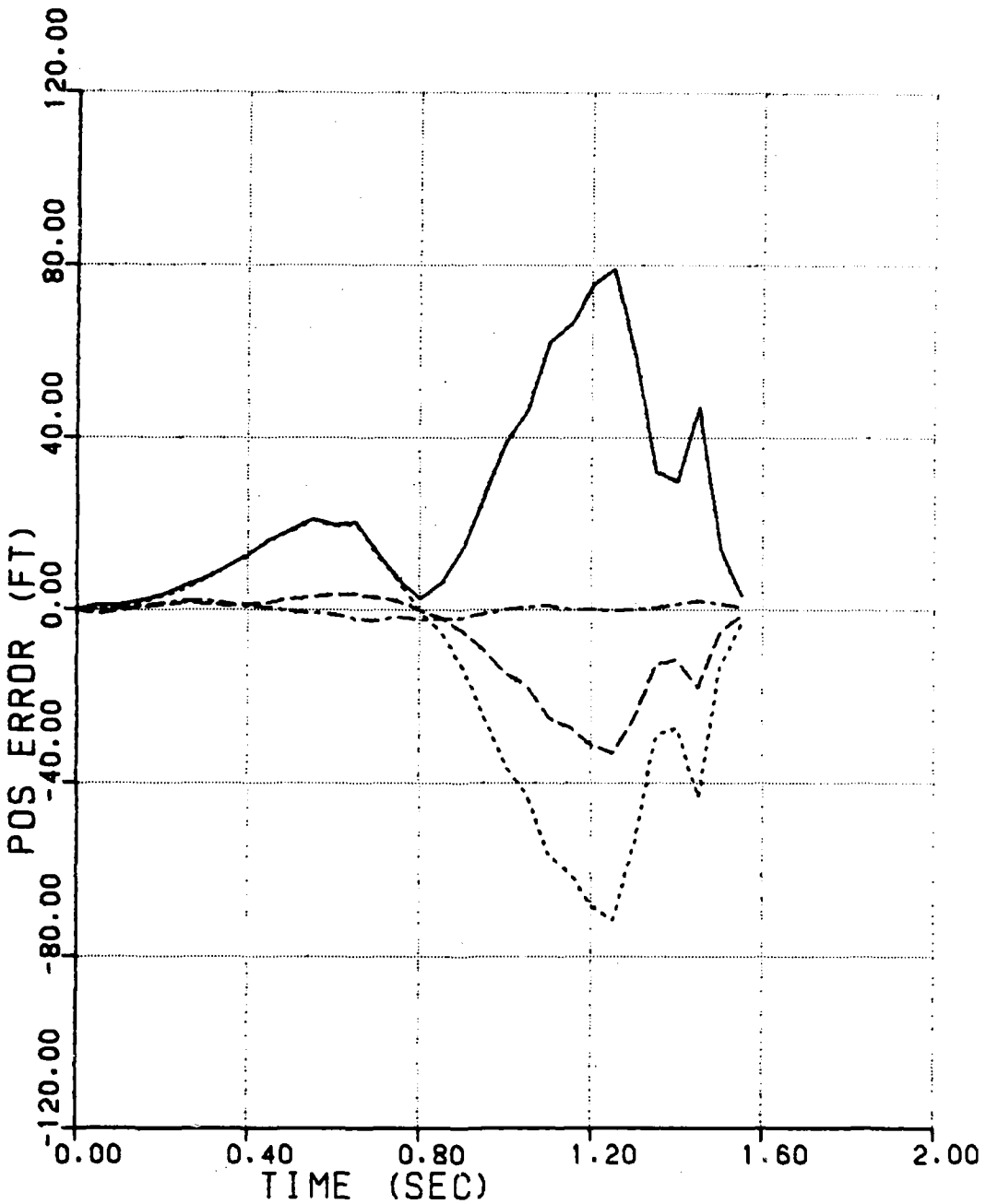

Figure 48. Position Error History for Engagement 4, Filter 3

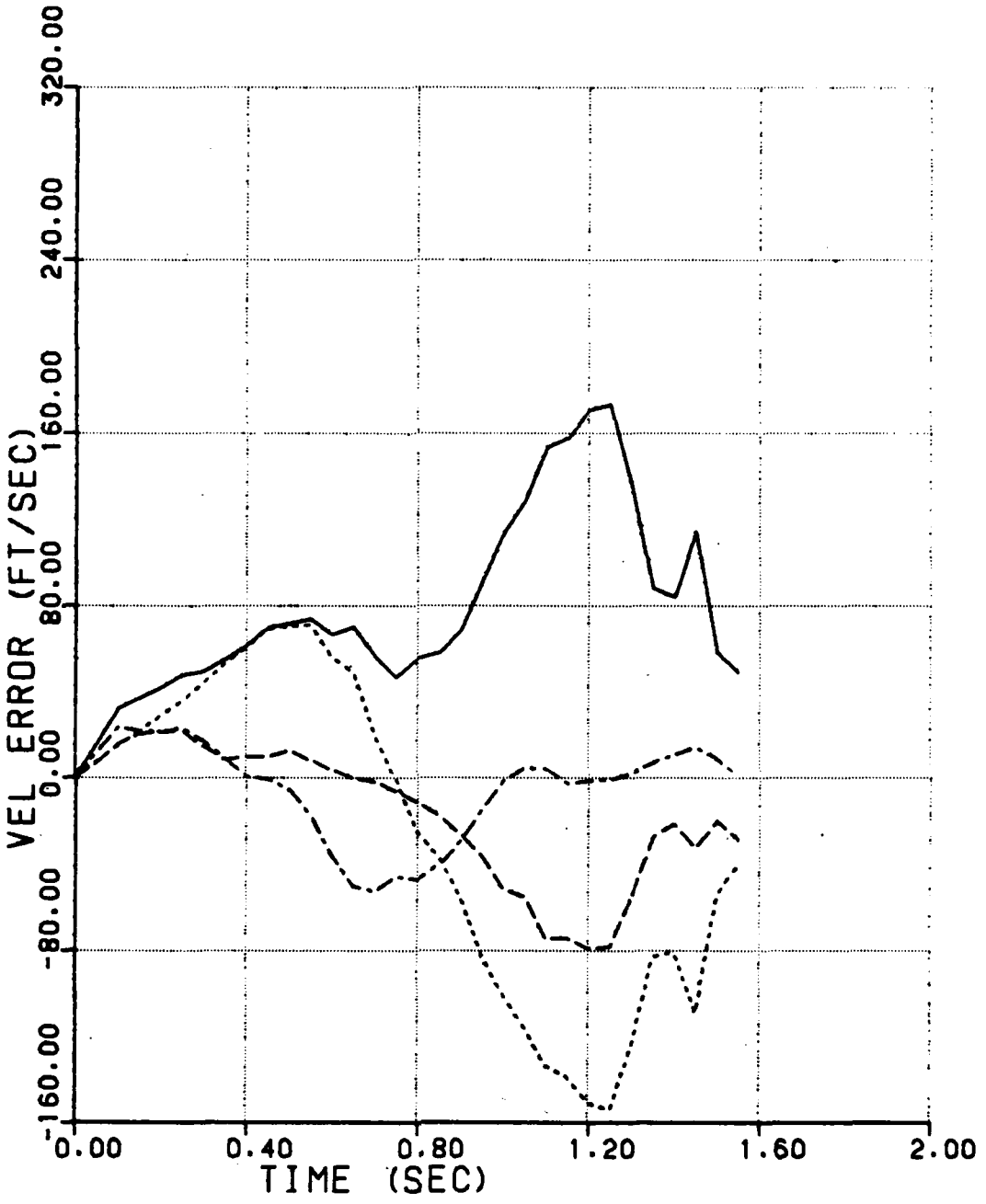

Figure 49. Velocity Error History for Engagement 4, Filter 3

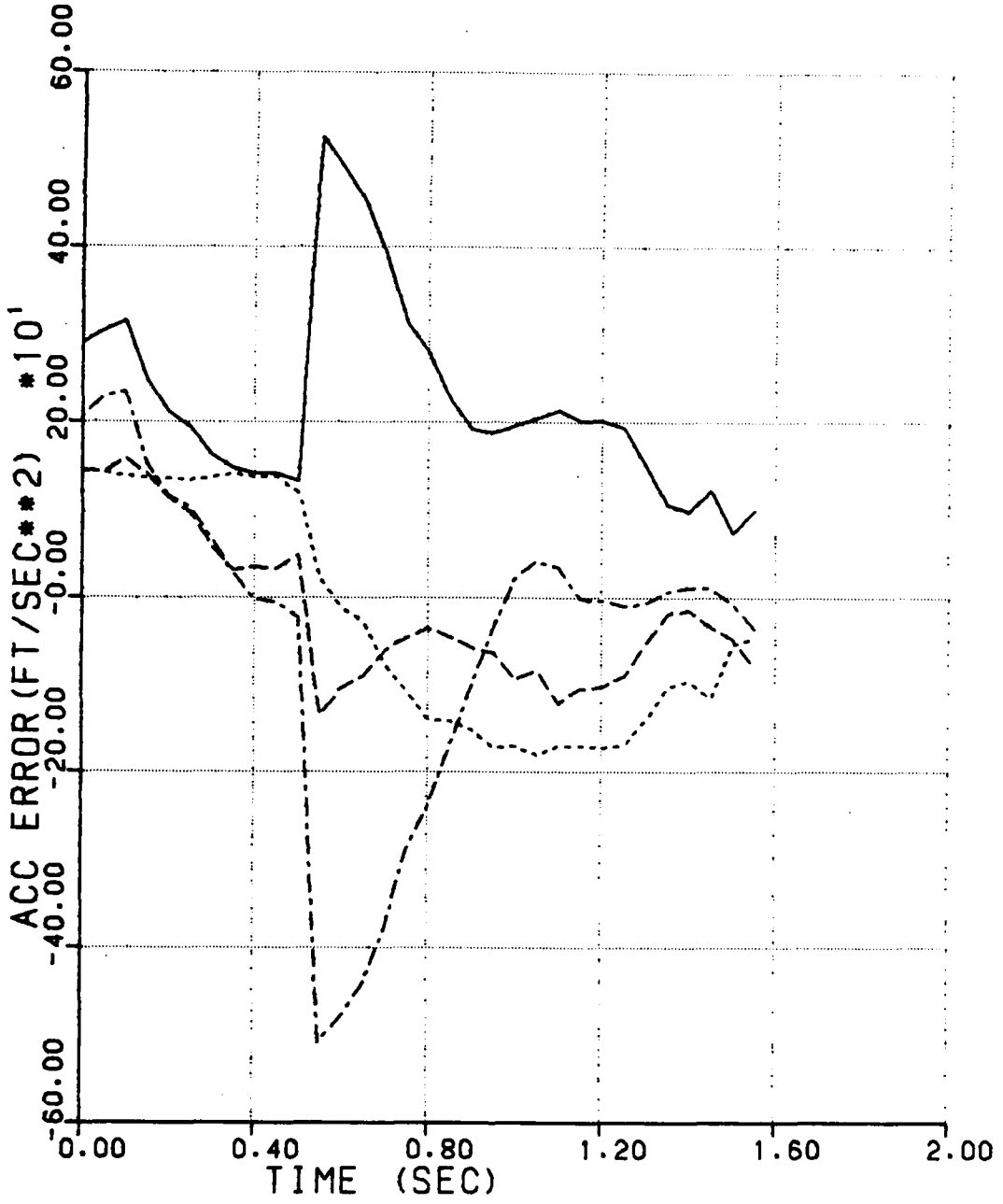

Figure 50. Acceleration Error History for Engagement 4, Filter 3

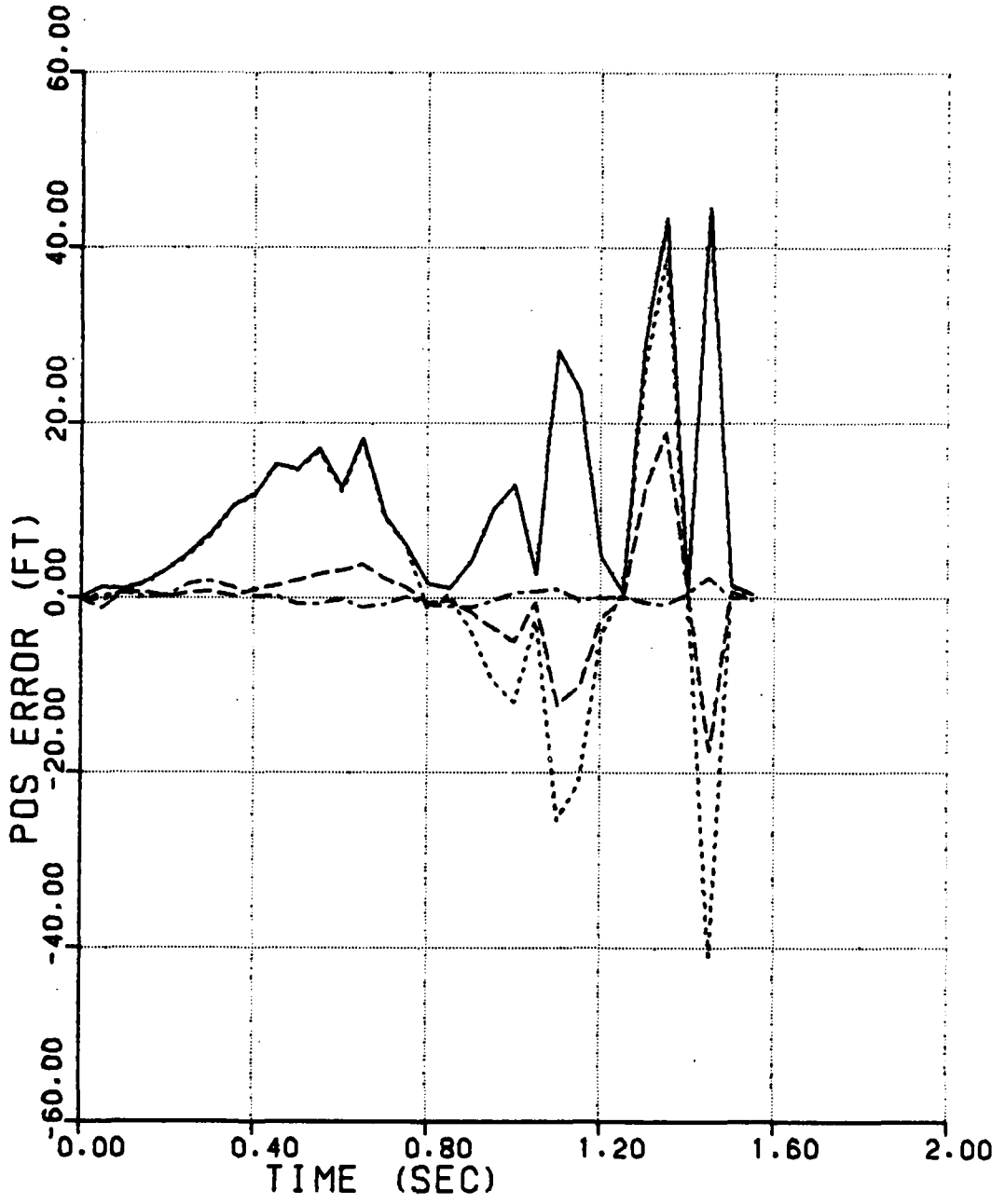

Figure 51. Position error History for Engagement 4, Filter 4

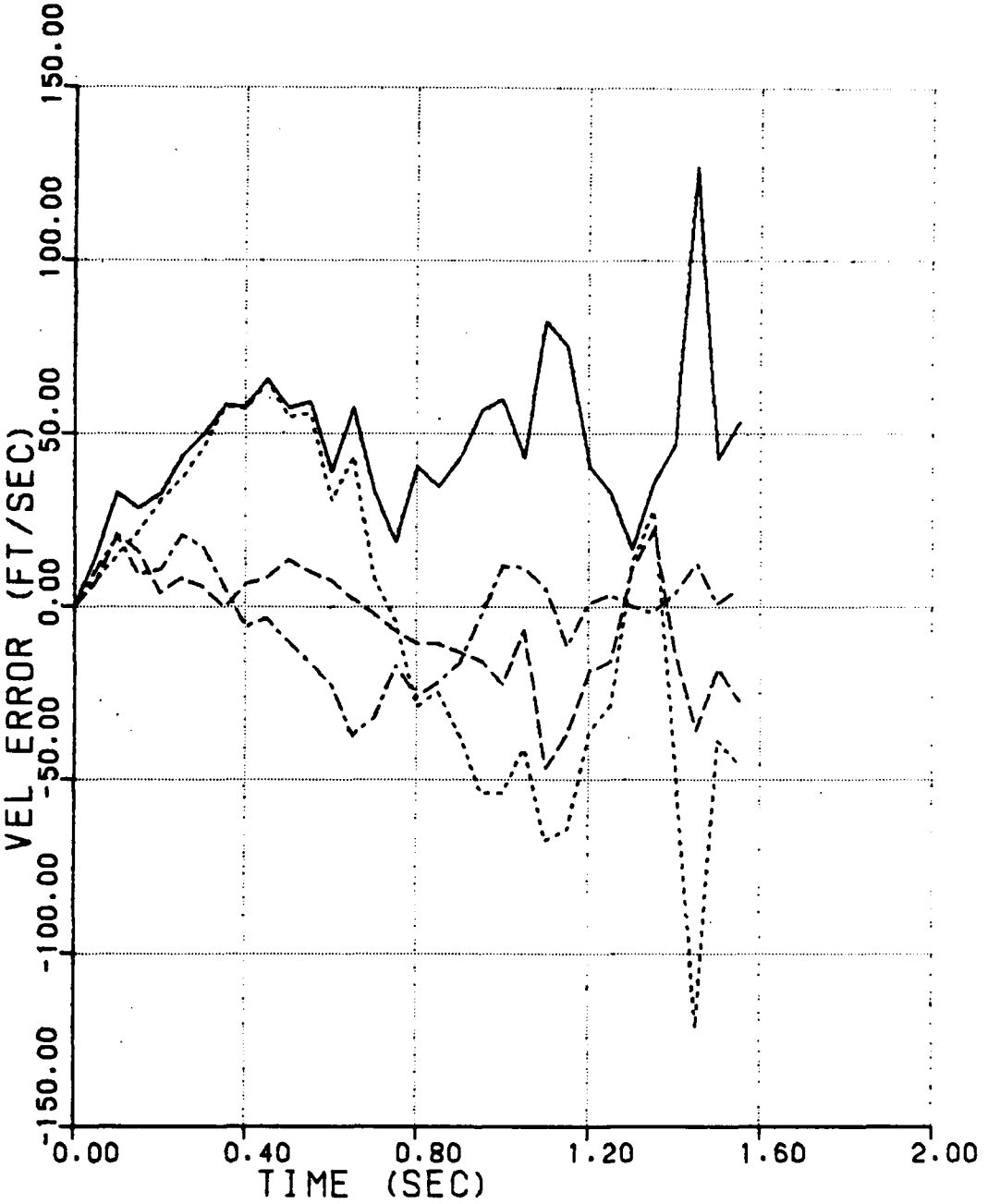

Figure 52. Velocity Error History for Engagement 4, Filter 4

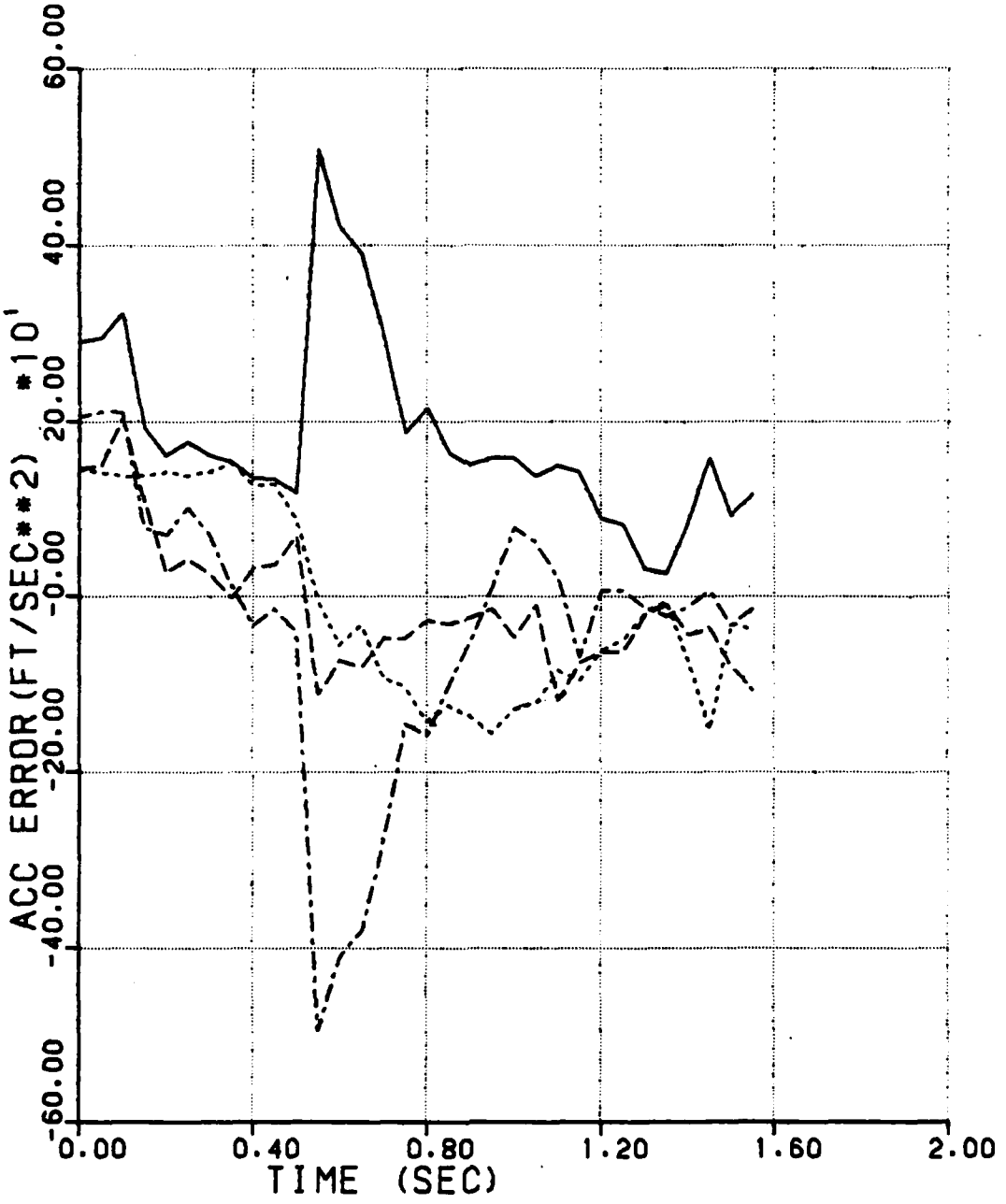

Figure 53. Acceleration Error History for Engagement 4, Filter 4

e. Engagement 5

The initial problem geometry for engagement 5 is presented in Figure 54. Again, the carrier aircraft is flying northward at 10,000 feet and a speed of Mach = 0.9 at launch. The target aircraft is also at 10,000 feet but is located on a line 40 degrees east of north relative to the carrier aircraft. The target aircraft is traveling southeastward at Mach = 0.9. The initial range is 3500 feet.

This is another short range problem with severe starting conditions. All of the filters performed acceptably in this condition which might cause problems with conventional proportional navigation systems. Surprisingly, the time-weighted adaptive extended Kalman filter performed poorest of the group (but still performed acceptably) while the iterated extended Kalman filter performed best of the group.

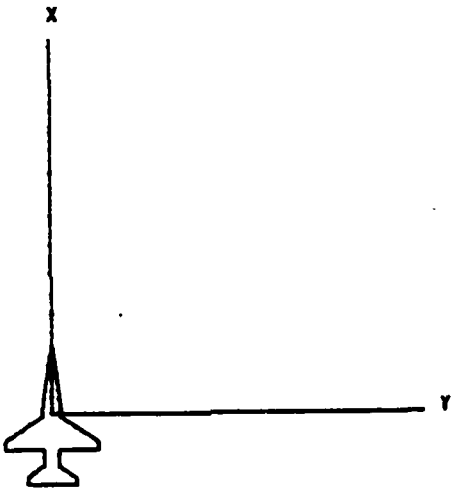

Figure 54. Engagement 5 Geometry

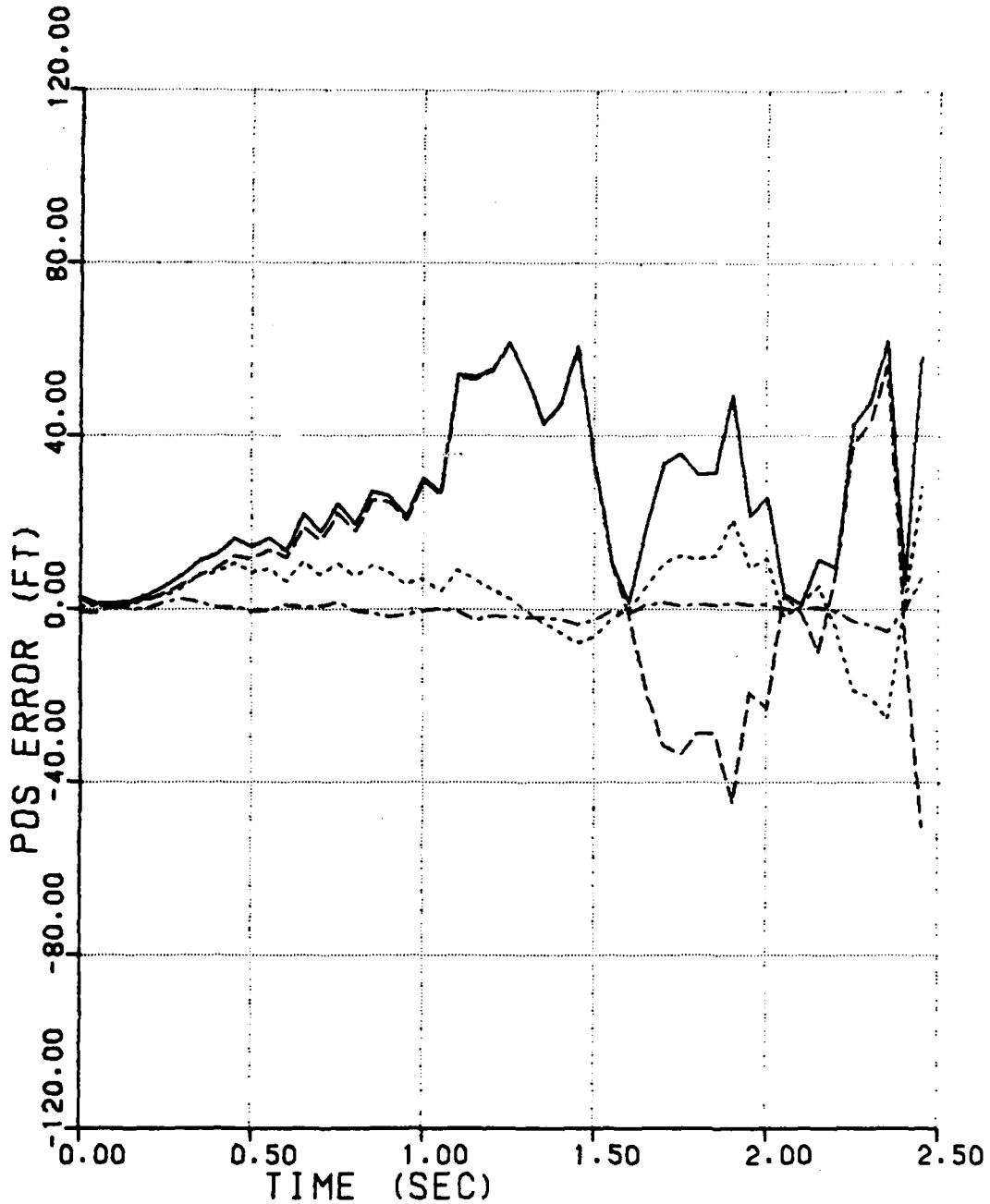

Figure 55. Position Error History for Engagement 5, Filter 1

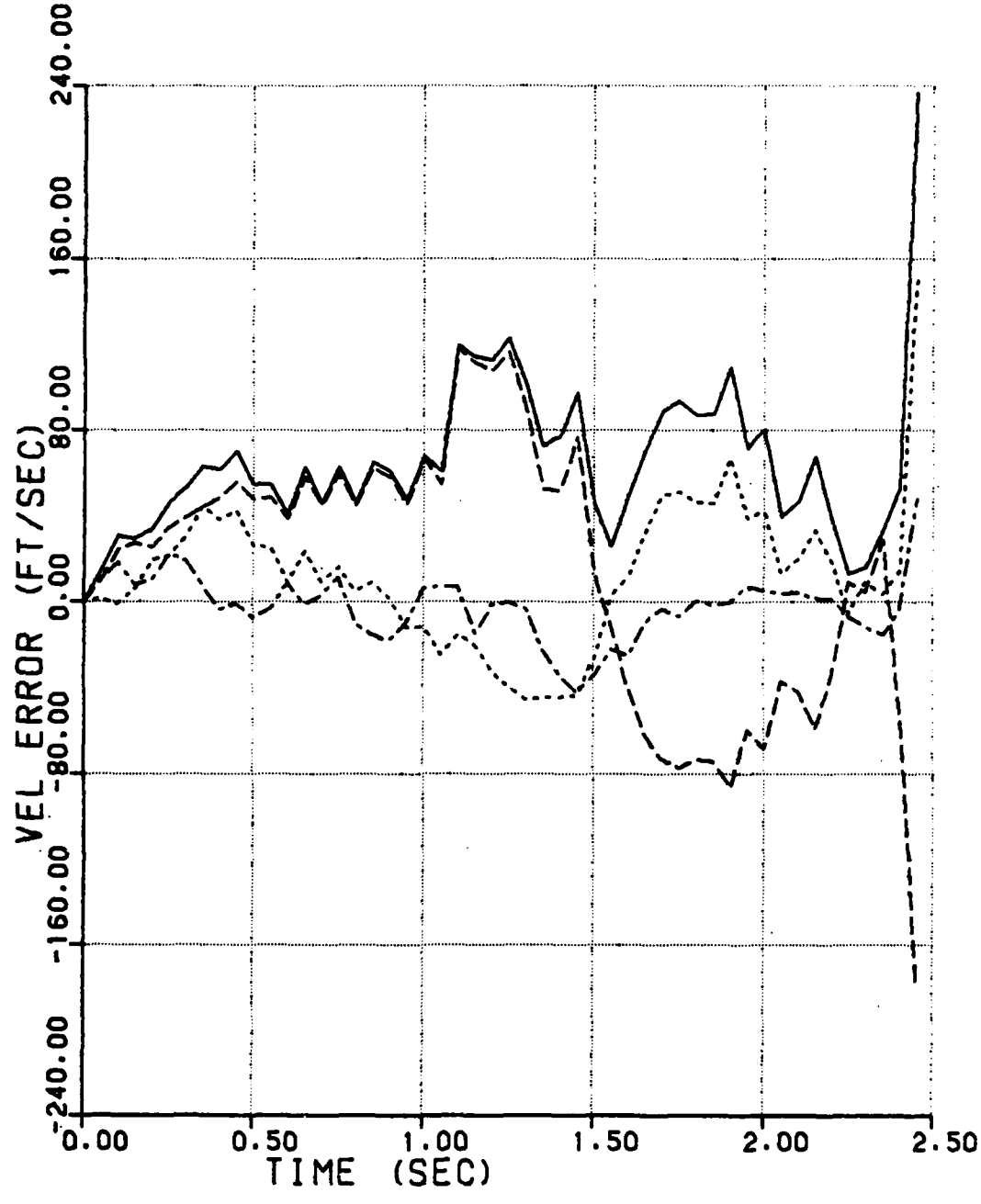

Figure 56. Velocity Error History for Engagement 5, Filter 1

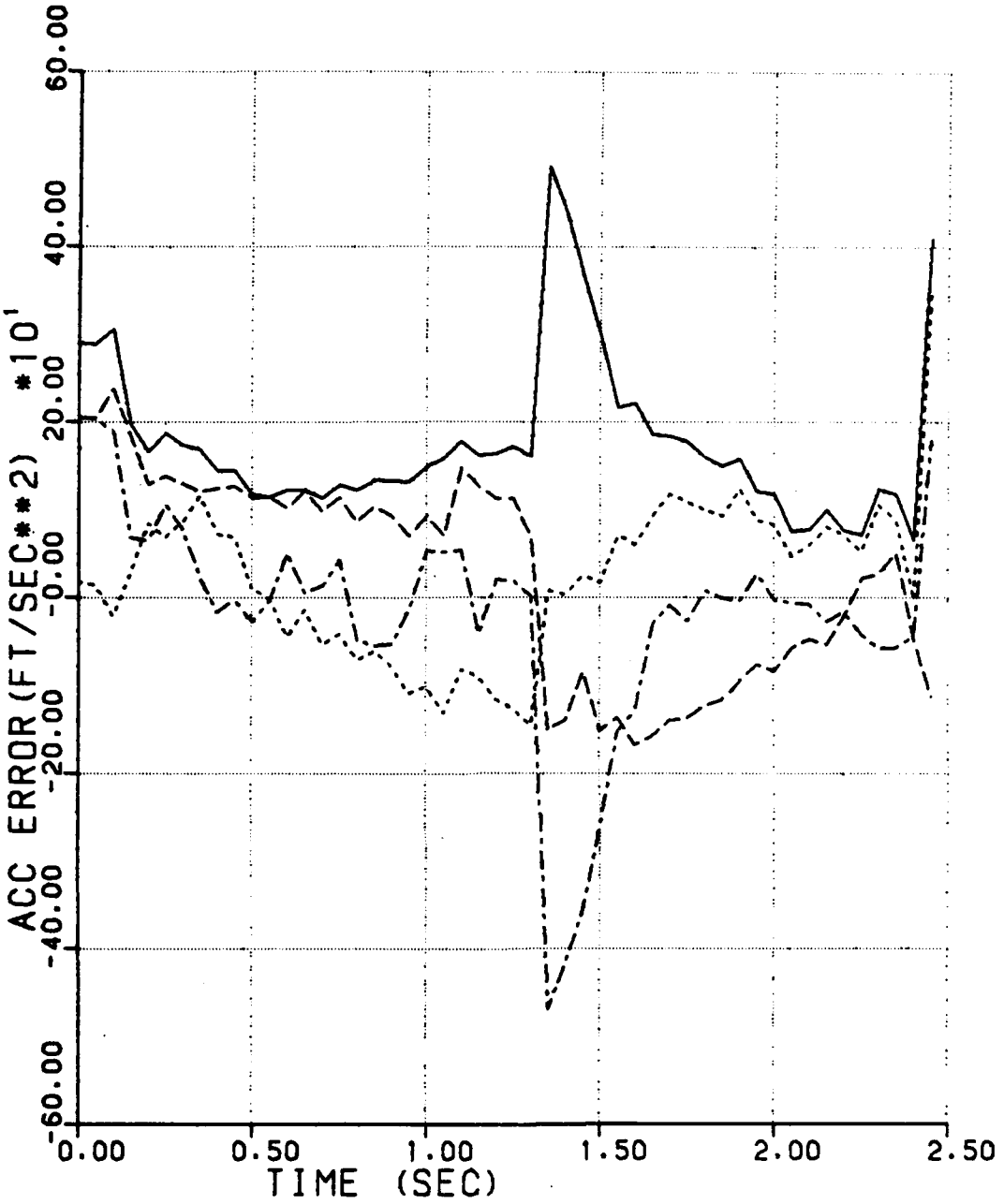

Figure 57. Acceleration Error History for Engagement 5, Filter 1

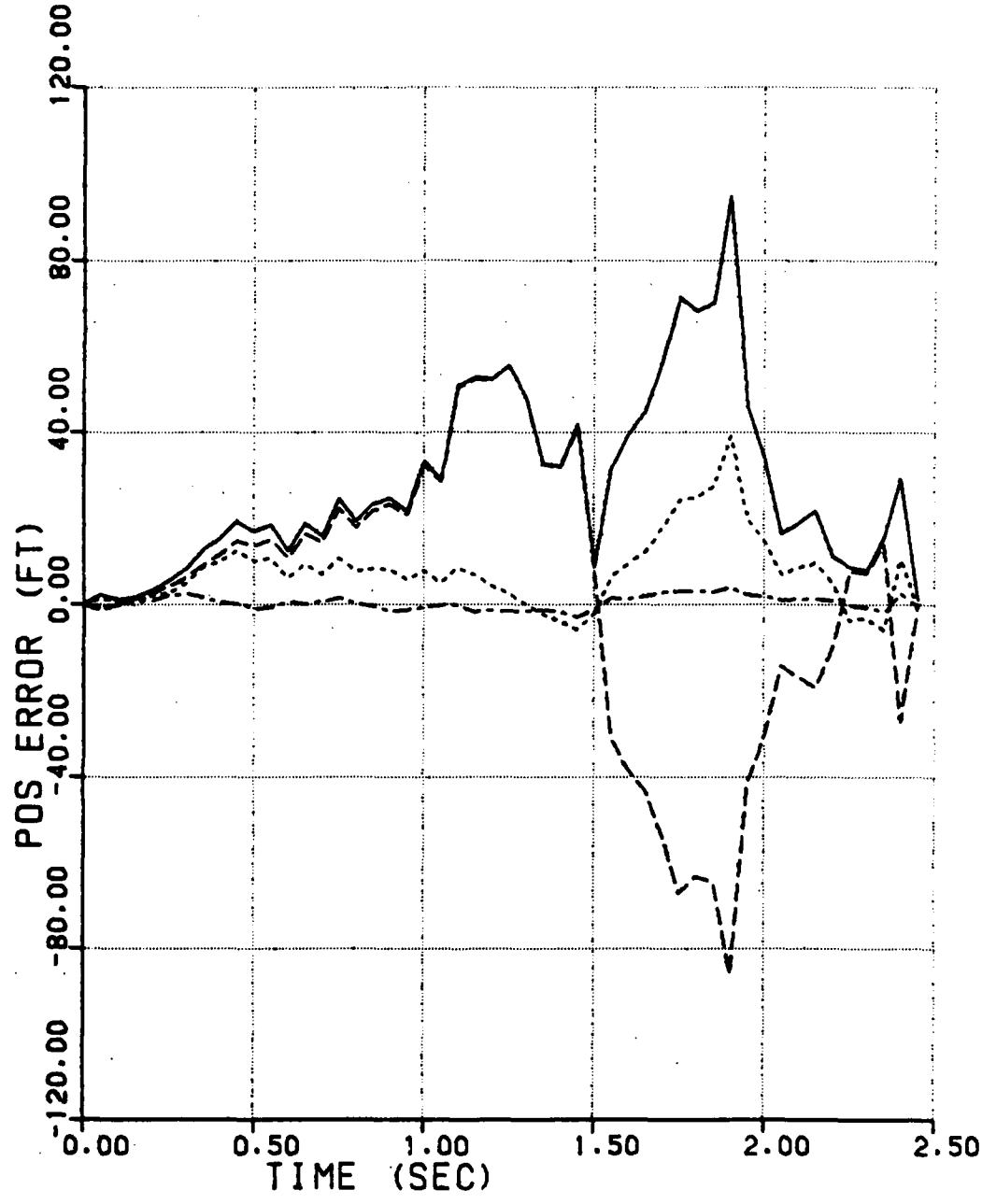

Figure 58. Position Error History for Engagement 5, Filter 2

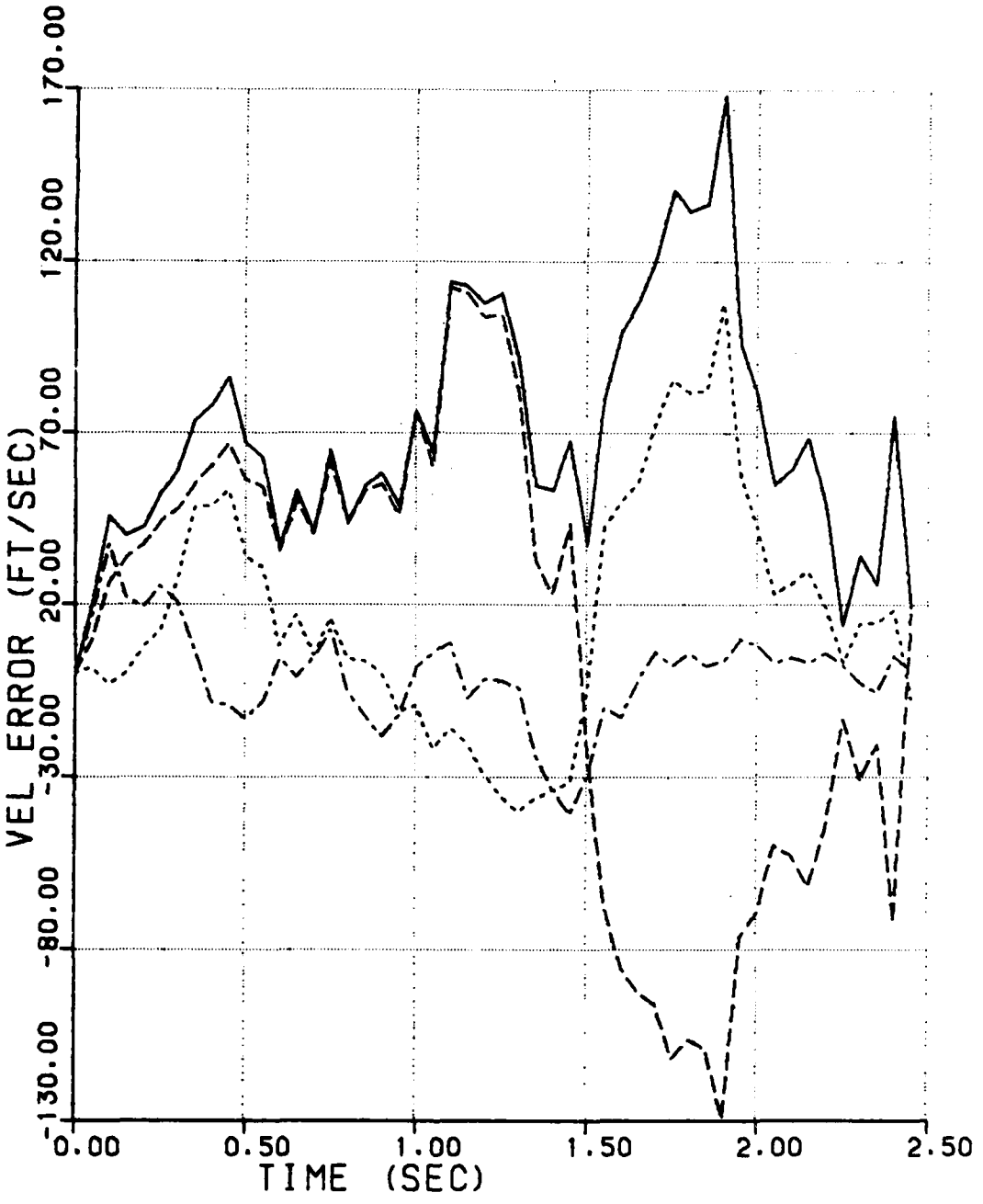

Figure 59. Velocity Error History for Engagement 5, Filter 2

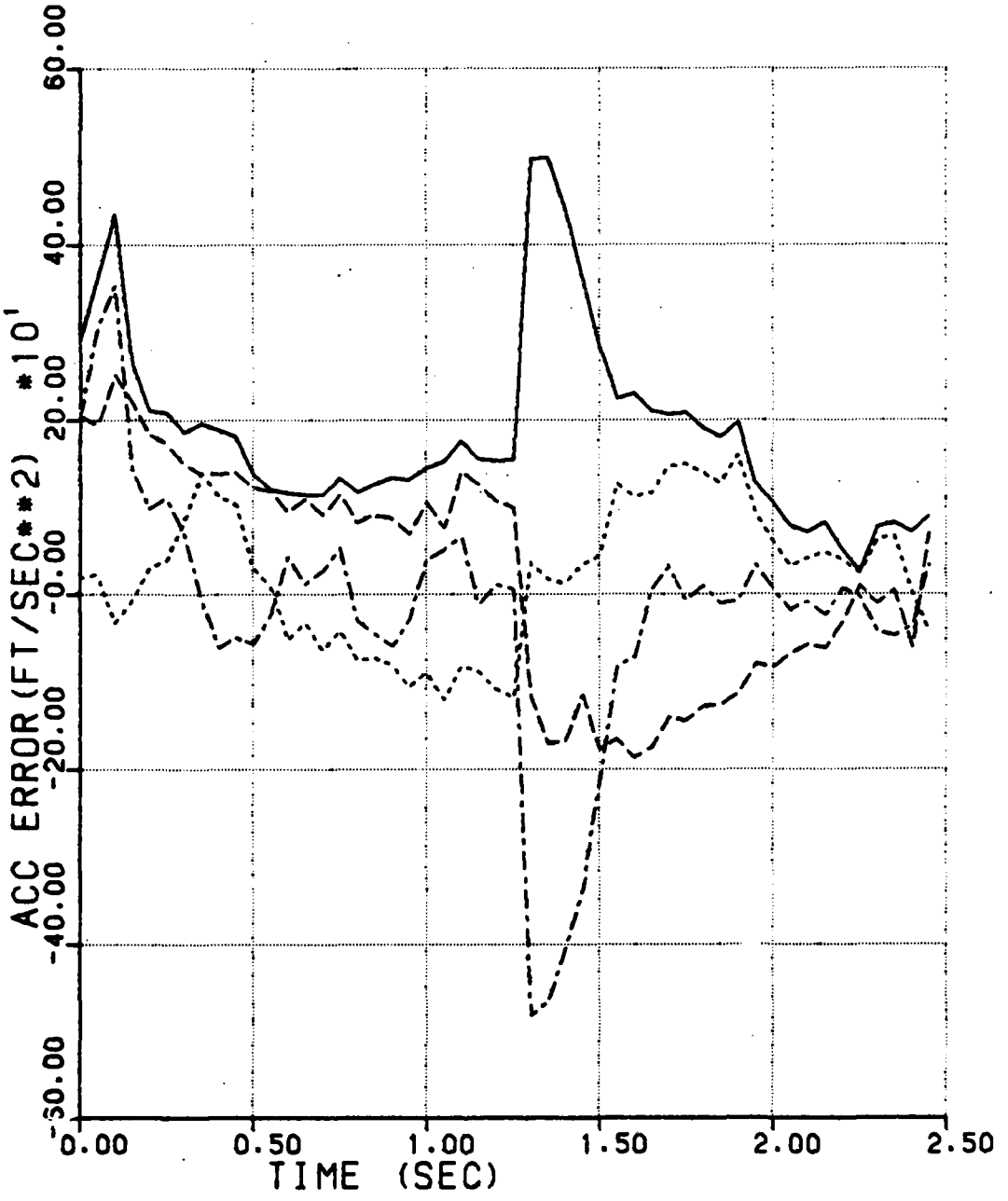

Figure 60. Acceleration Error History for Engagement 5, Filter 2

AD-A141 535 DEVELOPMENT AND COMPARISON OF ESTIMATION ALGORITHMS FOR AIRBORNE MISSILES(U) MISSISSIPPI STATE UNIV MISSISSIPPI STATE DEPT OF AEROPHYSICS A... K R HALL FEB 83 2/2

UNCLASSIFIED AFATL-TR-83-14 F08635-82-K-0107 F/G 12/1 NL

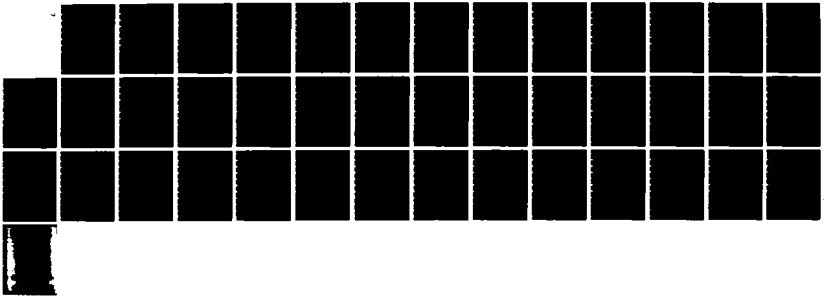

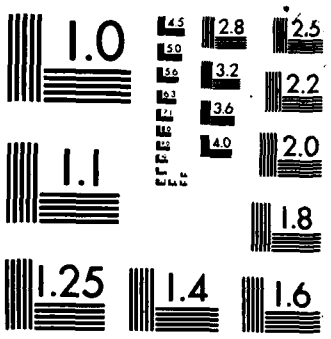

MICROCOPY RESOLUTION TEST CHART
NATIONAL BUREAU OF STANDARDS-1963-A

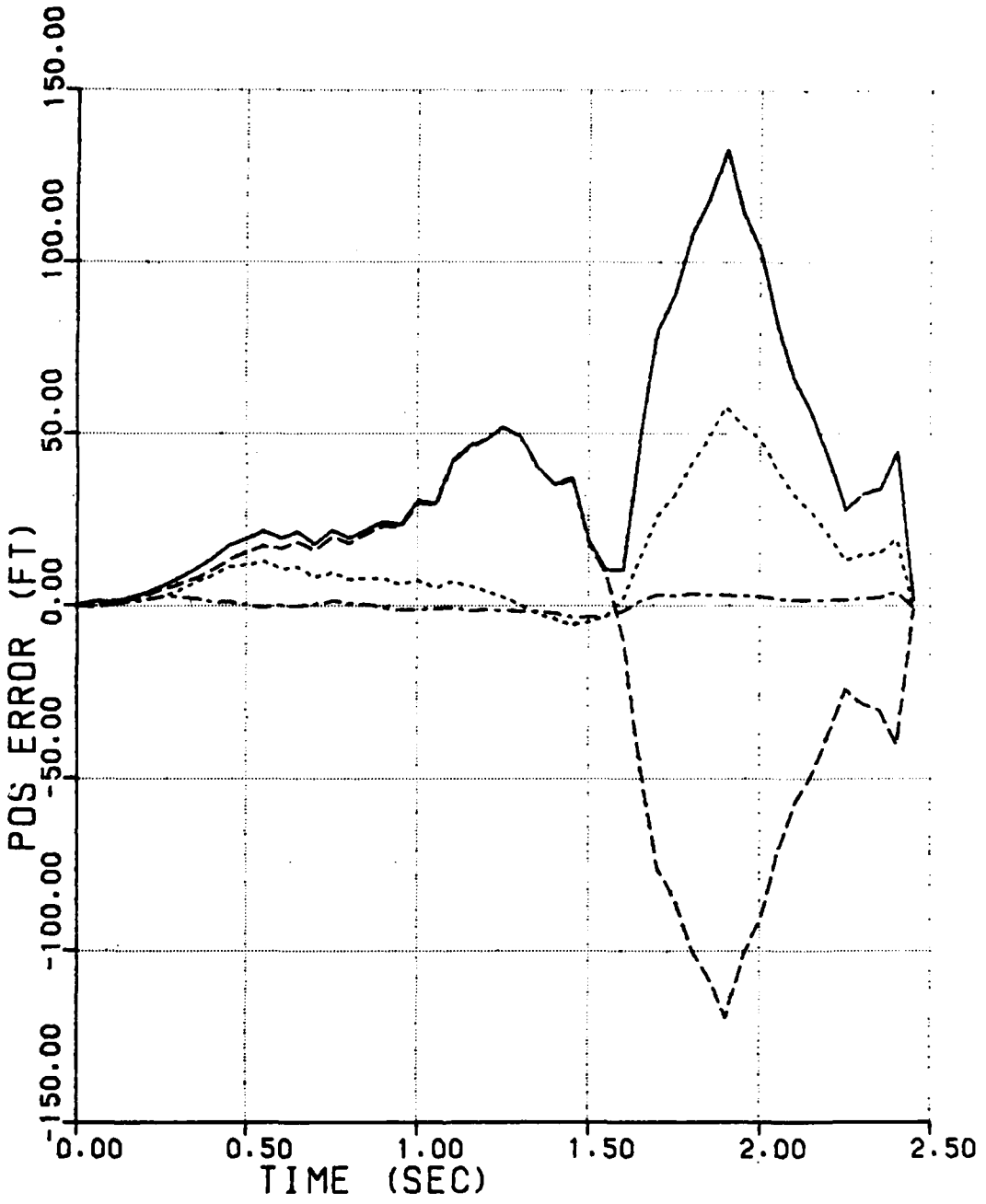

Figure 61. Position Error History for Engagement 5, Filter 3

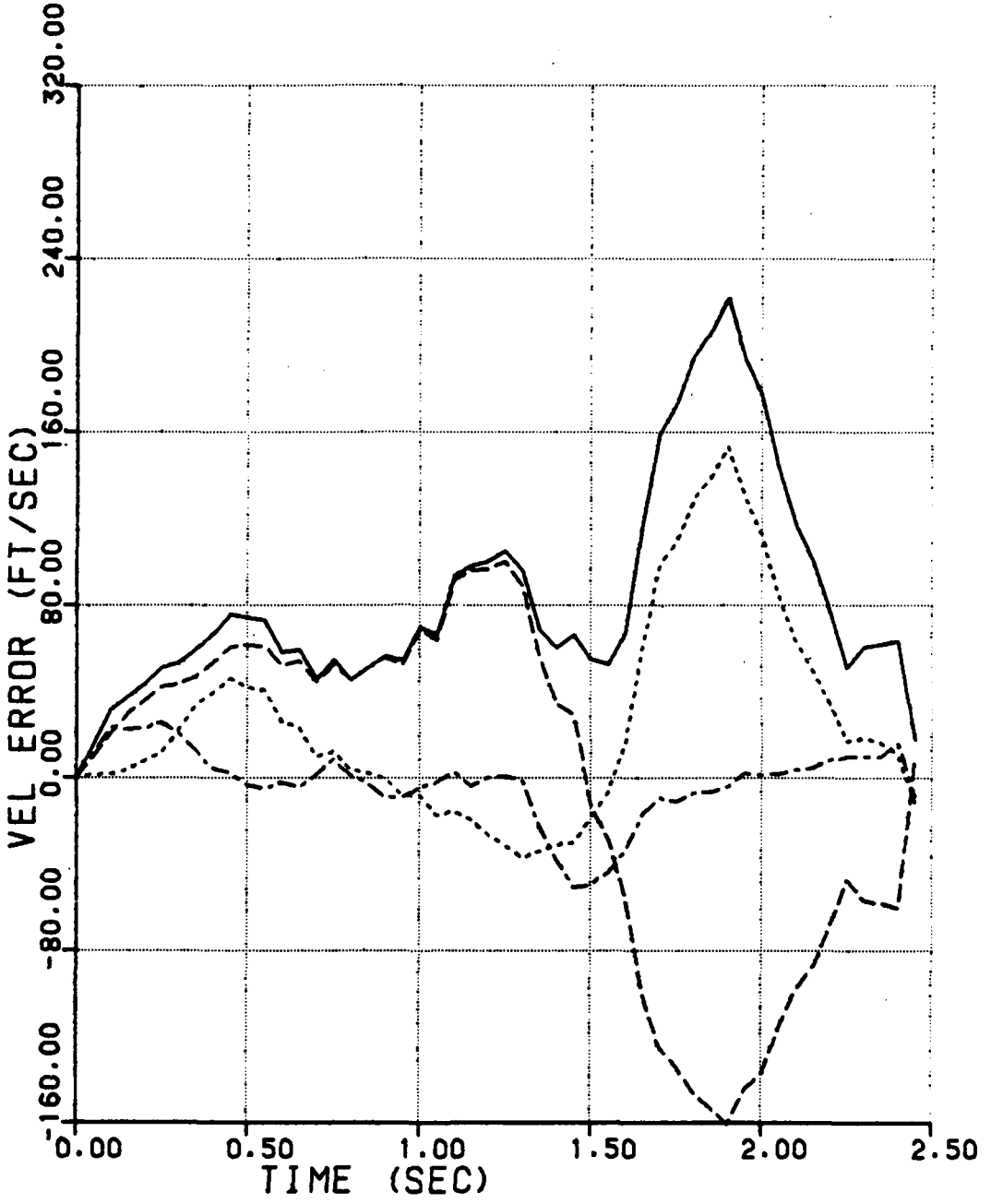

Figure 62. Velocity Error History for Engagement 5, Filter 3

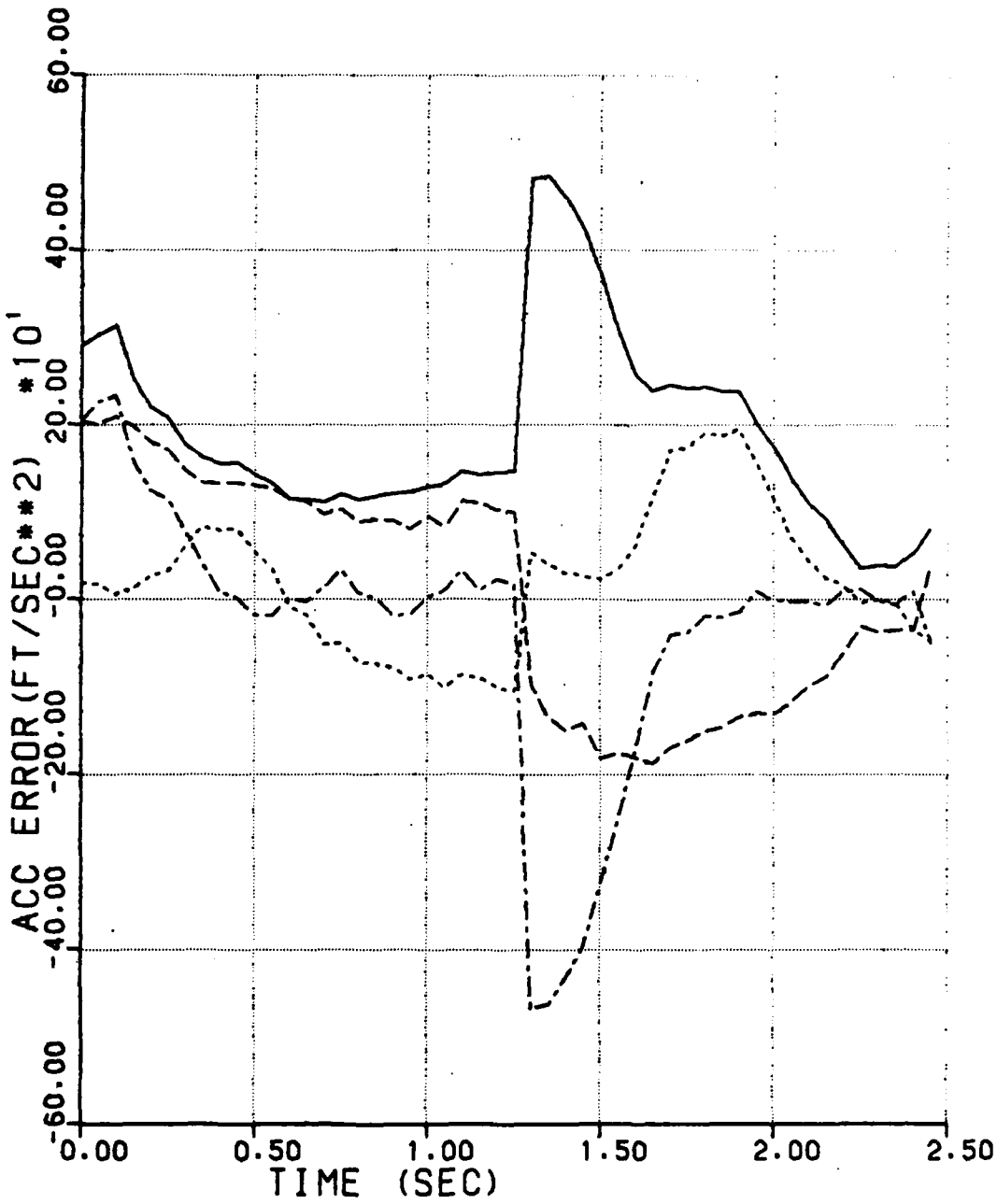

Figure 63. Acceleration Error History for Engagement 5, Filter 3

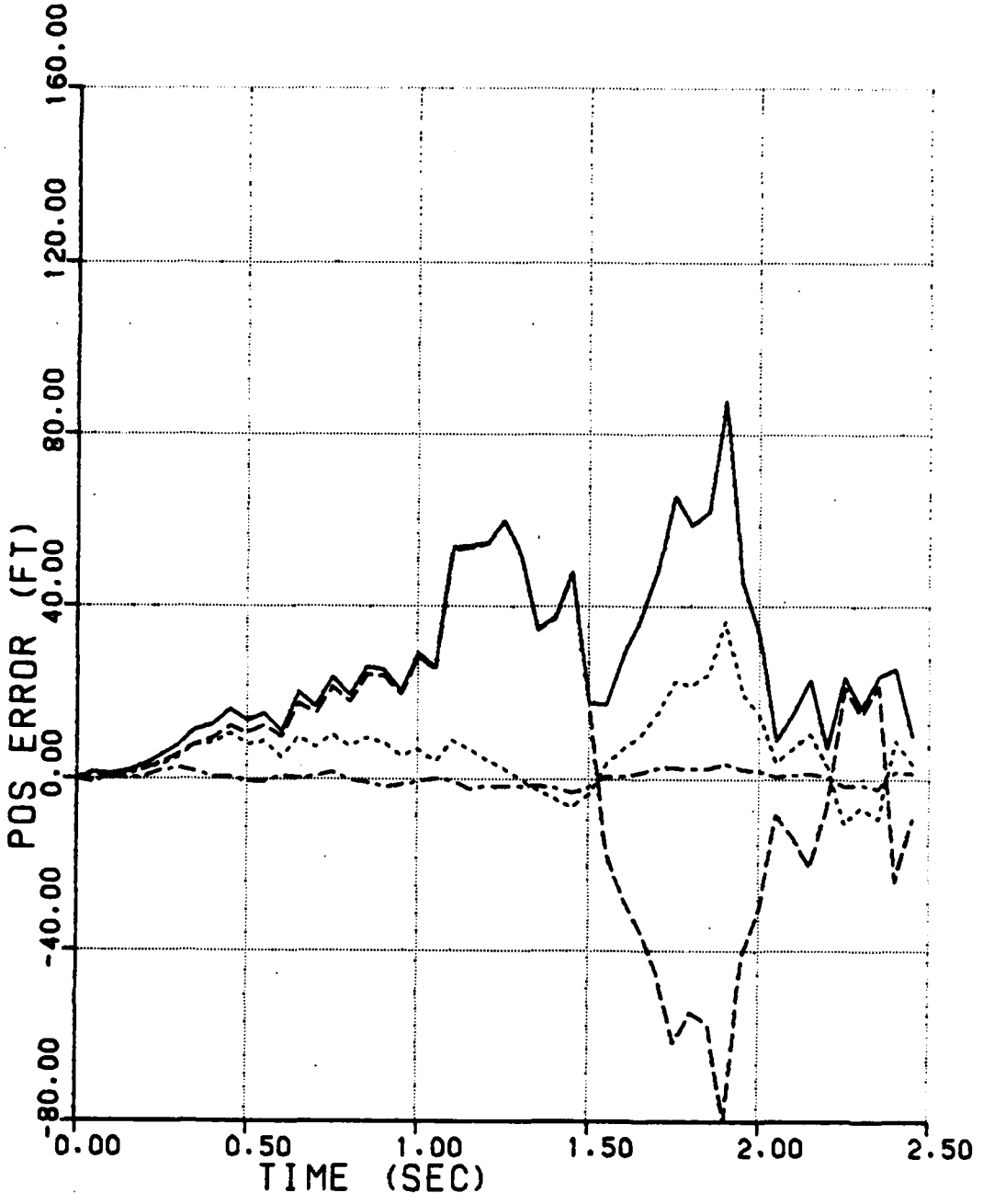

Figure 64. Position Error History for Engagement 5, Filter 4

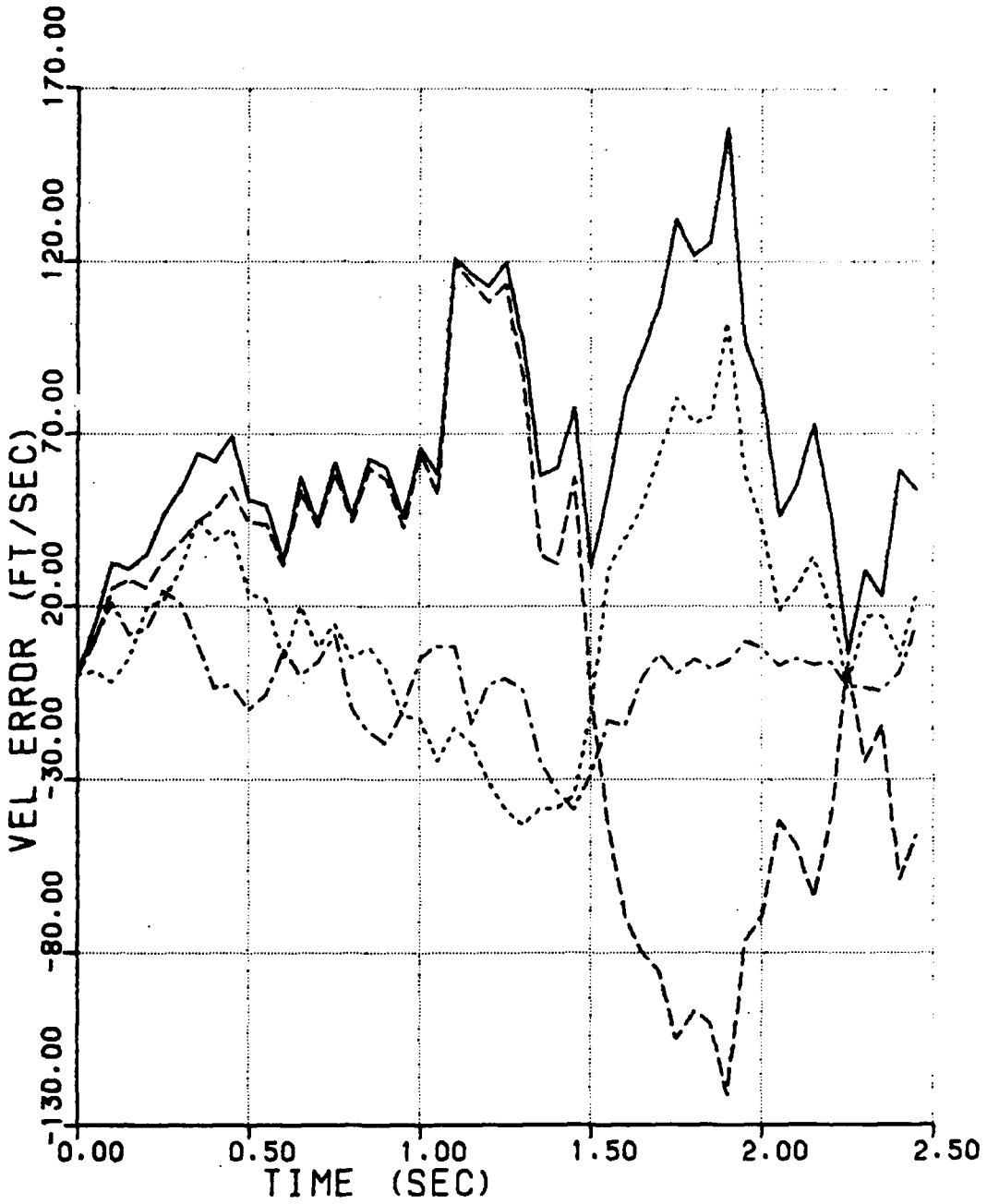

Figure 65. Velocity Error History for Engagement 5, Filter 4

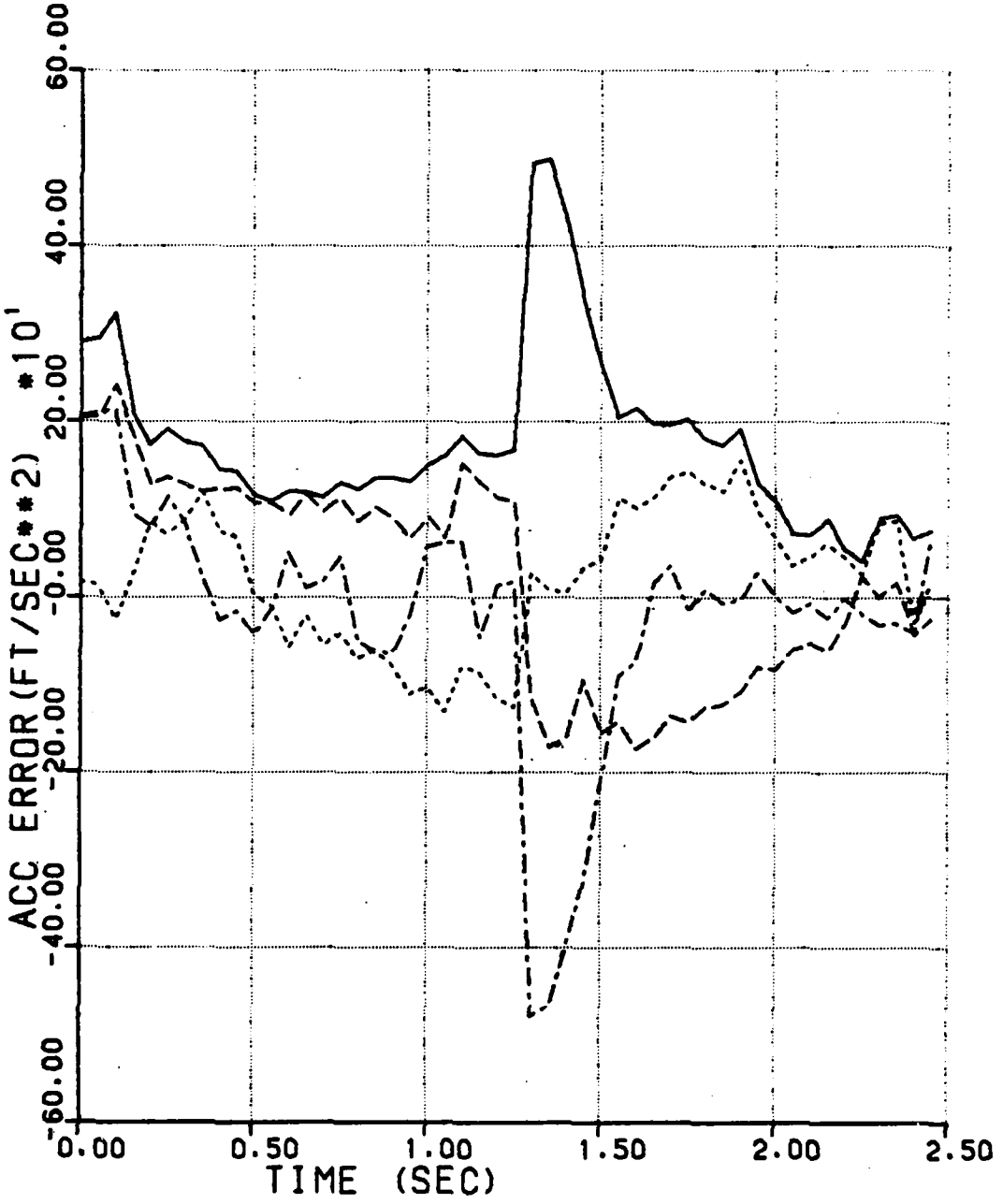

Figure 66. Acceleration Error History for Engagement 5, Filter 4

2. Numerical Comparisons

FILTER NO.	FILTER BEGINS TO DIVERGE (SEC)	MAX ERR (FT)	TIME OF MAX ERR (SEC)	ENSEMBLE MISS DIS (FT)
----------Engagement 1 Results----------				
1	1.65	3156	5.5	5.23
2	2.00	2124	5.3	4.47
3	2.60	870	5.3	2.19
4	2.00	3106	5.3	5.25
----------Engagement 2 Results----------				
1	1.70	3245	5.3	5.24
2	2.15	1715	5.5	3.31
3	2.25	494	5.6	2.90
4	1.70	2865	5.45	5.25
----------Engagement 3 Results----------				
1	2.00	2789	5.1	7.48
2	2.00	1954	5.3	4.55
3	3.10	589	5.8	3.95
4	2.00	2528	5.2	6.10
----------Engagement 4 Results----------				
1	0.05	40.5	1.45	4.42
2	0.05	52.6	1.45	7.00
3	0.10	78.6	1.25	3.81
4	0.05	44.6	1.45	6.61
----------Engagement 5 Results----------				
1	0.10	61.9	2.35	3.75
2	0.10	71.4	1.75	3.32
3	0.15	132.7	1.90	3.81
4	0.10	87.8	1.90	2.62

SECTION V

CONCLUSIONS

Four forms of the extended Kalman filter have been investigated for five different launch conditions in a simulated air-to-air combat scenario. All of the estimation algorithms performed in an acceptable manner in that all filters allowed the missile to come within ten feet of the target and that is considered a hit. The comparison of the filter performance along the entire trajectory provides more insight into the filter performance than comparing miss distance alone. The regular extended Kalman filter consistently performs the poorest when maximum estimation error and rapidity of adjustment to changing conditions are the judging criteria. The use of an adaptive filter which uses a local window of measurements to compute the measurement noise statistics significantly improves the performance of the regular extended Kalman filter. The use of time weighting of the measurement data again significantly improves the filter performance in reducing the maximum estimation error and also in adaptation to changing conditions. The iterated extended Kalman filter did not perform as well as expected, but additional work in this filter is expected to be profitable. The iterative nature of the filter is expected to smooth the error history and provide better estimates. At the current time, the use of the extended Kalman filter which uses adaptation to local conditions with time weighting to improve the rapidity of adjustment to changing conditions is highly recommended.

One note of caution for the casual reader these filters have been used with a linear quadratic control law where the determination of the final time is paramount in determining the optimal control. The best filter will perform poorly if

coupled with a poor control system. The future work of this group in exploring the options for the control system hold great promise for improving the overall system performance and thereby improving the estimation process.

APPENDIX A

DISCRETE STATE PROPAGATION EQUATIONS

Let the following expression represent the vector differential equation for a system governed by a set of linear, first order, ordinary differential equations.

$$\dot{X} = A\,X + B\,U$$

In the equation above, the coefficient matrices A and B may be constant matrices, matrices which are functions of time explicitly , or matrices which are functions of X as well as time. For this application, the matrices are constant coefficient matrices.

The control vector U may be time varying, but for this application, the control vector will be considered piecewise constant. This means that the control value will be held constant between commands and that the control reaches the commanded value immediately. This is an obvious approximation, but this is the development of a model for the estimation process, so the approximation is acceptable.

The solution of the state propagation equation is most easily obtained through use of the principle of superposition.

Let the state at some time t(k) be propagated from the state at some time t(k-1). Let X(k)=Y(k)+Z(k) where Y(k) represents the propagation of the initial conditions from t(k-1) to t(k) with zero forcing function and Z(k) represents the state response at t(k) to the forcing function between t(k-1) and t(k) calculated from zero initial conditions.

First, consider the Y response.

$$\dot{Y} = A\ Y$$

$$Y(k) = e^{A\ [t(k)-t(k-1)]}\ Y(k-1)$$

Let F(k,k-1) designate the state transition matrix which is represented by the exponential matrix term.

$$F(k,k-1) = e^{A\ [t(k)-t(k-1)]}$$

Now, the solution to the linear, homogenous, ordinary vector differential equation may be written in terms of the state transition matrix in the following manner.

$$Y(k) = F(k,k-1)\ Y(k-1)$$

Now, consider the response to the forcing function independently of the response to the initial conditions. Again, let Z(k) denote the response at time t(k) due to any forcing function between t(k-1) and t(k). For simplification, we will consider the forcing function B U to have a zero value everywhere within the interval t(k-1) to t(k) except for a small time interval "dt" located at time t(j) between t(k-1) and t(k). The response at t(k) will therefore be the response to an impulse occurring at t(j).

$$\dot{Z} = A\ Z + B\ U$$

Since this equation begins with zero initial conditions, the response will remain zero until reaching the time t(j) when the forcing function becomes non-zero. The time interval "dt" over which there is a non-zero forcing function is considered to be so small that the differential equation governing this portion of the total response may be represented by the following equation.

$$\dot{Z} = B\ U$$

At the end of the interval, "dt", the forcing functon is removed and the Z-response at this time is given by the following equation.

$$Z\ [t(j) + dt] = B\ U\ [t(j)]\ dt$$

The interval, "dt", over which the impulsive forcing function is defined is so small that the result may be interpreted as an instantaneous change in the state occurring at time t(j). The response at time t(k) may now be obtained by propagating this initial condition from time t(j) to time t(k) with no forcing function.

$$Z(k) = F(k,j)\ Z(j) = F(k,j)\ B\ U(j)\ dt$$

If there are two small intervals located at times t(i) and t(j), over which there is an impulsive forcing function, then the total response at time t(k) is the sum of the individual responses at time t(k).

$$Z(k) = F(k,i)\ B\ U(i)\ dt(i) + F(k,j)\ B\ U(j)\ dt(j)$$

For many small intervals of non-zero values of the forcing function, the total response at t(k) may be written as a summation of the individual responses to the individual impulses.

$$Z(k) = \sum_i F(k,i)\ B\ U(i)\ dt(i)$$

As the series becomes large and the size of the intervals becomes small, then the series becomes an integral. In this way, we may consider any continuous function between t(k-1) and t(k) to be composed of an

infinite number of small intervals with the function continuous within each small interval but varying from small interval to small interval.

$$Z(k) = \int_t F(k,t)\ B\ U(t)\ dt$$

The total solution at time t(k) may now be obtained from superposition.

$$X(k) = Y(k) + Z(k)$$

$$X(k) = F(k,k-1)\ X(k-1) + \int_{t(k-1)}^{t(k)} F(k,t)\ B\ U(t)\ dt$$

If we now assume instantaneous response of the control and assume that the control is held constant in the interval between t(k-1) and t(k), the discrete times when the state is available, the equation above may be simplified.

$$X(k) = F(k,k-1)\ X(k-1) + \int_{t(k-1)}^{t(k)} F(k,t)\ B\ U(k-1)\ dt$$

Let us investigate the quantity in brackets. Assume that the state propagation process occurs in steps of constant time increments given by DT = t(k)-t(k-1). The limits on the integration can be made to be "0" and "DT" for this process. All appearances of t(k)-t(k-1) which happened in the earlier development may now be replaced with DT.

$$F(k,k-1) = e^{(A\ DT)}$$

The state transition matrix F(k,k-1) is a constant matrix for a constant coefficient matrix ,"A", and for a constant interval, "DT". This constant state transition

matrix will be identified with a single letter "F" from this time on.

Define a control transition matrix, G(k,k-1), which may be used to show the influence of the constant control in the interval t(k-1) to t(k) upon the state response at time t(k).

$$G(k,k-1) = \int_{t(k-1)}^{t(k)} F(k,t)\ B\ dt$$

Note that the functional form of the state transition matrix "F" is used in the evaluation of the control transition matrix "G", not the constant "F". Also note that for a constant interval "DT", the control transition matrix will be a constant matrix. The single letter "G" will be used to refer to the constant control transition matrix.

The values of F and G may be precomputed and stored as they are constant matrices. Thus, the continuous differential equations governing the state propagation may be replaced with the discrete recursive state propagation equations.

$$\dot{X} = A\ X + B\ U$$

becomes

$$X(k) = F\ X(k-1) + G\ U(k-1)$$

This is the form to be used in subsequent developments.

APPENDIX B

LINEAR QUADRATIC CONTROL LAW

This section of the report considers the development of the control law which provides optimal control to a system trying to minimize a chosen performance index.

The control law will be developed for a system which obeys a set of linear, first order, ordinary differential equations with constant coefficient matrices. Following the notation used in the equations of Appendix A, the linear differential equations of motion may be represented as follows.

$$\dot{X} = A\,X + B\,U$$

Beginning at some time T, the problem is to determine the control law which is used to specify the control "U" such that some measure of performance ("J", the performance index) may be minimized. For this particular problem, the performance index is chosen as a combination of the final state and the integral control power required to produce the final state.

$$J = .5\ XF'\ S\ XF + \int_{T}^{TF} .5\ U'(t)\ W\ U(t)\ dt$$

The matrices S and W are positive-definite, weighting matrices with S being the final state weighting matrix, and W being the control power weighting matrix. Both of these matrices are constant matrices for this problem. The symbol XF refers to the state value at the time TF.

Now, considering that at some time T, the current

state is known, the problem is to determine U which produces the optimal trajectory based upon the performance index while obeying the differential equations of motion.

An augmented performance index is formed by appending the differential equation constraints to the original performance index through the use of a costate vector, "P".

$$H = .5\ U'W\ U + P'(A\ X + B\ U - \dot{X})$$

$$AJ = .5\ XF'\ S\ XF + \int_{T}^{TF} H(t)\ dt$$

In the expressions above, "H", the augmented integrand of the performance index is known as the numerical Hamiltonian. The augmented performance index, "AJ", can now be minimized with no constraints, and this is equivalent to minimizing the original performance index with the differential constraints.

Set the first variation of the augmented performance index equal to zero, and obtain the necessary conditions to produce a minimum of the augmented performance index and a minimum of the original performance index. Note that the original performance index was a quadratic form with positive definite weighting matrices, so only a minimum exists for this problem. Determining the necessary conditions will therefore completely solve the problem.

Setting the first variation of the augmented performance index equal to zero produces the following conditions.

Boundary condition:

$$[XF'\ S - PF']\ DXF + HF\ DTF = 0$$

State differential equations:

$$\dot{X} = A\,X + B\,U$$

Costate differential equations:

$$\dot{P} = -A'\,P$$

Optimality condition:

$$U = -W^{-1}B'P$$

The boundary condition furnishes a final value of the costate variable in terms of the final value of the state variable. For now, the final time will be considered fixed and the allowable change in the final time, "DTF", will be zero. If the optimality condition is used to eliminate the control from the state and costate differential equations, a classic two point boundary value problem will result with the values of the state known on the initial time boundary and the value of the costate known on the final time boundary. Most problems of this nature must be solved by an iterative procedure, but this particular problem possesses an analytical solution in terms of the final time.

Refer to the mathematical development section of this report for the development of the state differential equations.

$$A = \begin{bmatrix} A1 & 0 & 0 \\ 0 & A2 & 0 \\ 0 & 0 & A3 \end{bmatrix}$$

$$A1 = A2 = A3 = \begin{bmatrix} 0 & 1 & 0 \\ 0 & 0 & 1 \\ 0 & 0 & 0 \end{bmatrix}$$

$$B = \begin{bmatrix} B1 \\ B2 \\ B3 \end{bmatrix}$$

$$B1 = \begin{bmatrix} 0 & 0 & 0 \\ -1 & 0 & 0 \\ 0 & 0 & 0 \end{bmatrix} \quad : \quad B2 = \begin{bmatrix} 0 & 0 & 0 \\ 0 & -1 & 0 \\ 0 & 0 & 0 \end{bmatrix} \quad : \quad B3 = \begin{bmatrix} 0 & 0 & 0 \\ 0 & 0 & -1 \\ 0 & 0 & 0 \end{bmatrix}$$

$$S = \begin{bmatrix} S1 & 0 & 0 \\ 0 & S2 & 0 \\ 0 & 0 & S3 \end{bmatrix}$$

$$S1 = S2 = S3 = \begin{bmatrix} 1 & 0 & 0 \\ 0 & 0 & 0 \\ 0 & 0 & 0 \end{bmatrix}$$

$$W = \begin{bmatrix} w & 0 & 0 \\ 0 & w & 0 \\ 0 & 0 & w \end{bmatrix}$$

The definition of the control weighting matrix as a diagonal matrix in combination with the diagonal form of the final state weighting matrix allows one to express the performance index for the full nine state problem as the sum of three independent performance indices, one for each of the coordinate axes. This follows from the fact that the state differential equation for the full nine state problem could be expressed in three independent sets, one for each of the coordinate axes.

$$J = [\ J1 + J2 + J3\ ]$$

$$J1 = .5\ XF'\ S1\ XF + \int_{T}^{TF} .5\ w\ U1(t)^2\ dt$$

$$J2 = .5\ YF'\ S2\ YF + \int_{T}^{TF} .5\ w\ U2(t)^2\ dt$$

$$J3 = .5\ ZF'\ S3\ ZF + \int_{T}^{TF} .5\ w\ U3(t)^2\ dt$$

The following terms are used in the expressions above.

$X' = [\ X1,X2,X3\ ]$

$Y' = [\ Y1,Y2,Y3\ ]$

$Z' = [\ Z1,Z2,Z3\ ]$

$U' = [\ U1,U2,U3\ ]$

The individual state differential equations are:

$$\dot{X} = A1\ X + B1\ U1$$

$$\dot{Y} = A2\ Y + B2\ U2$$

$$\dot{Z} = A3\ Z + B3\ U3$$

For the sake of simplicity, we will solve one of the independent three state problems and use that result to infer the solution to the full nine state problem. Choose the x-axis as the one for analysis, and redefine the state vector and performance index to reflect the three state analysis.

$$X' = [\ X1, X2, X3\ ]$$

$$\dot{X} = A1\ X + B1\ U1$$

$$J1 = .5\ XF'\ S1\ XF + \int_{T}^{TF} .5\ U1'(t)\ w\ U1(t)\ dt$$

Following the usual procedure for minimizing a performance index subject to a set of differential constraints, we will form an augmented performance index by introducing the costate vector "P" which will have the same dimension as the state vector "X". The augmented performance index "AJ1" may be written in the following manner.

$$H1 = .5\ w\ U1^{2} + P'(A1\ X + B1\ U1 - \dot{X})$$

$$AJ1 = .5\ XF'\ S1\ XF + \int_{T}^{TF} H1(t)\ dt$$

The quantity "H1" in the expression above is the numerical Hamiltonian. Performing the perturbation mathematics about the optimal trajectory leads to the following necessary conditions for the optimal path.

$$\dot{X} = A1\ X + B1\ U1$$

$$\dot{P} = -\ A1'P$$

$$U1 = -\ \frac{1}{w}\ B1'P$$

$$PF = S1\ XF$$

Consider the analytical integration of the costate

differential equations which are linear, homogenous , differential equations with constant coefficients.

$$P' = [\ P1, P2, P3\ ]$$

$$\dot{P} = -\ A1'P$$

$$PF = S1\ XF$$

$$\dot{P}1 = 0 \quad : \quad P1F = X1F$$

$$\dot{P}2 = -\ P1 \ : \quad P2F = 0$$

$$\dot{P}3 = P2 \quad : \quad P3F = 0$$

Integrating the differential equations from the known time T to the unknown time TF yields the following expressions for the costate vector.

$$P1 = X1F$$

$$P2 = X1F\ (TF-T)$$

$$P3 = X1F\ \frac{1}{2}\ (TF-T)^2$$

The analytical solutions for the costate differential equations are now known in terms of the parameters of final time and final position. While these parameters have not yet been evaluated, continue to express the rest of the solution in terms of these two parameters. Using the optimality condition, the optimal control can be expressed in terms of the parameters as follows.

$$U1 = -\frac{1}{w} B'P$$

becomes:

$$U1 = \frac{1}{w} X1F\ (TF-T)$$

The optimal control is now expressed in terms of the parameters of final time and final position. The use of the state transition matrix approach will allow further simplification of this problem.

$$X(TF) = F(TF,T)\ X(T) + \int_{T}^{TF} F(TF,t)\ B\ U1(t)\ dt$$

Where:

$$U1(t) = \frac{1}{w} X1F\ (TF-t)$$

Since the analytical form of the state transition matrix is required for the integration, the following evaluation is helpful.

$$F(T,t) = e^{A\ (T-t)}$$

yields:

$$\dot{F} = A\ F \quad : \quad F(t,t) = I, \text{ the identity matrix}$$

Using the values of the matrices for this particular problem yields the following state transition matrix for this problem.

$$F(TF,t) = \begin{bmatrix} 1 & (TF-t) & \frac{1}{2}(TF-t)^2 \\ 0 & 1 & (TF-t) \\ 0 & 0 & 1 \end{bmatrix}$$

The analytical expression for the state transition matrix may now be used to propagate the state from the current time "T" to the final time "TF". The expression for X1F is the following.

$$X1F = X1 + X2\,(TF-T) + X3\,\frac{1}{2}(TF-T)^2 - X1F\,\frac{1}{3w}(TF-T)^3$$

The first three terms in the equation above arise from propagating the current state to the final time using the state propagation matrix. The last term arises from the integration of the optimal control influence upon the state between the current time and the final time. Since the difference between the current time and the final time is the true parameter instead of final time, define the "time-to-go" parameter, TTG = TF-T, and use this expression in the following work. Solving for the final state from the equation above yields the following expression.

$$X1F = C1\,[\,X1 + X2\,TTG + X3\,\frac{1}{2}\,TTG^2\,]$$

Where:

$$C1 = (3\,w) / (3\,w + TTG^3)$$

Therefore:

$$U1 = C2\,[\,X1 + X2\,TTG + X3\,\frac{1}{2}\,TTG^2\,]$$

Where:

$$C2 = (3\ TTG) / (3\ w + TTG^3)$$

Now, from similarity, the optimal control expression for the other two directions can be inferred from the one dimensional example. The optimal control for each of the three directions may be expressed as follows

$$U1 = GN [\ X1 + X2\ TTG + X3\ \tfrac{1}{2}\ TTG^2\ ]$$

$$U2 = GN [\ Y1 + Y2\ TTG + Y3\ \tfrac{1}{2}\ TTG^2\ ]$$

$$U3 = GN [\ Z1 + Z2\ TTG + Z3\ \tfrac{1}{2}\ TTG^2\ ]$$

Where:

$$GN = (3\ TTG) / (3\ w + TTG^3)$$

The optimal control for this problem has now been expressed in terms of the current state and the single parameter "TTG", the time-to-go. The specification of TTG in combination with the current state knowledge will provide a unique value for the optimal control.

The determination of a value for the parameter "TTG" is a study in itself. Even assuming perfect knowledge of the state at the current time, how does one predict the time required for the airborne missile to reach a maneuvering target whose actions are unpredictable? The solution for TTG is usually obtained from an assumptiom about the future target acceleration and from the knowledge of the missile acceleration along its body x-axis which is uncontrollable. In the simplest case, assume that the target acceleration is

zero and that the missile closing velocity is constant. The value of TTG is then obtained by dividing the target distance from the missile by the closing velocity. Other means of obtaining TTG involve approximating the closing acceleration as a constant value and solving the resulting quadratic for TTG. More exotic means of calculating TTG exist but all of the methods suffer from the same malady. The value of TTG obtained is valid only for the condition used to obtain TTG. Changes in the thrust acceleration of the missile or changes in the target acceleration will cause discontinuities in the TTG calculations. For this particular problem, major discontinuities occur when the missile exhausts its fuel supply, and when the target begins its evasive maneuver. A variation of the constant closing acceleration method is used in determining TTG for this report, but this technique is not advocated above the others. Future studies will explore additional information concerning the determination of TTG as this is a most important parameter.

With the determination of TTG, the optimal control law is completely specified in terms of the current state vector information. One should remember the assumptions made in the determination of the guidance law and in the determination of the parameters which provide a unique value for the control.

APPENDIX C

DEVELOPMENT OF AN ESTIMATION ALGORITHM

This section of the report deals with the development of an estimation algorithm, a computational technique for extracting desired information from available information. In Appendix B, the optimal control law was developed presuming that all information regarding the state vector was available. The estimation process is used to furnish the necessary state information to the guidance system. The combination of a Linear Quadratic control law with an estimation algorithm which assumes Gaussian noise characteristics produces a control system known as a Linear Quadratic Gaussian (LQG) control system.

For control of an airborne missile with a passive seeker, the available sensors provide information about the inertial acceleration of the missile and the angles defining the line-of-sight direction from the missile to the target. All measurements are corrupted by some form of additive white noise, and there is uncertaintity in the initial state vector quantities at the beginning of the engagement. From the noisy measurements and the uncertain starting conditions, the estimation algorithm is expected to furnish to the control law the target's position and velocity relative to the missile, and the inertial acceleration of the target--the full nine state vector.

1. Extended Kalman Filter

For fully linear systems, systems obeying linear state propagation equations and linear measurement equations, the optimal estimation algorithm is the Kalman filter. For those systems with nonlinear state propagation equations or

with nonlinear measurements, the standard estimation process is the extended Kalman filter, a suboptimal filter which linearizes the nonlinear part of the process about a "best estimate". The extended Kalman filter is the base algorithm for this report and all other estimation algorithms will be compared to the extended Kalman filter.

The estimation algorithm relies upon a model of the process by which the state vector describing the system is propagated in time. This problem is assumed to obey the linear model developed in the Mathematical Development section of this report with an extra term to account for any unmodeled terms, incorrectly modeled terms, or any other errors in state propagation which can be included in the category of "process noise". The true state vector propagation is represented by the linear vector differential equation below.

$$\dot{X} = A\,X + B\,U + C$$

Where:
X is an N-state vector
A is an NxN matrix of constants
B is an NxM matrix of constants
U is an M-control vector
C is an N-vector of noise

The integration of the state differential equations utilizing the state transition matrix provides the following discrete recursive equation governing the true state propagation.

$$X(k+1) = F\,X(k) + G\,U(k) + q(k)$$

Where:

X(k) is the state vector at the k-th time point
F is the constant state transition matrix
G is the constant control transition matrix
U(k) is the control vector at the k-th time point
q(k) is the process noise for the k-th interval

At this time, note that if the exact initial state vector is known, if the exact control vector is known, and if the exact state propagation model is known, then this model would yield the true state vector with no additional work. The only inputs required by the model would be the time for which the state vector is required.

The fault with this line of reasoning is that there are no "exact" quantities in the real world. For problem solution in the real world, we must make a "best guess" or estimate of the initial state vector, produce a control vector based upon the estimated state vector, and propagate the state estimate to a new time based upon an "assumed form" or model of the state propagation process. At the new time, information in the form of real world measurements is used to correct or "update" the state estimate. The estimation process consists of a continuous sequence of propagation and updating of the state estimate.

Let XT denote the true value of the state vector, let XH denote the best state estimate using all available information, and let XB denote the propagated state before including new measurement information.

$$XB(k+1) = F\,XH(k) + G\,U(k)$$

$$XT(k+1) = F\,XT(k) + G\,U(k) + q(k)$$

Remember that the true state XT is not known and that

the XT propagation equation above is written for comparison with the XB propagation equation only.

The real use for the equations above is the determination of a state estimate error propagation equation. Define the error terms as follows.

$$XBe = XB - XT$$
$$XHe = XH - XT$$

Subtracting the true state propagation equation from the estimated state propagation equation yields the following state estimate error propagation equation.

$$XBe(k+1) = F\ XHe(k) - q(k)$$

The error propagation equation above is not really used to propagate the state estimate error as we would use the error value and make the estimate correct if possible. The error propagation equations are useful for propagating error bounds which can be established. Next, the sign of the state estimation error is unknown, so the sign of the error bound is also unknown. The use of a covariance matrix solves some of these problems. Define the covariance matrix for an error vector as the expected value of the outer product of the error vector with itself.

$$PB = E\{\ XBe\ XBe'\ \}$$
$$PH = E\{\ XHe\ XHe'\ \}$$

In the expressions above, "PB" is the covariance matrix for the propagated state estimate error, and "PH" is the covariance matrix for the updated state estimate error. The use of the covariance matrices relieves us from the necessity of guessing the appropriate signs of the error terms as the diagonal terms of the covariance matrix are the squares of the error terms.

The use of the covariance matrix also relieves us from the task of guessing the initial estimation errors. Assume that the initial estimation errors are uncorrelated with zero expected values. This allows us to set the initial values of the off-diagonal terms in the covariance matrices to zero and the diagonal terms to the square of the initial error bounds. Remember that the state estimation error covariance matrix is a measure of the confidence which can be placed in the state estimate as indicated by the growth or decline of the estimation error bounds. The equation for the propagation of the state estimation error covariance matrix is obtained as follows.

$$PB = E\{ XBe\ XBe' \}$$

Where:

$$XBe(k+1) = F\ XH(k) - q(k)$$

Thus:

$$PB(k+1) = F\ PH(k)\ F' + Q(k)$$

Where:

$$E\{ F\ XHe\ XHe'\ F' \} = F\ PH\ F'$$
$$E\{ F\ XHe\ q' \} = 0$$
$$E\{ q\ XHe'F' \} = 0$$
$$E\{ q\ q' \} = Q$$

Where Q is the process error covariance matrix.

The initial state vector can be estimated and the propagation equation used to propagate the estimate to a new time. At the same time, the initial state estimation error bounds can be established and the error bounds used to initialize the state estimation error covariance matrix. The estimation error covariance matrix may be propagated to the new time along with the state estimate. One requirement

for this propagation is that the process error covariance matrix "Q" must be defined. An estimate must be made of the error between the model equation used to propagate the state estimates and the real world propagation of the true states. This error may be used to establish an error bound for the process error and the error bound may then be used to create the process error covariance matrix. For this problem, the process error covariance matrix was constant throughout the engagement. Note that the process error covariance matrix always increases the estimation error covariance matrix.

Once the estimate of the state vector is propagated to a new time, the relationship of the state vector to the measurement vector can be used to estimate what the measurements should be. Comparison of the estimated measurements to the true measurements provides a means of correcting or updating the state estimates. Let MT denote the true or actual real world measurements and let MB denote the estimate of the measurements based upon the propagated state estimate and the state-measurement relationship model. Let "MB = h(XB)" be the model of the state-measurement relationship and let "MT = h(XT) + r" be the actual state-measurement relationship. The quantity "r" is the measurement noise term similar to the process noise term in the state propagation equations. The measurement error is defined in a manner similar to the state error.

$$MBe = MB - MT$$
$$MBe = h(XB) - h(XT) - r$$

Linearize the last equation about the propagated state estimate where XT = XB - XBe. This will give an equation relating the measurement residual or error to the propagated state estimate error.

$$MBe = HX\ XBe - r$$

The matrix "HX" in the equation above denotes the partial derivative matrix for the measurement equation evaluated at XB. Note that this error equation is linear even though the original error equation was not. This is what differentiates the extended Kalman filter from the regular Kalman filter which deals with a totally linear problem.

For completeness, define the measurement error covariance matrix, "CM", in the following manner.

$$CM = E\{ MBe\ MBe' \}$$
$$= E\{ (HX\ XBe - r)\ (HX\ XBe - r)' \}$$
$$= HX\ PB\ HX' + R$$

Where:

$$E\{ (HX\ XBe)\ (HX\ XBe)' \} = HX\ PB\ HX'$$
$$E\{ (HX\ XBe)\ (-r)' \} = 0$$
$$E\{ (-r)\ (HX\ XBe)' \} = 0$$
$$E\{ (-r)\ (-r)' \} = R$$

Where R is the measurement noise covariance matrix.

The incorporation of the measurement data into the estimation process will allow us to correct or update the state estimate in order to make the measurement estimate conform more closely to the actual measurement. A relationship must be established between the measurement residual and the updated state estimate in order to accomplish this. For obtaining a linear, unbiased state estimate, the updated state estimate will be formed from a linear combination of the propagated state estimate and the measurement residual. The updated quantities are given by the following equation.

$$XH = XB - KG\ (MB - MT)$$

$$XHe = XBe - KG\ MBe$$

$$= (I - KG\ HX)\ XBe - KG\ r$$

$$PH = (I - KG\ HX)\ PB\ (I - KG\ HX)' + KG\ R\ KG'$$

Note the introduction of the gain matrix "KG" which is the Kalman gain matrix. The matrix "KG" is an NxM matrix. The discussion below is concerned with the determination of a value for KG.

The manner in which KG is determined specifies the estimation technique. If KG is chosen to minimize the estimation error in some way, then the estimator is a minimum error estimator. If the value of KG is chosen to minimize the estimation error covariance in some way, then the estimator is a minimum variance estimator. This report is concerned with the minimum variance type of estimator.

Take a first variation of the PH equation with KG as the perturbation variable. Setting the first variation equal to zero will yield the following expression for KG.

$$KG = PB\ HX'\ (HX\ PB\ HX' + R)^{-1}$$

Note the pleasing result--that the value of KG can be determined from the propagated state estimate, propagated state estimate error covariance, and the measurement error covariance. This means that KG can be determined explicitly from propagated and measured quantities. There is no iteration necessary in determining KG.

Substitution of this expression for KG into the equation for PH allows an alternate expression for PH as given below.

$$PH = (I - KG\ HX)\ PB$$

This expression for PH is computationally more efficient than the previous expression, but the insight that PH is a symmetrical positive semidefinite matrix is not available from the latter expression. Likewise, periodically one should perform a check that the latter means of calculating PH does retain the positive semidefinitness of PH.

The following provides a flowchart for the extended Kalman filter algorithm which has just been developed.

Precompute: $F = F(DT,0)$
$G = G(DT,0)$

Initialize: XH,PH,Q,R

Begin:

Propagate: $T(k+1) = T(k) + DT$
$XB(k+1) = F\ XH(k) + G\ U(k)$
$PB(k+1) = F\ PH(k)\ F' + Q(k)$

Measure: $MT(k+1)$

Compute: $MB(k+1) = h(XB(k+1))$
$MBe = MB - MT$
$HX(XB)$

Compute: $KG = PB\ HX'\ (HX\ PB\ HX' + R)^{-1}$

Update: $XH(k+1) = XB(k+1) - KG\ MBe$
$PH = (I - KG\ HX)\ PB$

2. Adaptive Kalman Filter

In the development of the extended Kalman filter, it was noted that potential difficulty exists in the manner of specification of the process error covariance matrix "Q", and the measurement noise covariance matrix "R". Adaptive estimation algorithms attempt to alleviate the problems by allowing the filter to adjust to the unknown noise statistics. Ideally, adaptive filtering would allow the estimation process to account for nonlinearities, for error sources not included in the model, and for all forms of noise. Practically speaking, this is not realizable, but the adaptation should improve the filter operation and allow an improvement in the estimation of the states.

The measurement residuals provide an excellent source of information for the estimation of the measurement noise statistics. A moving window sample of measurement residuals will be used to produce an unbiased estimate of the measurement noise covariance matrix. The following relationships will be used for calculating the characteristics of the measurement noise.

Measure: MT(j): j=1,nm
Calculate: MB(j): j=1,nm
Determine: MBe(j): j=1,nm

Define: C1=1/nm
Define: $em = C1 \sum_j MBe(j)$

Define: C2=1/(nm-1)
Define: $CS = C2 \sum_j [MBe(j)-em]\,[MBe(j)-em]'$

Remember: CM = HX PB HX' + R
Approximate: R = CS - HX PB HX'

The above expressions allow the online determination

of the measurement noise statistics based upon the measurement residuals and the assumption that the sample covariance can be used to approximate the global covariance. The validity of this approximation is borne out in the filter comparisons where the adaptive filter consistently improves upon the performance of the regular extended Kalman filter. The only fault that one could find with the approximation is that the accuracy is dependent upon the size of the sample used in the computations. In almost all cases, a sample window of 20 measurements provided the best performance, so the adaptive filter window size was fixed at this value.

BIBLIOGRAPHY

1. Brown, C. M. and Price, C. F., A Comparison of Adaptive Tracking Filters for Targets of Varible Maneuverability, The Analytic Sciences Corporation, Report No. TR-480-6, April, 1976.

2. Bryson, Arthur E. and Yu-Chi Ho, Applied Optimal Control, Blaisdell Publishing Company, Waltham, Mass.,1969.

3. Clark, B. L., Development of an Adaptive Kalman Target Tracking Filter and Predictor for Fire Control Applications, Naval Surface Weapons Center Report No. NSWC/DL TR-3445, March, 1977.

4. Emmert, R. I., Ehrich, R. D., and Longenbaker, W. E., Strapdown Seeker Guidance and Control Integration Technology for Tactical Weapons, Phase I - Air-to-Air Feasibility Study, Rockwell International Corporation, Report No. AFATL-TR-80-65, June, 1980.

5. Fiske, P. H., Advanced Estimation and Control Concepts for Air-to-Air Missile Guidance Systems, The Analytic Sciences Corporation, Report No. AFATL-TR-79-29, Feb., 1979.

6. Gelb, Arthur,Ed., Applied Optimal Estimation, The M.I.T. Press, Cambridge, Mass.,1977.

7. Gottfried, B. S. and Weisman, J., Introduction to Optimization Theory, Prentice-Hall, Englewood Cliffs, N. J., 1973.

8. Hall, Kenneth R., "An Investigaton into State Estimation for Air-to-Air Missiles", AFOSR-SCEEE Summer Faculty Research Program, Eglin AFB, Florida, 1981.

9. Kirk, Donald E., Optimal Control Theory, Prentice-Hall, Englewood Cliffs, N. J., 1970.

10. Lauer, D. S., and Sandell, N. R., A Characterizaton of Maneuver Observability Via Cramer-Rao Bounds, Alphatech Inc., Report No. TR-109, Sept., 1980.

11. Leondes, C. T., Ed., Theory and Applicatons of Kalman Filtering, AGARDograph No. 139, Technical Editing and Reproduction Ltd., London, 1970.

12. McClendon, J. R. and Vergez, P. L., "Applications of Modern Control and Estimation Theory to the Guidance of Tactical Air-to-Air Missiles", Proceedings of the Second Meeting of the Coordinating Group on Modern Control Theory, 1980.

13. Maybeck, Peter S., Stochastic Models, Estimation, and Control, Volume 1, Academic Press, New York, 1979.

14. Myers, Kenneth A., Filtering Theory and Applications to the Orbit Determination Problem for Near-Earth Satellites, AMRL 1058, The University of Texas at Austin, Nov., 1973.

15. Sammons, J. M., Balakishnan, S., Speyer, J. L., Hull, D. G., Development and Comparison of Optimal Filters, The University of Texas at Austin, Report No. AFATL-TR-79-87, Oct., 1979.

16. Vergez, P. L. and McClendon, J. R., "Optimal Control and Estimation for Strapdown Guidance of Tactical Missiles", Proceedings of the Second Meeting of the Coordinating Group on Modern Control Theory, 1980.

17. Warren, M. E. and Bullock, T. E., Development and Comparison of Optimal Filter Techniques with Application to Air-to-Air Missiles, The University of Florida, Report No. AFATL-TR-80-50, April, 1980.

INITIAL DISTRIBUTION

DTIC-DDAC	2
AUL/LSE	1
ASD/ENSZ	1
AFATL/DLODL	2
AFATL/CC	1
USAF/SAMI	2
OO-ALC/MMWR	1
AFIS/INTA	1
ASD/ENESS	1
TAC/DRA	1
HQ USAFE/DOQ	1
AFATL/CCN	1
HQ PACAF/DOQQ	2
HQ TAC/INAT	1
ASD/XRX	1
USA TRADOC-SYSTEMS ANAL ACTY	1
COMIPAC (PT-2)	1
HQ PACAF/OA	1
USA BALLISTIC RESCH LAB	1
AFWAL/AADM	1
HQ AFSC/XRL	1
ASD/EN	3
HQ TAC/XPS	1
AFWAL/FIB	1
NWC (CODE 03A4)	2
AD/XRS	1
AFATL/DLMA	5
NWC (CODE 335)	1
DRSMI-RPR	2
AFATL/DLMM	1
AFATL/DLYV	1
AFWAL/FIGC	1
SAF/ALR	1
MIT LINCOLN LABS	1
AFWAL/FIGX	1
AEDC LIBRARY	1
NWC (CODE 3905)	1
NSWC (CODE K-21)	2
DRSMI-RGN	1
AFIT/ENG	1
AFOSR/NM	1

(The reverse of this page is blank)

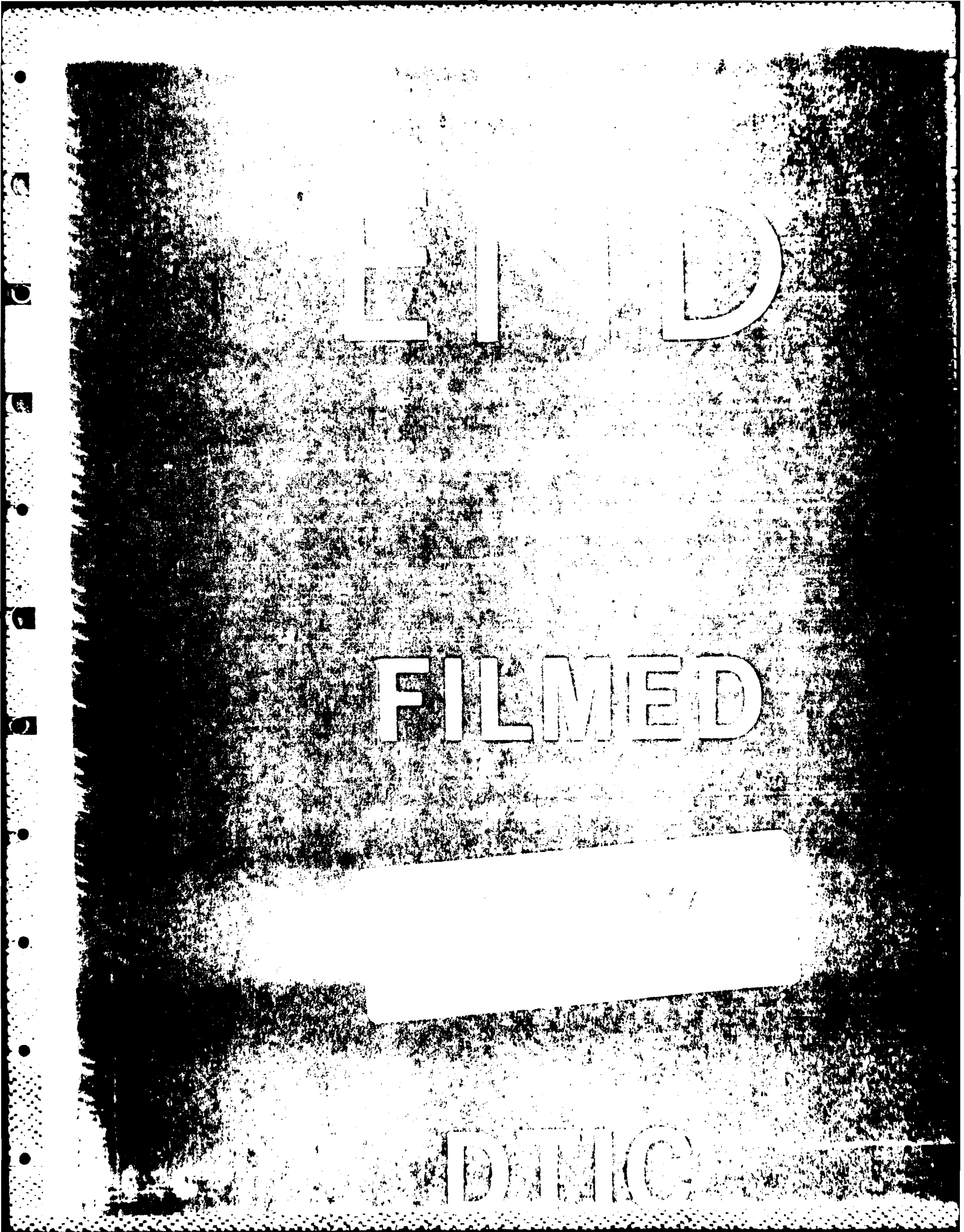
FILMED
DTIC